

Journal of Architectural Environment & Structural Engineering Research



December
2018
• Volume 1 Issue 1



**BILINGUAL
PUBLISHING CO.**
Pioneer of Global Academics Since 1984

Editor-in-Chief Seyed Mojtaba Sadrameli Tarbiat Modares University, Iran

Editorial Board Members

Müslüm Arıcı, Turkey
Yonggao Yin, China
Rangika Umesh Halwatura, Sri Lanka
Seifennasr Sabek, Tunisia
Mehdi Shahrestani, UK
Andrzej Łączak, Poland
Reda Hassanien Emam Hassanien, Egypt
Mario D’Aniello, Napoli
Mohammed Ali Khan, India
Humphrey Danso, Ghana
Khaled M Bataineh, Jordan
Alireza Joshaghani, USA
Mohamadreza Shafieifar, USA
Sina Memarian, Iranian
Mohamed El-Amine Slimani, Algeria
Vanessa Giaretton Cappellesso, Brazil
Trupti Jagdeo Dabe, India
Lobanov Igor Evgenjevich, Russian
Vincent SY Cheng, Hong Kong
Hamed Nabizadeh Rafsanjani, USA
Ramin Tabatabaei Mirhosseini, Iran
Dario De Domenico, Italy
Amos Darko, Hong Kong
Rahul Sharma, India
Guillermo Escrivá-Escrivá, Spain
Selim Altun, Turkey
Yangang Xing, UK and P.R.China
Ahmed Mohamed El shenawy, Canada
Fengyuan Liu, UK
Anastasia Fotopoulou, Italy
Caroline Hachem-Vermette, Canada
Hua Qian, China
Elder Oroski, Brazil
Mohammadreza Vafaei, Malaysia
Yacine Gouaich, Algeria
Chiara Tonelli, Italy
António José Figueiredo, Portugal
Shuang Dong, China
Amirpasha N/A Peyvandi, USA

Ece Kalaycioglu, Turkey
Ali Tighnavard Balasbانه, Malaysia
Sadegh Niroomand, Iran
Amirreza Fateh, UK
Latefa Sail, Algeria
Chi Kuen Henry Hung, Hong Kong
Suman Saha, India
José Ricardo Carneiro, Portugal
Payam Sarir, China
Amjad Khabaz, Syria
Jingfeng Tang, China
Mohammad Ahmed Alghoul, Saudi Arabia
Jian-yong Han, China
Huaping Wang, China
Jun-Ling Song, China
Chiara Belvederesi, Canada
Yukun Li, USA.
Giovanni Rinaldin, Italy
Alper Aldemir, Turkey
Yushi Liu, China
Amin Jabbari, Iran
Rawaz M.S.Kurda, Portugal
Nasir Shafiq, Malaysia
Ahmed Elyamani Ali, Spain
Mohammed Jassam Altaee, Iraq
Nadezda Stevulova, Slovakia
Anderson Diogo Spacek, Brazil
Tatjana Rukavina, Croatia
Yuekuan Zhou, Hong Kong
Pramod Kumar Gupta, India
Rabah Djedjig, France
Abdullah Mahmoud Kamel, Egypt
Xiuli Liu, China
Biao Shu, China
M^a Dolores Álvarez Elipe, Spain
Jing Wu, China
Mohammad Jamshidi Avanaki, Iran

Volume 1 Issue 1 • October 2018 ISSN 2630-5232 (Online)

Journal of Architectural Environment & Structural Engineering Research

Editor-in-Chief

Seyed Mojtaba Sadrameli



**BILINGUAL
PUBLISHING CO.**

Pioneer of Global Academics Since 1984

Contents

Article

- 1 Simulation of Self-compacting Concrete Properties Containing Silica Quicksand Using ANN Models**
Ramin Tabatabaei Mirhosseini Mohsen Shamsadineei

- 10 Impact of Glazing Type and Orientation on the Optimum Dimension of Windows for Office Room in Hot Climate**
Chahrazed Mebarki Essaid Djakab Sidi Mouhamed Karim El Hassar
Mohamed El-Amine Slimani

- 16 Feature Identification for Non-Intrusively Extracting Occupant Energy-Use Information in Office Buildings**
Hamed Nabizadeh Rafsanjani

Review

- 25 Early Stage Design Workflow for High Energy Performance Multi-storey Residential Buildings**
Caroline Hachem Robert Beckett

- 39 Anthropic Principle Algorithm: A New Heuristic Optimization Method**
Elder Oroski Beatriz S. Pês Rafael H. Lopez
Adolfo Bauchspiess

Copyright

Journal of Architectural Environment & Structural Engineering Research is licensed under a Creative Commons-Non-Commercial 4.0 International Copyright (CC BY- NC4.0). Readers shall have the right to copy and distribute articles in this journal in any form in any medium, and may also modify, convert or create on the basis of articles. In sharing and using articles in this journal, the user must indicate the author and source, and mark the changes made in articles. Copyright © BILINGUAL PUBLISHING CO. All Rights Reserved.

ARTICLE

Simulation of Self-compacting Concrete Properties Containing Silica Quicksand Using ANN Models

Ramin Tabatabaei Mirhosseini* Mohsen Shamsadineei

Department of Civil Engineering, Islamic Azad University, Kerman Branch, Kerman, 761, Iran

ARTICLE INFO

Article history:

Received: 24 October 2018

Accepted: 14 November 2018

Published: 19 January 2019

Keywords:

Quicksand density

Silica fume

Compressive strength

Mechanical properties and
artificial neural network (ANN)

ABSTRACT

Self-compacting concrete (SCC) mix designs demonstrate complexities in their mechanical properties due to natural compounds of the material and the diversity and abundance of factors that affect the properties. In this paper, a set of SCC mix designs is made using silica quicksand (as a filler) instead of rock powder with other required materials. The tests of fresh concrete such as the slump flow, J-ring, V-funnel, L-box tests and the hardened concrete tests are investigated and considered. The test results are shown that, a high quality has been achieved for SCC mixture contains the quicksand and silica fume contents with low lubricant admixture dosage. The research is embodied the use of a branch of Artificial Neural Networks (ANN) as a quick and reliable method of such concrete experimental testing. The results confirm that the ANN technique can perform as a satisfactory algorithm to provide speedy prediction of optimum silica quicksand content must be added prior to SCC mix design. Carry out experiments are usually costly and time consuming, therefore, the proposed algorithm can be used as an approximate method.

1. Introduction

Self-Compacting Concrete or SCC was carried out by Okamura for the first time in late 1980 in Japan for earthquake-prone buildings that were located in areas with a high density of reinforcement.^[1,2] Recently, this type of concrete is widely applied in many countries in order to vary the shape of the structure has been used.

Self-Compacting Concrete or SCC is treated as a mix of lubricant admixtures such as rock powder, silica fume (SF), fly ash (Fly-Ash) and superplasticizer (SP) contents and a very low water to cement ratio. Granulometry and heat treatment have been optimized to obtain excellent mechanical and durability properties. Starting point of

the SCC mix design is the packing theory. These types of concrete are very smooth and without undergoing any significant separation that can be spread readily into place and fill the framework without any consolidation, thus SCC mixes, which requires less-skilled workers, in construction's development can be found.^[3]

The strength and durability of SCC as the main criteria for success are the properties of fresh concrete mixes, but it is much wider than conventional concrete is compacted by vibration. In general the relation between compacting and mechanical properties of concrete is known, and usually a granulometric curve of the solid components such as gravel, sand, filler (rock powder, fly ash and silica fume) and cement is selected. These mixes are extensive-

**Corresponding Author:*

Ramin Tabatabaei Mirhosseini,

Department of Civil Engineering, Islamic Azad University, Kerman Branch, Kerman, 761, Iran;

E-mail: tabatabaei@iauk.ac.ir

ly tested, both in fresh and hardened states, and meet all practical and technical requirements such as a low cement and admixtures.^[4]

However, SCC mixture should maintain continuity and no separation between aggregate grains occur. The Japanese method suggest that the coarse aggregate content in the SCC mix corresponds to generally fixed at 50 percent of the total solids volume, the fine aggregate content is fixed at 40 percent of the mortar volume and the water / powder ratio is assumed to be 0.9-1.0 by volume depending on the properties of the powder and the SP contents. In many countries, the Japanese method has been adopted and used as a first step for training on the development of the SCC mix design.^[5]

A new mix design method developed for creating SCC, henceforth was referred to as Chinese method.^[5] First, in this recent method the amount of all aggregates requirement is determined, and the paste is then filled into the void space of the grading aggregates to guarantee that the concrete thus obtained has flowability, compactability, without segregation and other desired SCC properties. Recently, several researchers follow that the particle size distribution (PSD) of all aggregates in the concrete mix should follow the grading line of the modified Andreasen and Andersen (A&A) model. This line grading comprises the fine aggregate and goes down to a particle size of typically 150 μ m. In order to model the SCC mix design, all solid components should be considered, so also the cement and the filler.^[5] This modified model verifies the positive relation between the rheological properties and the compacting of the SCC mix: accomplishing full compacting, the enough water is available to perform as lubricant for the solid components, and the better flowability. Both the Japanese and Chinese methods do not consider the PSD values of the aggregates.^[6]

The amount of aggregates, powders, water/filler ratio and water/cement ratio, as well as type and dosage of superplasticizer to be used are the major factors influencing the properties of SCC mixture.^[7,8]

The principal consideration of the SCC mix design method is that the void space of the aggregate is filled with paste requirement (cement, water and rock powder). Further, the grading of the fine and coarse aggregates is an important characteristic because it determines the paste to obtain suitable workability. Further, the paste is the factor calculating the price, since the increase of the cost of paste is use of higher powder content and it can also be reduced by use of various mineral materials such as rock powder, fly ash, metakaolin etc., as partial replacement of cement. However, it is generally noted that, the mineral materials also improve the mechanical properties and durability

of the SCC^[9,10]. It is therefore desirable to accomplish, the more aggregate, the less paste and consequently, less flowability. Subsequently, the cement content is evaluated. This quantity is assessed by the required mechanical properties and durability of the hardened concrete stage.^[11]

A serious lack of the mineral material resources (such as rock powder and fly ash) increases the cost of SCC production. Therefore, in some countries natural substitute materials such as quicksand can be used. Mineral materials which are also known as mineral admixtures have been used as replacement cements for a long time ago. There are two types of materials crystalline and non-crystalline. Micro silica (or called silica fume) is very fine of non-crystalline type. But it should be noted that the use of the micro silica has led to an increase in the cost of filler, and the price of SCC.

Over the last two decades, the development of an acceptable artificial neural network (ANN) model is necessary for the prediction of reliable results for a problem such as mechanical properties of concrete.^[12]

In the literature, many researchers either selected the different data mining methods to input the variables for their ANN models in studying the compressive strength of concrete^[13-17]. Therefore, the correct selection of the input and output of ANN algorithms can be likely to be impressive. Thus do the steps of data preparation and training/testing are very sensitive and important. To achieve an optimal result, several iteration steps are usually required. Usually the Backpropagation (BP) layout of neural network model is used. In fact, BP is kind of the training algorithm in which pattern provided direction of the data flow, either forward or backward. BP requires at least three layers in order to predict correctly, and training is conducted in a supervised processes. Training of a BP neural network occurs in two steps.^[18]

The purpose of this study was to examine tiny silica quicksand (at Kerman desert) as filler for a broad range of SCC concrete mixes. This was achieved by mix the quicksand ratio for 5, 10, 15 and 20% by weight, as a substitute for concrete rock powder. The quicksand is considered as filler and its price is about 1/4 the price of the rock powder. The natural silica quicksand is usually a gray colored powder somewhat similar to some micro silica and they are generally classified as filler content.

The empirical studies show that, the quicksand treats as rock powder and fly ash and it was initially suitable as cement replacement material and sometimes it can view as an alternative to micro silica. As known that, micro silica content may be used as costly pozzolanic admixtures. Following the previous references methods, the concrete paste lines are considered for significant water/powders

(cement, fly ash and rock powder). A general relation is achieved between the compacting and specific surface area of each solid, and the water required for bleeding, flowing and deformability of paste phase. The effects of quicksand content in addition to rock powder, silica fume (SF) and superplasticizer (SP) dosage on fresh and hardened concrete properties of SCC are considered. This mix is introduced all practical and technical requirements such as a low cement and powder content, therefore the experimental results are illustrated that the mix design has the high compressive strength and low cost.

As mentioned, due to the variation in the SCC concrete constituents has different behavior. As a result, it is necessarily the view of the mechanical properties such as compressive strength and workability is reviewed. In this research the objective goal was not the evaluation of concrete durability. Therefore, the two artificial neural network (ANN) models that were selected for the present study are predictions of SCC mechanical properties. These two models are developed to predict the following attributes of the SCC mix design: 1) mechanical property, 2) rheological property.

In order to present study, the results of forty-five experimental samples are utilized to develop these two ANN models, incorporating some of the effective parameters on their mechanical properties.

2. Experimental Stage

The experiment stage is consisted of six studies on forty-five full scale mixes. Each study is built upon techniques and observations as the SCC mix designs are limited to standard mix designs at a constant, moderate level of workability. Furthermore, the studies are statistically designed to estimate all of the possible properties variation that might occur in SCC preparation, as explained in the next sections. The materials used are chosen to allow the optimal use of standard requirements, which proved to be vital in extracting information from the data in the previous studies.

2.1. Materials

Cement: The cement used was type II of Portland cement with a specific gravity 3.15 ton/m^3 , produced by Kerman cement factory. The XRD test results show that chemical characteristics of the cement satisfy the ASTM C150 Standard Specification.

Fine aggregate: The fine aggregate

(sand) used in the samples was the natural siliceous clean and free of impurities crushed stone sand with a specific gravity 2.7 ton/m^3 . It was obtained from Kerman aggregate mine in eastern south of Iran. Its maximum nominal size (4.75 mm) is suitable to be used in SCC and absorption of the sand found 0.7% . Granulometric curve of the used fine aggregate is shown in Fig. 1. Sieved sand over sieve of size 0.6 mm was discarded as impurities. This indicates that the fine aggregate is unstable and contains void. Adequate grading and packing is therefore required to obtain workable fresh concrete.

Coarse aggregate: Two types of coarse aggregates used to make mix design were obtained from Kerman crushed aggregate mines. Maximum size of the coarse aggregate used in concrete was 19 mm .

Specific gravity and water absorption of the coarse aggregates (gravels) under examination are determined using ASTM standard C127. The values of specific gravity and water absorption of aggregates are found 2.7 ton/m^3 and 0.7% , respectively. Sieve testing results of the used coarse aggregates are shown in Fig. 1.

Silica fume (SF): It is a product of micro silica consisting mainly of amorphous silica (SiO_2) and non-combustible particles. It was produced by Ferro Alloys Corporation Ltd. The main constituent material in SF is silica (SiO_2), the content of which is normally over 90% . Table 1 shows chemical components obtained by the XRD test of a commercially available silica fume. The silica fume used was

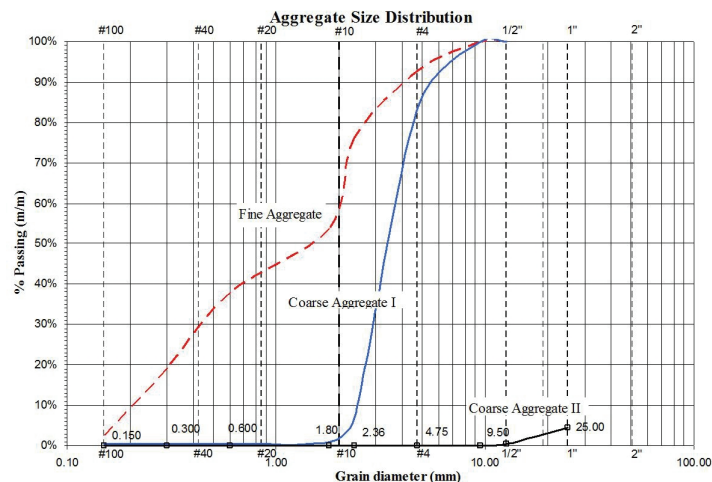


Figure 1. Sieve analysis of fine and two types of coarse aggregates

Table 1. The chemical components of the silica fume

Chemical Composition	SiO_2	Al_2O_3	Fe_2O_3	CaO	MgO	K_2O	Na_2O	N_2O	P_2O_5	Cl
Average (%)	93.6	1.32	0.87	0.49	0.97	0.87	0.50	1.01	0.16	0.04

satisfied with the main requirements of ASTM C1240.

Superplasticizer: In order to improve the workability of fresh phase without an additional amount of water, the high-range water-reducing admixtures, often referred to as superplasticizer was added to the mixture. In this study a naphthalene sulphonate group based superplasticizer, supplied by Chemical Supply Manufactory was used. The main properties of the used superplasticizer were conformed to ASTM C494-Type F.

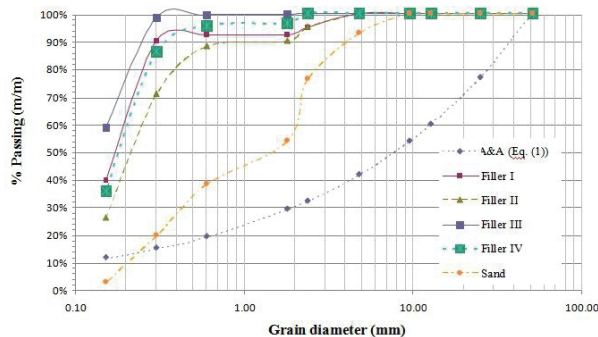


Figure 2. Particle Size Distribution(PSD) of fillers and sand

Quicksand: Because of its unique nature, some of the silica quicksand has the potential to significantly reduce SCC costs. There is not currently an exact standard requirements regard to proportioning of the quicksand in the SCC mixes.

In this study, the clean silica quicksand materials as filler were prepared from deserts around Kerman province. The physical properties (granulometric tests and SE) have been used as examples of fine aggregate (sand). As the A&A model accounts for fillers ($<250\mu m$) better, it is better suited for designing SCC and when the cumulative PSD satisfies equation as follows [6],

$$P(D) = \left(\frac{D}{D_{\max}} \right)^q \quad (1)$$

The parameter P is a fraction that is based on the size of sieve D , D_{\max} is the maximum particle size of the aggregate components and q has a value between 0 and 1. Based on Andreasen and Andersen (A&A) research, the optimum packing will be obtained when value of $q \approx 0.37$.

The sieve analysis results of the used fillers and the fine aggregate are compared in Fig. 2. The results are implied that all of the quicksand materials (Type I to IV) are within the specified limit and these values are suitable as filler for construction work (see Fig. 2).

2.2. Mix design

In present study, the effects of the quicksand (as filler) instead of the rock powder content are investigated for a

broad range of SCC concrete mixes. This was achieved by mixing the quicksand ratio for 5, 10, 15 and 20% by weight, as a substitute for concrete rock powder.

At first step, the most important consideration is that the voids between incompact aggregates are filled with paste, and that the packing of the aggregates is minimized.

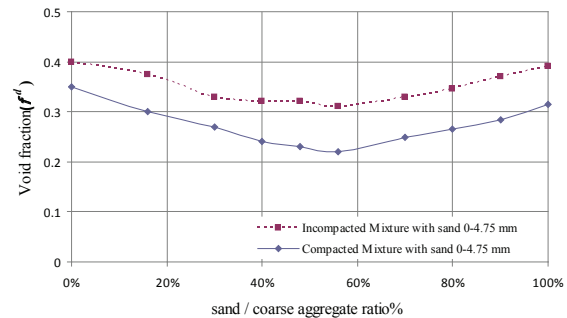


Figure 3. Void fraction of aggregates mixes, before and after compaction process

Therefore, the locally fine aggregate (sand) and a gapped grading has been used for the coarse aggregates (2 types) made by combining what has been retained on the sieve #4. Hence, the density of the aggregate components depends on the sand/coarse ratio, and not only to the value of sand or gravel alone.

The void fraction of the densely packed aggregate is determined as follow [5],

$$\phi^d = 1 - \frac{\rho_a^d}{\rho_a} \quad (2)$$

where ρ_a^d and ρ_a are density of the compacted aggregate (referred to apparent density) and its specific density (or particle), respectively.

Fig. 3 shows the void fraction values with sand/coarse (mass) ratios of both in loose and compacted situation. As shown in this figure, the fine aggregate (sand 0-4.75mm) achieves a minimum value of the void fraction when its content is 56% in combination with coarse aggregate.

The second step is the addition of the powders (cement and filler) contents. The concrete samples are carried out based on replacement of powder by the quicksand as filler material. The required cement content is directly related to the desired compressive strength. In the most previous researches, a linear relation between the mechanical properties of the hardened concrete and the cement content is assumed. Furthermore, the quantity of water for the cement and the powders follows from the flowability requirement. Then the mix designs were carried out according to number of trail mixes to produce SCC without segregation and bleeding. In the trail mixes, it can be noted that the quan-

tity of water for the cement and the filler can be achieved in fresh mix according to the flowability requirement. For this study, SCC mixes were prepared with a different filler ratio.

These mix designs are introduced in detail here, whereby the quicksand and other supplementary cementitious materials are now also included as filler content.

As shown in Table 2 the more details on the preparation procedure of the SCC mixes have been contained the following specifications, Mix QS expresses a concrete with just quicksand content, Mix RP and Mix SF represent mixes create just containing rock powder and Silica Fume, respectively, Mix RP + SF and Mix QS + SF concretes related to mix design by rock powder plus silica Fume and mix using quicksand in combination with silica Fume, respectively, and Mix RP + QS introduce mix include rock powder and quicksand as filler material content.

Table 2. Dosage of developed SCC mixes

Material (kg/m^3)	Mix QS	Mix RP	Mix RP + QS	Mix RP + SF	Mix QS + SF	Mix SF
Cement	450	450	450	450	450	450
Rock powder	--	250	125	120	--	--
Fine aggregate (sand)	850	800	850	850	850	850
Coarse aggregate I	450	450	450	450	450	450
Coarse aggregate II	400	400	400	400	400	400
Quicksand	250	--	125	--	125	--
Water	170	140	170	130	145	145
Silica Fume (SF)	--	--	--	50	125	250
Superplasticizer (SP)	20	20	20	20	15	10
Water/cement ratio	0.38	0.31	0.38	0.29	0.32	0.32
Water/(QS+SF) ratio	0.68	0.56	0.68	0.77	0.58	0.58

Finally, the plastic and hardened properties of the SCC were monitored and measured.

2.3. Fresh Concrete Experiments

Several tests for the fresh properties (paste phase) of SCC have been proposed [19]. Tests was included density, air content, slump flow and passing ability that are measured by L box, V-funnel time and J-ring. Further, characterizing method for the mortar properties were proposed and the indices for deformability and viscosity were defined as Γ_m and R_m [4].

$$\Gamma_m = (d_1 d_2 - d_0^2) / d_0^2 \quad (3)$$

d_1, d_2 : Measured flow diameter through slump flow

d_0 : Flow cone diameter

$$R_m = 10/t \quad (4)$$

t (sec): Measured time (sec) for mortar to flow through the V-funnel

In Eqs. (3) and (4) a larger Γ_m shows higher deformability and a smaller R_m indicates higher viscosity.

The test results of the fresh concrete are given in Table 3 according to the different standard reference methods.

Table 3. Results of fresh SCC tests according to standards

Result	Mix QS	Mix RP	Mix RP + QS	Mix RP + SF	Mix QS + SF	Mix SF
Slump (mm)	665	631	684	671	709	720
Slump flow time T_{50} (sec)	4.9	4.7	4.5	4.6	4	2.8
L-Box (h_2/h_1) %	81	76	80	79	89	90
V-funnel time (mm)	12	13	12	9	10	8
J-ring diameter (cm)	64.5	61	66.1	66.3	69.9	71.2
J-ring ($h_2 - h_1$) (mm)	11	13	11	7	7	5
Superplasticizer (kg/m^3)	20	20	20	20	15	10
Superplasticizer/powder (%)	8	8	8	11.8	6	4
Air content (%)	1	1	1	1	1	1
Density (kg/m^3)	2590	2510	2590	2470	2560	2555

The properties of the freshly-prepared SCC mixes are tested including density as the specified limit by European standard.

Table 4. Results of hardened SCC tests

Result (kg/cm^2)	Mix QS	Mix RP	Mix RP + QS	Mix RP + SF	Mix QS + SF	Mix SF
28 days compressive strength	300	480	380	585	820	660
modulus of elasticity ($\times 10^5$)	2.60	3.29	2.92	3.63	4.20	3.85

2.4. Hardened SCC Experiments

Hardened concrete tests on SCC included compressive strength and modulus of elasticity.

The six different mixes have been cast in standard cubes of $150 \times 150 \times 150 \text{ mm}^3$ for the compressive strength testing at 28 days, (standard BS EN 12350-1). At ages of 7, 14 and 28 days, four cubes per mix QS+SF with a quicksand ratio as much as 5% to 20% (of the weight) are tested, and the mean values of the tests results are represented in Fig. 4.

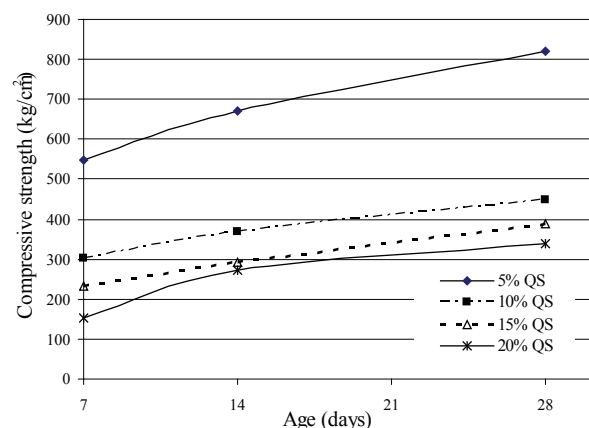


Figure 4. Compressive strength versus age (Mix QS+SF)

The data regarding the compressive strength for all the mixes is presented in Table 4 and indicates that average 28 days strengths of 820 kg/cm² obtained for 5% quicksand content (Mix QS + SF).

Based on results of hardened concrete tests, using the quicksand (as filler) instead of the rock powder, decreases the amount of SP. Additionally, there is a consistent behavior for both 7 and 28 days compressive strengths have been observed. When the amount of the quicksand content exceeds 5%, the compressive strength is decreased with the same SP dosage. Further, a condition of good dispersion of mortar with more content of the quicksand (greater than 5%) due to high SP dosage could increase the amount of weak zones, interfacial transaction zone. thereby decrease the compressive strength of mortar. More importantly, the experimental results pointed out that there exists a critical unit quicksand volume for mortar with W/C = 0.32 of the Mix QS + SF included content of SP dosage. The compressive strength of mortar would be affected when the content of quicksand exceeded this critical volume. It was due to the differences of effective thickness of paste around aggregates. The maximum compressive strength has been achieved for this critical volume (see Fig. 4).

3. Investigating the Alkali-Silica Reaction (ASR)

In this section, standard test method for evaluating the potential Alkali-Silica Reactivity of combinations of the pozzolan and the aggregates is investigated. Materials required for the Accelerated Mortar-Bar Method (AMBM) are selected based on the norm ASTM C 1260 recommendation. In all tests, to determine the effect of pozzolanic activity on the ASR, the rate of deformation of specimens from concrete components (with constant value) containing different percentages of the pozzolan to the cement was observed over a period of approximately 14 days and compared to the control specimen reviewed.

Table 5. Mortar-Bar mixing with different pozzolan replacement ratios

Specimen No.	Oven-dry aggregate (kg)	Cement (kg)	Water (kg)	(w/c)	Special Weight (kg/m ³)	Poz-zolan (%)	Air-En-trained (%)
P-1	878	350	200	0.47	2274.3	0	2.49
P-2	878	350	200	0.47	2251.9	5	0.48
P-3	878	350	200	0.47	2237.6	10	1.11
P-4	878	350	200	0.47	2224.1	20	1.71
P-5	878	350	200	0.47	2215.7	35	1.89
P-6	878	350	200	0.47	2054.8	50	1.70

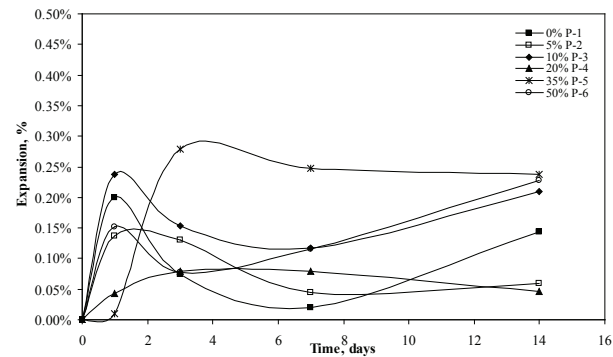


Figure 5. Specimens expansion containing Pozzolan for a period of 14 days

It should be noted that, in the AMBM test, expansion of specimens is considered to be more than 0.1% for 14 days as ASR criteria. Fig. 5 show the expansion rate of specimens against the alkali solution. Figure demonstrated that mortar with 20% pozzolan replacement (instead of cement) are activated with an alkali solution and expand less than 0.1% after almost 14 days.

4. ANN modeling stage

Experimental studies of engineering issues are time-consuming and expensive. Particularly in concrete mixing designs, the selection of suitable components may be due to an error. So using simulation methods to predict results can be very useful. One of the most commonly used simulation methods in engineering issues is artificial neural network (ANN). In this section, application of artificial neural network (ANN) to develop two models for predicting SCC mix design properties is presented. These two models are developed to predict the following attributes: 1) mechanical property (ANN1), 2) rheological property (ANN2). In this study, two proposed ANN models are initially converted into an input layer, multi-hidden layers, and an output layer. The final layers for these two models are as shown in Fig. 6. As seen in the figure, in the multi-hidden layer case, the output of each hidden layer is used as an input for the next hidden layer. In fact, in ANN1 model, the inputs are the values of concrete components and the output is an estimate of the compressive strength of different ages. In ANN2 model, inputs are the same values as components, and the output represents the parameters that illustrate the workability of fresh concrete phase.

In this research, in both ANN1 and ANN2 models, the tansig transfer function in the hidden and output layer was used. Furthermore, the feed-forward Back propagation (BP) learning algorithm is used to find a local minimum of the error functions of the training data set.

Results from two models were evaluated based on three error functions: the square of the correlation coefficient (R^2), root mean squared error (RMSE), and mean absolute error (MAE). If the calculated error of the test set was less than the previous optimal network, the current network would be saved; these steps would continue until no upgrading in the current network occurred. An average error for all training cases would then be calculated for comparison purposes. However, a lower calculated error would indicate that the network performance is better.

4.1. ANN steps

After modeling, its computational operations are carried out in two basic steps: 1) The preparation of the training

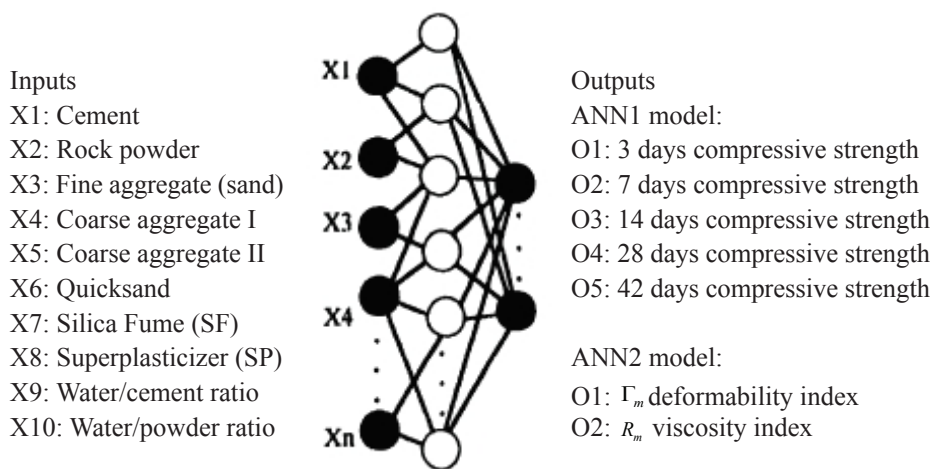


Figure 6. The basic structure of the created two ANN models

data; and 2) training/testing.

① The preparation of the training data

As shown in Fig. 6, the parameters for input (X1 to X10) and output (O1 to O5 in ANN1 model and O1 to O2 in ANN2) was introduced to the network. In order for the architecture design of the network, 70% of experimental data for training, 15% for validation and 15% for testing was chosen. Selecting the data was random using the software. In the architecture of neural networks, the number of neurons in the input layer is similar to the number of the input parameters, i.e. number 10. The number of neurons in the hidden layer neurons initially was considered 10 and then the optimum number of the neurons was determined. Also, the number of the output layer neurons depends on the number of the output parameters of each model. According to the Fig. 6, the output data of ANN1 and ANN2 models was 6 and 2, respectively.

The training process was set for 100 epochs (or in order to modify the values of the weight are 100 times the all data entered) and the best case was obtained nearly in 20 times. This process is repeated until the error reaches the priority level. Recent step is very time-consuming and reduces the efficiency of the ANN method. A common way

to select the appropriate number of neurons in each hidden layer is to perform a parametric analysis of the network and check the accuracy of the results. In each iteration step using Eq. (5) between the input data will be summed together with their weight values and with the bias,

$$\Delta W(t) = -\eta(\text{error}) + \alpha \Delta W(t-1) \quad (5)$$

where η , α are training rate and momentum factor, respectively.

The parameters η , α both are in the range 0 to 1. The weight and bias values will be initially selected as random numbers and then adjusted according to the obtained results of the training process. This method causes the model to become agile and decreases during the execution of the operation.

② The training/testing

The validity of the proposed ANN models is then tested by applying training/testing on the results of the experimental data. So that, 30% of the experimental data results were initially set aside for simulation purposes at this step. It should be noted that, these data are not used for training step, and if they can accurately predict the results, then

it can be said that the network is

reliable and usable.

5. Results and Discussion

To determine the optimum number of neurons in the hidden layer, with neural network architecture is mentioned only by the number of different neurons from 1 to 30 was created by neurons and minimum RMSE, MAE and R^2 of each of the two obtained the network that the results shown in Table 6. Results shown that, the maximum errors for 45 test results are about less than 20%, on the other hand, it can be seen that 98% of the output results has errors less than 15%.

Table 6. Performance results for the two ANN models

Model	Network Architecture	Maximum error (%)	R^2	RMSE	MAE
ANN1	Backpropagation	14.5	0.925	3.972	3.521
ANN2	Backpropagation	15.3	0.928	3.859	3.126

According to Table 6, the minimum error and the maximum correlation coefficient in 11 neurons was happened. The value of the squared error has decreased for 1 to 11 neurons and then increased. Also, the value of the correlation coefficient has increased slowly with increasing the

number of the neurons. Meanwhile, with the increase in the number of neurons to more than 11, the value of the squared error has increased sharply and the value of the correlation coefficient with large slope is reduced. This means that, increasing the number of neurons is not always improves network performance, but also the number of neurons is dependent on the number of all input data of a neural network. In this research the number of all input data is 45 and the number of the appropriate neurons in the hidden layer is 11. Therefore, the number of neurons in the hidden layer must be approximately 1/4 to 1/5 of the number of all input data.

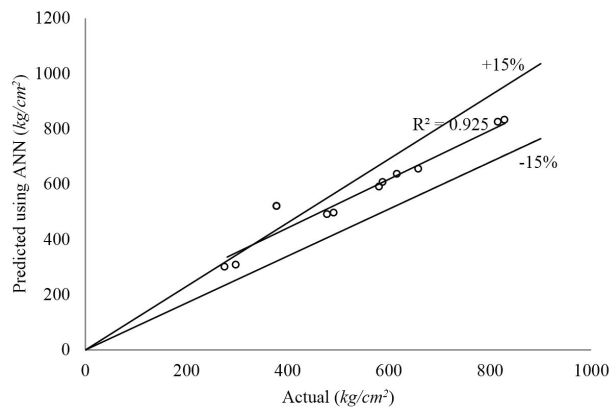


Figure 7. Actual v/s predicted results of the 28-day compressive strength(kg/cm²) using ANN1

Fig. 7 shows a plot of actual compressive strength against corresponding ANN1 model predication for testing data. A linear correlation can be observed and the square of the correlation coefficient is found to be 0.925. Thus it can be concluded that the model successfully predicted the compressive strength of concrete in good manner.

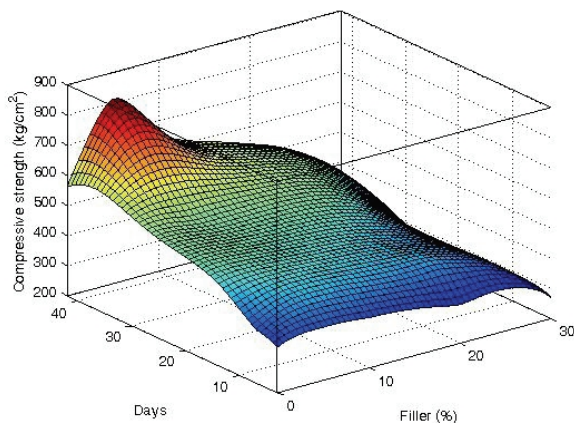


Figure 8. Predicted results of the comprehensive strength (kg/cm²) using ANN1

Fig. 8 shown that, the results suggest that ANN, can effectively be used to predict the compressive strengths of the SCC included different percent of the filler content.

There is a wide variation of two parameters i.e. the concrete age (days) and the percent of quicksand content (filler %) which can be used.

The second model (ANN2) involved choosing the ideal model for the rheological property of the SCC, again by minimizing the weighed errors produced for model and by also evaluating the ability of the network to produce results for deformability and viscosity indices. The results for the optimum model for ANN2 are shown in Fig.9. The results are suggested the prediction of the rheological property based on characterizing method for the mortar properties were proposed using the Γ_m and R_m indices. Hence the square of the correlation coefficient was found to be 0.928.

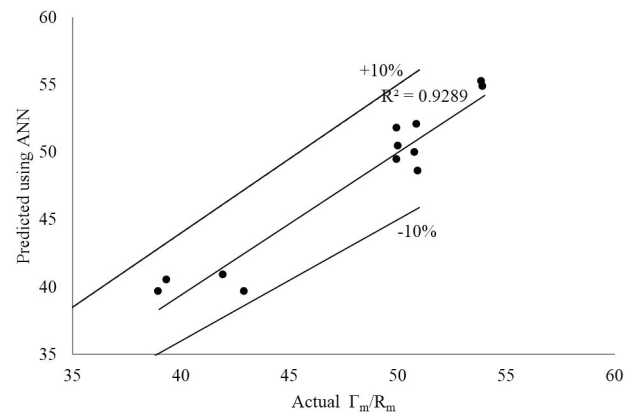


Figure 9. Actual v/s predicted results of the deformability and viscosity indices using ANN2

As shown in Fig. 10, separate training and testing was conducted for rheological property model (ANN2 model) which predicted the deformability and viscosity for different percentage of the filler content.

It is anticipated that the results for both networks could only improve with the addition of further experimental data for training and testing the networks.

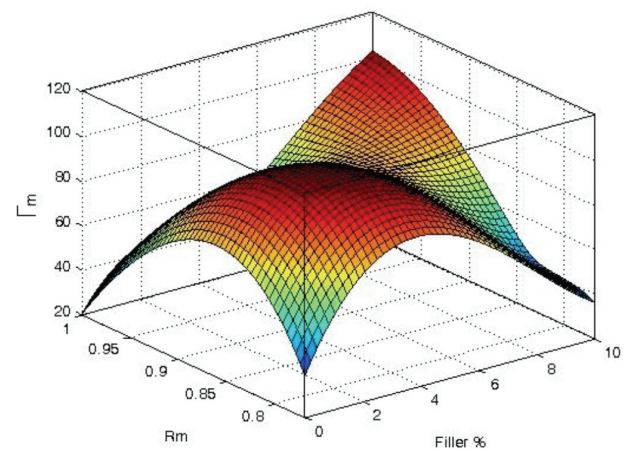


Figure 10. Predicted results of the deformability and viscosity using ANN2

6. Conclusions

The process of choosing a suitable silica quicksand content material to make SCC is considered with the aim of determining the relative amounts of concrete produced economically as possible and with the maximum of required properties, particularly compressive strength, compactability and flowability. Based on these considerations, increasing the amount of quicksand (as filler) instead of rock powder samples of SP is reduced.

Characteristics of fresh SCC tests show that, high compactability and restrained flowability is usually depends on the shape, size and quantity of the aggregate, and the friction between the solid particles, which would be reduced by adding the amount of quicksand to the mortar. It was due to the quicksand act as a roller between the aggregates. Further, the segregation phenomena is usually related to the cohesiveness of the paste of the fresh concrete, which can be improved by some combination of increasing the volume of paste, reducing the free water content and the coarse aggregate, which would be achieved by adding the quicksand content to the SCC mixture.

Further, adding silica quicksand as much as 5% (of the weight of the cement) in the concrete, the concrete strength will be seen, as 28-day compressive strength increased by 40% compared to the control sample (using both rock powder and silica fume materials). Slump flow, V-funnel, L-flow, J-ring tests were carried out to examine the performance of fresh concrete, and the results indicate that using the quicksand in the mixture could produce successfully SCC of high flowability, without segregating and saves cost. Mortar with 20% pozzolan (instead of cement) are activated with an alkali solution and expand less than 0.1% after almost 14 days.

Two ANN models for both mechanical and rheology properties of SCC containing silica quicksand (as filler) have been developed. The optimal network is a three-layer network with 11 neurons in the hidden layer. The use of the Levenberg-Marquardt training function and the tansig transfer function in the hidden and output layers and the number of neurons between 1/5 to 1/8 of the input data will have the suitable results for predicting the properties of the self-compacting concrete. Results of each model were trained with input and output experimental data. Statistical values such as the square of the correlation coefficient, RMSE and MAE that are calculated for comparing experimental data with two ANN models. Consequently, compressive strength and flowability properties of SCC can be predicted in the two models without attempting any experimental program.

References

- [1] Okamura, H. (1997), Self-compacting High-Performance Concrete, *Concrete International*, 19(7), 50- 54.
- [2] Nagamoto, N. and Ozawa, K. (1997), "Mixture properties of self- compacting, high-performance concrete", *Proceedings of Third CANMET/ACI International Conferences on Design and Materials and Recent advances in Concrete Technology*, SP-172, V. M. Malhotra, American Concrete Institute, Farmington Hills, Mich., 623-637.
- [3] Okamura, H. and Ouchi, M. (1999), "Self-Compacting Concrete—development, present, and future", *Proceedings of 1st International RILEM Symposium on Self-Compacting Concrete*, Stockholm, Sweden.
- [4] Okamura, H. and Ouchi, M. (2003), "Self-compacting concrete", *J. Adv. Concre. Technol.*, 1(1), 5-15.
- [5] Brouwers, H.J.H. and Radix, H.J. (2005), "Self-compacting concrete: theoretical and experimental study", *Cem. Concre. Res.*, 35 (1), 2116 – 2136.
- [6] Andreasen, A.H.M. and Andersen J. (1930), "Ueber die beziehungzwischenkornabstufung und zwischenraum in produktenauslosenkonkretm (miteinigen Experimenten)", *Kolloid-Zeitschrift*, 50 (1), 217– 228 (in German).
- [7] Aggarwal, P., Siddique, R., Aggarwal, Y., Gupta, S. and Gupta, M. (2008), "Self-compacting concrete - procedure for mix design", *Leonardo El. J. Pract. Technol.*, 7(12), 15-24.
- [8] Su, N., Hsu, K.C. and Chai, H.W. (2001), "A simple mix design method for self- compacting concrete", *Cem. Concre. Res.*, 31(12), 1799–1807.
- [9] Su, N. and Miao, B. (2003), "A new method for mix design of medium strength concrete with low cement content", *Cem. Concre. Comp.*, 25(1), 215– 222.
- [10] MD Nor, A. and Hanizam, A. (2011), "The compressive and flexural strengths of self-compacting concrete using raw rice husk ash", *J. Eng. Sci. Technol.*, 6(6), 720-732.
- [11] Rocco, C.G. and Elices, M. (2009), "Effect of aggregate shape on the mechanical properties of a simple concrete", *Eng. Fract. Mech.*, 76(2), 286-298.
- [12] Gupta, S., (2013), "Using artificial neural network to predict the compressive strength of concrete containing nano-silica", *Civil Eng. Archit.*, 1(3), 96-102.
- [13] Saridemir M., Ozcan F., Severcan M.H., and Topçu I. B. (2009). "Prediction of long-term effects of GGBFS on compressive strength of concrete by artificial neural networks and fuzzy logic". *Constr. Build. Mater.*, 23(3), 1279-1286.
- [14] Alshihri, M.M., Azmy, A.M., and El-Bisy, M.S. (2009), "Neural networks for predicting compressive strength of structural light weight concrete", *Constr. Build. Mater.*, 23 (6), 2214-2219.
- [15] Demir, A. (2015), "Prediction of Hybrid fibre-added concrete strength using artificial neural networks". *Engineering, Comput. Concrete*, 15 (4), 503-514.
- [16] Atici, U. (2011), "Prediction of the strength of mineral admixture concrete using multivariable regression analysis and an artificial neural network", *Expert. Sys. Appl.*, 38 (8), 9609-9618.
- [17] Khan, M., Noor, M. and Fazal, R. (2015), "Modeling shotcrete mix design using artificial neural network", *Comput. Concrete*, 15 (2), 167-181.
- [18] Chauvin, Y. and Rumelhart, D.E., (1995), "Backpropagation: Theory, Architectures, and Applications. Lawrence Erlbaum Assoc., Inc., Publ., Hillsdale, N.J.
- [19] The European Guidelines for Self-Compacting Concrete Specification, Production and Use. (2005).

ARTICLE

Impact of glazing type and orientation on the optimum dimension of windows for office room in hot climate

**Chahrazed Mebarki^{1*} Essaid Djakab¹ Sidi Mouhamed Karim El Hassar¹
Mohamed El-Amine Slimani²**

¹ Laboratory built in the environment, University of science and technology Houari Boumediene, 16111 Bab Ezzouar, Algiers, Algeria

² Department of Energetic and Fluid Mechanics, Faculty of Physics, University of Science and Technology Houari Boumediene (USTHB), 16111 Algiers, Algeria

ARTICLE INFO

Article history:

Received: 5 November 2018

Accepted: 26 November 2018

Published: 21 December 2018

Keywords:

Energy consumption

Window size

Optimization

Daylight

Hot climate

Cooling loads

ABSTRACT

This study aims to analyse the impact of orientation and glazing type on optimum glazing size in hot climate using genetic algorithms. In winter the optimization of glazing size is obtained considering the thermal gains from solar radiation. Heating demands of the building are reduced by taking into account the free heat gains from the sun. In summer the optimization of glazing size is complex. In this case, the glazing is considered as a heat gains element. Indeed, for a hot climate, daylighting can be used as a passive strategy to reduce energy consumption. Thus an optimal window size allows avoiding problems of glare and overheating. ASHRAE proposed a Window to Wall Ratio (WWR) which is considered as the optimal glazing size that ensures minimum annual thermal loads. This coefficient neglect different parameters such as (Glazing type, the orientation and daytime). A typical office room located in Ghardaia (South of Algeria) is selected as a case study. The results show that daylight is a key factor in limiting the glazing size in hot climate. ; this study shows that the optimal window size varies with daytime. Hence, the WWR cannot be considered as optimal for the whole year.

**Corresponding Author:*

Laboratory built in the environment,

University of science and technology Houari Boumediene,

16111 Bab Ezzouar, Algiers, Algeria;

Email: cmebarki@usthb.dz

1. Introduction

Energy consumption of buildings has a negative impact on the environment. They are responsible for approximately 40% of the total world annual energy consumption. Most of this energy is for the provision of lighting, heating, cooling, and air conditioning. Increasing awareness of the environmental impact of CO₂ and NO_x emissions and chlorofluorocarbons triggered a renewed interest in environmentally friendly cooling and heating technologies [1]. Windows are generally the weakest link of buildings regarding energy conservation. Approximately one-third of the energy loss from a typical house occurs from windows [2].

In many countries, codes are regulating minimum window size to provide problems of glare and overheating. The window size is generally defined as a WWR which is related to an annual thermal loads calculation. However, this coefficient neglects several parameters that have a direct influence on thermal loads such as the orientation. Alan Pino and al [3] analyzed the thermal and luminous behavior of an office building in Santiago, for different design conditions through a year, by changing four architectural parameters that are the window to wall ratio (WWR), the outdoor solar protection devices, the type of glazing and the orientation. In winter, the window is a thermal losses element and also a source of thermal gains due to solar radiation. Taking into account this thermal gains reduce heating loads; in this case the window has an optimal size. In summer, the window is only as a thermal gains element, this means that the optimal window size is 0m². Consequently, the WWR cannot be considered as optimal for the whole year. This makes the optimization of the window size much complex for cooling-dominated climates.

The window as a thermal loads element is also a source of daylight, according to Scartzzini and al [4] daylighting strategies can contribute to curb the energy consumption of buildings, as well as the related carbon emissions, by reducing their artificial lighting and cooling needs.

In this study, the effect of using different types of glazing taking into account the daylight on optimized window dimensions of an office room (for 4 different orientations: North; South; East; West) is investigated. The Algerian standards (DTR) [5] and the Hourly Analysis Program (HAP software) are used to calculate the required hourly cooling loads (for 15th of July as an example study) for different types of glazing. Genetic Algorithm is used to determine the optimal size of the windows. The results of the hourly optimization are analyzed to evaluate the impact of a proper window optimal glazing area in a typical office room in Ghardaia city (south of Algeria) and to minimize

the energy impact of windows.

2. Description of the Referenced Room

An office of an arbitrary surface area of 25.9 m², located in Ghardaia region in south of Algeria (32.49° N latitude; 3.67°E longitude), is selected for this case study. It should be pointed out that Ghardaia is located in a hot climate with specific solar radiation (Fig.1 and Fig.2).

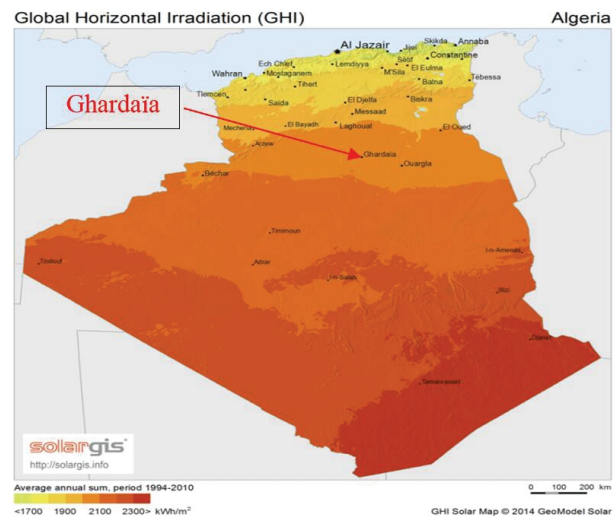


Fig 1. Solar radiation map for Algeria

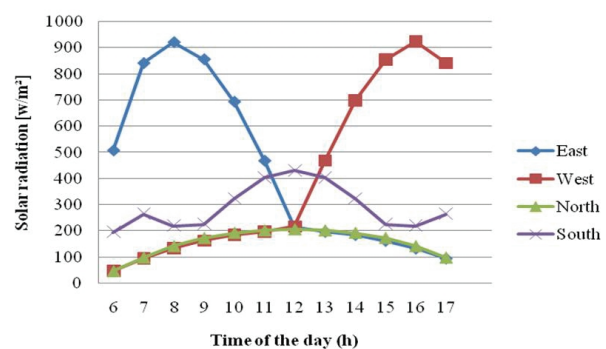


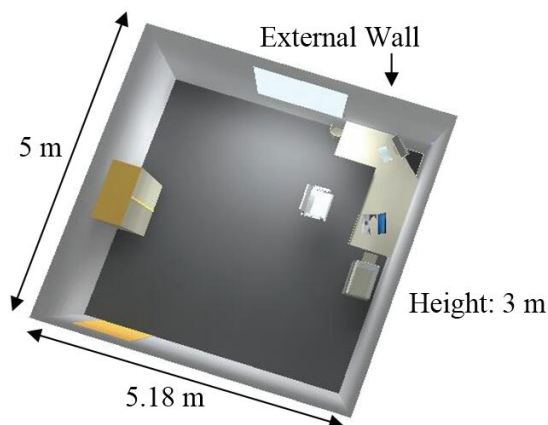
Fig 2. Solar radiation for Ghardaia region (ASHRAE method)

Figure 3 shows the schematic design of the office room. The dimension of the studied office room is 5.18 m long, 5 m wide and a height of 3 m. This model has one window placed on the external wall. Furthermore, all other opaque surfaces of the reference office room are considered as adiabatic (no heat exchanges) except the external wall. The usual external wall typology in Algeria has double wall (2 cm mortar, 15 cm brick wall, 5 cm air gap, 10 cm brick wall, 2 cm gypsum) with transmittance of 1.14 [W/m².°C]. Four orientations South, East, North and West are considered for load calculations. The optical properties of glazing are shown in Table 1. The same products have been studied by reference [6] where SF is the Solar Factor

Table 1. Glazing type characteristics

	Glazing type	SF [%]	U [W/m ² .C°]	τ [%]	Thickness [mm]
Type 1	Simple glazing	0.83	5.8	0.87	4
Type 2	Double glazing classic	0.75	3.3	0.81	4(6)4
Type 3	Double solar control glazing Air	0.47	2.8	0.41	6 (12) 6
Type 4	Double solar control glazing Air	0.12	2.3	0.07	6 (12) 6
Type 5	Double glazing (Reinforced Thermal Insulation) and solar control Air	0.08	1.4	0.07	6 (16) 6
Type 6	Double glazing (Reinforced Thermal Insulation) and solar control Argon 85 %	0.37	1.2	0.40	6 (16) 6
Type 7	Double glazing (Reinforced Thermal Insulation) and solar control Argon 85 %	0.08	1.2	0.07	6 (16) 6
Type 8	Double glazing (Reinforced Thermal Insulation) and solar control Argon 85 %	0.17	1.1	0.18	6 (16) 6
Type 9	Double glazing (Reinforced Thermal Insulation) and solar control Argon 85 %	0.08	1.1	0.07	6 (16) 6

[%], U is the thermal transmittance [W/m².C°] and τ is the luminous transmittance of the glazing [%]. Furthermore, these types of glazing are as commonly used in the Algerian building construction industry.


Fig 3. Schematic design of the office room

In this study, the cooling setpoint is considered equal to 26°C. Only cooling load of the glazing, the luminaires, and the external wall are considered. For a standard office room, the internal illuminance level is equal to 500 lux. For uniform control of the illuminance Spot luminaires has been chosen with unitary luminous flux of 1300 lm and electrical power of 11.6 w.

3. Methodology for Cooling Loads Optimization

For the total thermal loads calculation, the method given by the Algerian Standards DTR [5] is used. However, the mathematical models for thermal loads calculation used in the Algerian Standards are simplified. For accuracy purposes the Carriers' method implemented by the Hourly Analysis Program (HAP) is used to recalculate the total thermal loads considering the optimal parameters obtained

by the Genetic Algorithm. As the cooling loads are calculated on hourly basis, the ASHRAE [7] method is used to calculate solar irradiation intensity taking into account day-time for Ghardaia region. The objective function (Qt) to optimize is the total cooling loads due to glazing (Q_{glazing}), the external wall ($Q_{\text{external walls}}$) and the artificial lighting installation ($Q_{\text{luminaires}}$) that is:

$$Q_t = Q_{\text{luminaire}} + Q_{\text{glazing}} + Q_{\text{external walls}} \quad (1)$$

While satisfying an equality constraint which is expressed as follow:

$$E_{\text{luminaires}} + E_{\text{natural}} = 500 \text{ lux}, \quad (2)$$

$E_{\text{luminaires}}$ is the illumination level ensured by the electric lighting installation, E_{natural} is the natural illumination level ensured by the daylight. The internal illuminance level (E_i) calculation in the office room was carried out using the daylight factor DF Eq.3 The daylight factor method has been adopted by the C.I.E. (International Commission on Illumination) and is therefore internationally used [8]. In the formula for Daylight Factor calculation, the Orientation Factor (OF) is fixed (average value over a year) [9]. However, in the present work the Orientation Factor was not taken as fixed. Indeed its value varies with daytime and orientation and introduced in Eq.3 to consider the case of clear sky.

$$DF = [(Ag \times \tau \times M \times OF) / At \times (1 - R^2)] \times (E_i / E_e) \times 100 \quad (3)$$

Where Ag is the glazing area of the window; τ is the luminous transmittance of glazing; M is the maintenance correction factor $M=90\%$ (clean space); q is Vertical angle of visible sky from the center of the window $q=90^\circ$ (no obstacles); OF is orientation factor for glazing; At is the total area of room-surfaces; R^2 average reflectance of all room-surfaces $R^2=0.5$ (clear internal surfaces); E_i is the required illuminance (500lux recommended by the standards for office room) and E_e is the outside illuminance on horizontal surface given by the method of reference [10].

The solution methodology is illustrated by the flow-chart as depicted by Figure 3:

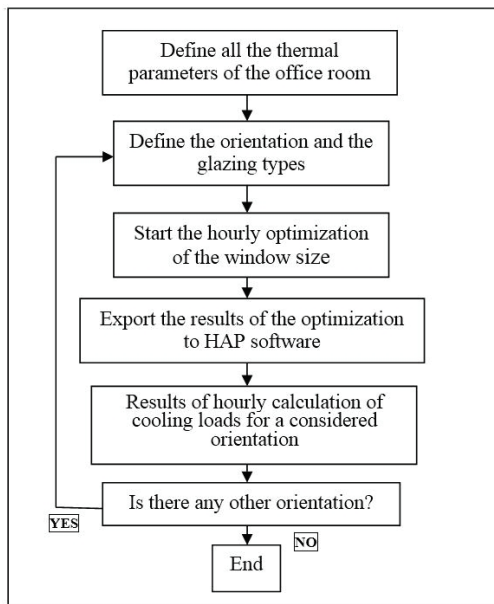


Fig 4. Structure of the proposed methodology

For the Genetic Algorithm optimization, the initial population ranges from 0 to 12 m². The number of generation is 100. The population is taken 50 individuals. The crossover and mutation fractions are respectively 80% and 10%.

4. Results

The cooling loads optimization for different type of glazing and orientations are depicted in Fig. 5, 6, 7, 8, 9, 10, 11 and 12:

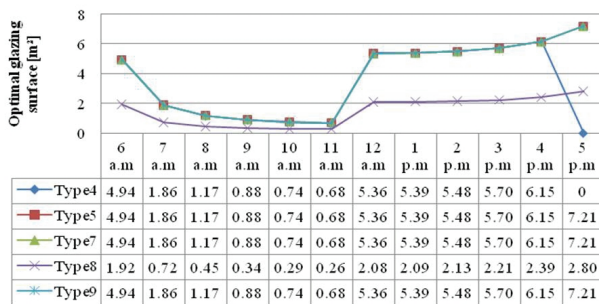
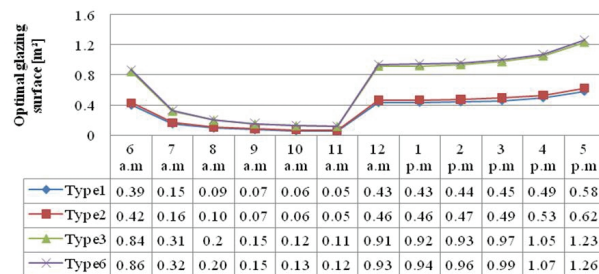


Fig 5. Variation of the optimal glazing surface for each type of glazing according to the time (East orientation)

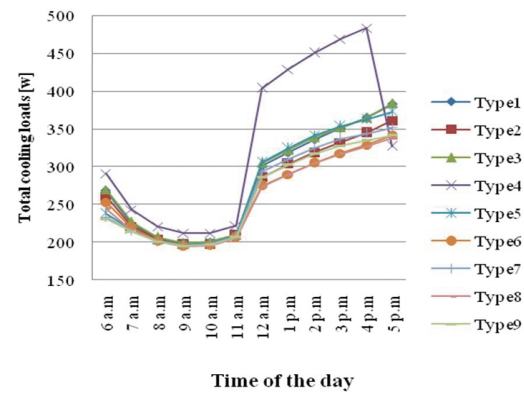


Fig 6. Variation of the total cooling load for different type of glazing (East orientation)

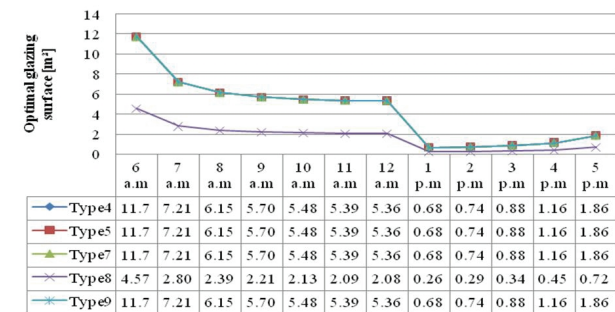
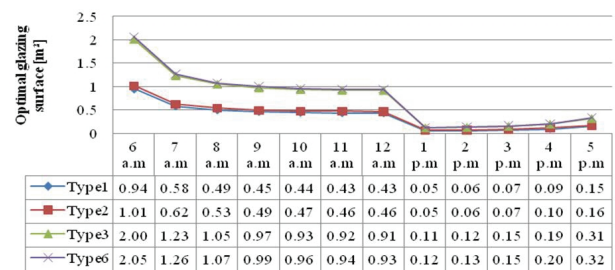


Fig 7. Variation of the optimal glazing surface for each type of glazing according to the time (West orientation)

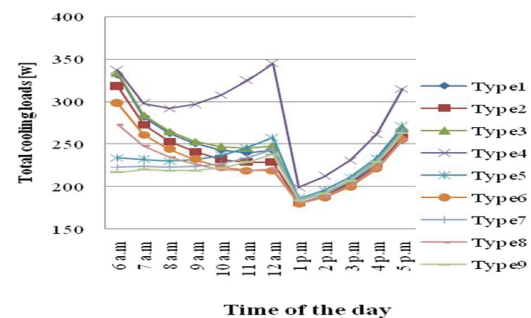


Fig 8. Variation of the total cooling load for each type of glazing (West orientation)

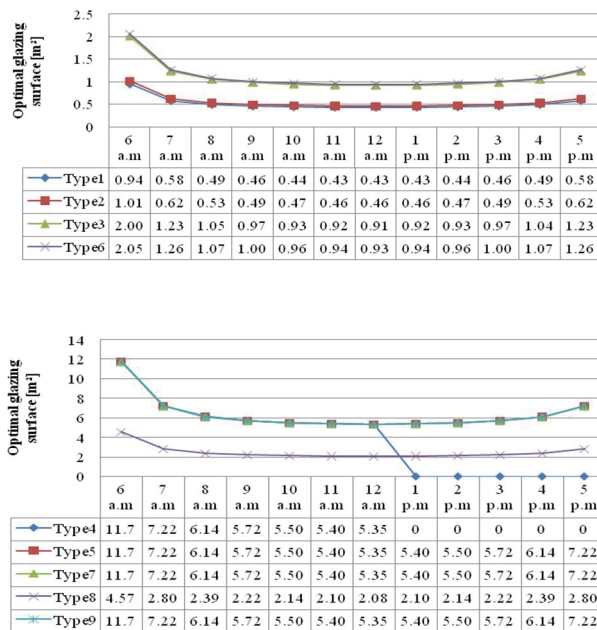


Fig 9. variation of the optimal glazing surface for each type of glazing according to the time (North orientation)

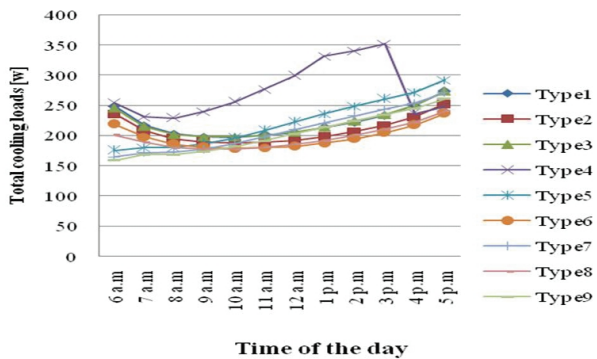


Fig 10. Variation of the total cooling load for each type of glazing (for North orientation)

5. Discussion

From previous work, it has been found that the optimal glazing surface calculation was related only to orientation, glazing types. However, in this study orientation, glazing types, daytime and clear sky have been considered. From the obtained results it can be said that:

For East Orientation, the optimal glazing size decreases for all glazing types (6 a.m to 11 a.m). This is due to the high solar radiation intensity. From 12 a.m to 5 p.m, the optimal glazing size increases (the external wall is in shade). The glazing types 1, 2, 3 and 6 give the minimum of optimal glazing area than glazing types 4, 5, 7, 8 and 9. The glazing type 4 gives a maximum of total cooling loads

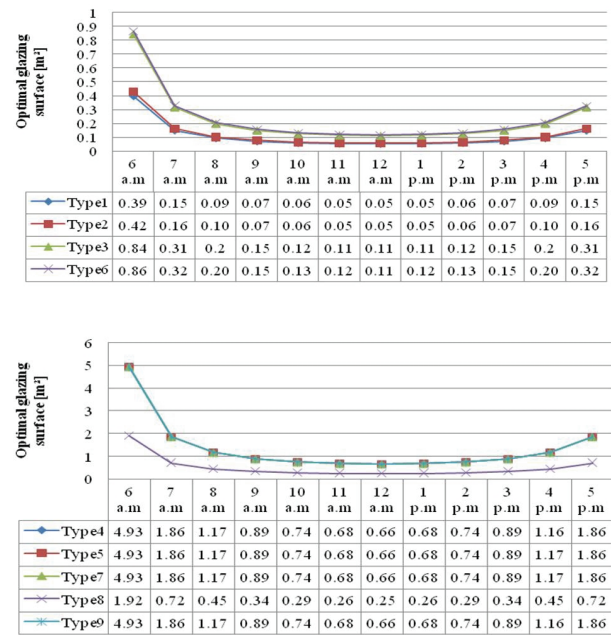


Fig 11. Variation of the optimal glazing surface for each type of glazing according to the time (South orientation)

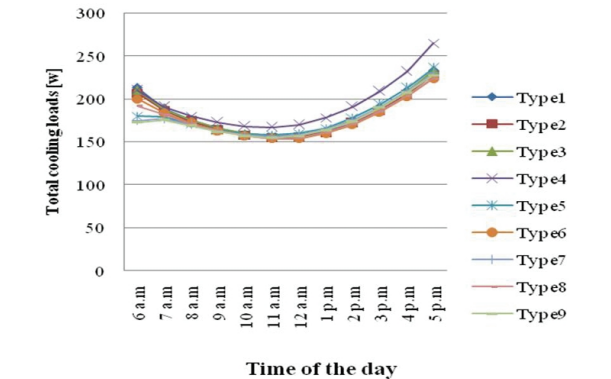


Fig 12. Variation of the total cooling load for each type of glazing (South orientation)

compared to all the other glazing types, which means that this glazing type is not adequate for this orientation. At 5 p.m the optimal glazing size for glazing type 4 is equal to 0 m² (in relation to a minimum cooling load). This can be justified by the fact that the heat transmission from the glazing is higher than daylighting transmission, because the glazing has a high thermal transmittance and a low luminous transmittance.

For West Orientation the optimal glazing size increases for all glazing types (6 a.m to 12 a.m) at this time the glazed area is in shade. From 1 p.m to 5 p.m, the optimal glazed size decreases, this is due to the high solar radiation intensity. The glazing types 1, 2, 3 and 6 give a mini-

mum of optimal glazing area than glazing types 4, 5, 7, 8 and 9.

The glazing type 4 gives a maximum of total cooling loads compared to all the other glazing types, which means that this glazing type is not adequate for this orientation.

For North orientation, the optimal glazing surface is the largest compared to all the other orientations. For this orientation the glazing area is in shade all the daytime. The glazing types 1, 2, 3 and 6 give a minimum of optimal glazing area than glazing types 4, 5, 7, 8 and 9. From 1 p.m to 5 p.m, the optimal glazing size for glazing type 4 is equal to 0 m², this can be justified by the fact that The heat transmission from the glazing is higher then daylighting transmission, because the glazing has a high thermal transmittance and a low luminous transmittance.

The glazing type 4 gives a maximum of total cooling loads compared to all the other glazing types, which means that this glazing type is not adequate for this orientation.

For South orientation, the optimal glazing size is the lowest compared to those obtained considering the other orientations. In this case the glazing is permanently exposed to the sun. The glazing types 1, 2, 3 and 6 give a minimum of optimal glazing area than glazing types 4, 5, 7, 8 and 9.

The glazing type 4 gives a maximum of total cooling loads compared to all the other glazing types, which means that this glazing type is not adequate for this orientation.

It is shown from the above analysis that the optimal glazing size depends on daytime, solar radiation intensity, orientation and glazing types.

The optimal glazing size increases when the luminous transmittance of the glazing decreases while giving a minimum of cooling loads.

Finally, it can be said that for hot climate, glazing with high thermal and luminous performances should be used in the construction industry.

6. Conclusion

This study evaluates the influence of daylight on optimized glazing size in an office room in hot climate. Un-

like the Wall to Window Ratio (WWR) method for glazing surface calculation, this study shows that the optimal window size depends on daytime, orientation, the glazing type and solar radiation intensity. In fact, the glazing type and room orientation have a large effect on cooling load when optimum dimension of glazing is considered under a clear sky. The results show also that daylight is a key factor in limiting the glazing size while having a minimum of cooling loads. Indeed, the choice of an adequate glazing type allows reducing cooling loads and increasing the window size. This result indicates that there is a significant effect of daylight on optimizing window size to reduce the energy consumption of an office room located in a hot climate.

Reference

- [1] Abdeen Mustafa Omer. Energy use and environmental impacts: A general review; *Journal of Renewable and Sustainable Energy* 1, 053101 (2009); <https://doi.org/10.1063/1.3220701>.
- [2] Hasan Karabay, Muslum Arıcı, Multiple pane window applications in various climatic regions of Turkey; *Energy and Buildings* 2012 (45): 67–71
- [3] Alan, P, Waldo, B, Rodrigo, E, Felipe, E, P. Thermal and lighting behavior of office buildings in Santiago Belgium. Elsevier. *Energy and Buildings* (2011) 47: 441–449.
- [4] Scartezzini, J.-L, Paule, B, Chuard, D, Simos, S (Eds.). *Principles of Lighting, RAVEL Swiss Action Programme for Rational Use of Energy, EDMZ, Bern, Switzerland* 1993 (81): 1166–1179..
- [5] Document Technique Réglementaire, Réglementation thermique des bâtiments d'habitation, CNERIB, Algérie, 1997
- [6] MEMENTO Saint Gobain Glass, 2007.
- [7] 2001 ASHRAE Fundamentals Handbook, chapter 30.
- [8] International Commission on Illumination, Daylight: International Recommendations for the Calculation of Natural Daylight No. 1970, Publication Cfi no.16 (E-3.2)).
- [9] Littlefair P. J. Predicting Annual Lighting use in Daylit Buildings. *Building and Environment* 1990; 25(1):43-54.
- [10] Sokol, D, Ardesir, M. A simple model for the derivation of illuminance values from global solar radiation data. Springer. *BUILD SIMUL.* 2013; 6: 379–383.

ARTICLE

Feature Identification for Non-Intrusively Extracting Occupant Energy-Use Information in Office Buildings

Hamed Nabizadeh Rafsanjani*

School of Environmental, Civil, Agricultural and Mechanical Engineering, University of Georgia, Athens, GA 30602, USA

ARTICLE INFO

Article history:

Received: 25 October 2018

Accepted: 8 November 2018

Published: 30 November 2018

Keywords:

Occupant energy consumption

Occupant energy-use features

Feature extraction

Non-intrusive load monitoring

Office buildings

ABSTRACT

Detailed energy-use information of office buildings' occupants is necessary to implement proper simulation/intervention techniques. However, acquiring accurate occupant-specific energy consumption in office buildings at low cost is currently a challenging task since existing intrusive load monitoring (ILM) technologies require a large capital investment to provide high-resolution electricity usage data for individual occupants. On the other hand, non-intrusive load monitoring (NILM) approaches have been proven as more cost effective and flexible approaches to provide energy-use information of individual appliances. Therefore, extending the concept of NILM to individual occupants would be beneficial. This paper proposes two occupancy-related energy-consuming features, delay interval and magnitude of power changes and evaluates their significances for extracting occupant-specific power changes in a non-intrusive manner. The proposed features were examined through implementing a logistic regression model as a predictor on aggregate energy load data collected from an office building. Hypotheses tests also confirmed that both features are statistically significant to non-intrusively derive individual occupants' energy-use information. As the main contribution of this study, these features could be utilized in developing sophisticated NILM-based approaches to monitor individual occupant energy-consuming behavior.

1. Introduction

Growing interest in reducing energy consumption in office buildings attract attentions from research and industry toward intervening occupants to keep energy-saving behaviors since this method has recently been considered as the most cost-effective approach for enhancing office buildings' energy conservation.^[1-7]

up to 24 percent energy savings can be achieved through intervening occupants' behaviors in an office building.^[8,9] For achieving this goal, personalized feedback approaches have been mainly considered as the most effective intervention technique to adapt energy-efficient behaviors.^[10,11] Effectively implementing of such approaches critically depends to the availability of occupant-specific energy-use

**Corresponding Author:*

Hamed Nabizadeh Rafsanjani

School of Environmental, Civil, Agricultural and Mechanical Engineering,

University of Georgia, Athens, GA 30602, USA;

E-mail: hr@uga.edu.

information. Such information is also extremely important in advancement of occupancy-related simulation techniques.^[12]

To acquire the energy-use information of an occupant of interest, conventional methods typically utilize intrusive load monitoring (ILM) approaches which require plug load sensors installed for the appliances controlled over by the occupant. These sensors then provide the energy-consuming information of the appliances and accordingly estimate the occupant's energy consumption. ILM methods generally provide data with high level of resolution and accuracy, however they are not economically feasible due to high capital investments and configuration efforts especially for a large scale deployment.^[13] By installing a sensor per occupant's workstation, Gulbinas and Taylor^[14] collected the data of individual occupants at a multi-story office building occupied by 115 employees; the data was used to examine the impact of organizational network energy-use feedbacks on intervening behaviors. Such studies highlight the high cost and installation complexity associated with implementing of ILM methods in an office setting. Therefore, utilizing alternative cost-effective methods for data acquisitions is necessary.

Increased interest in economically detailed energy sensing led to the emergence of non-intrusive load monitoring (NILM) which has been widely employed for more than two decades as an appropriate viable solution to perform energy monitoring of major appliances (e.g., HVAC systems) in residential and office settings.^[13,15-17] NILM is a technique which relies on the aggregate electrical energy-use information provided by a building's meter to disaggregate energy information at the appliance level and identify which appliance and when uses how much electricity.^[16] Accordingly, compared to the ILM, NILM is perceived as less expensive and more feasible approach to monitor appliance-specific energy consumption in office buildings.^[15,17,18]

Although current research has made a great advancement in economically tracking the energy use of individual appliances through NILM techniques, there is still a need for tools to economically monitor individual occupants' energy consumption in office buildings.^[2,9,19] As a springboard for developing a solution to address this need, extending the NILM concept from individual appliances to individual occupants could be investigated. Currently, the growing advancement in building' energy and occupancy sensors which deliver data with high granularities, provides the possibility of distinguishing the energy information of a single occupant from a group of people.^[2,9,12,14] Given this, a NILM-based approach might help in extracting this information.^[20-23] Recently,

there has been an especial emphasis in extending NILM concept to the occupancy sensing area. Through utilizing aggregate data provided by electricity meters in residential buildings, Chen et al.^[24] and Kleiminger et al.^[25,26] demonstrated that a meter can be used as an occupancy sensor in houses; such occupancy information of houses has typically been exploited for promoting smart grids. Within the office settings, Ardakanian et al.^[27] revealed how non-intrusive techniques could be utilized for real-time occupancy estimation; this information can make a great help in building system automation and demand-driven HVAC operation. Overall, such abilities in sensing occupancy information based on the NILM concept particularly indicate the possibility of extending this concept into occupancy energy consumption area.

In order to extend a NILM-based technique for monitoring occupant energy consumption, at the first step, the general structure of NILM approaches should be studied. In general, a NILM approach includes two main steps:^[13,15,16] (1) selecting and characterizing appliance-specific features; (2) developing an algorithm to detect the features of different appliances in aggregate load data in order to identify how much electricity consumed by each appliance and when. In particular, each appliance has specific electrical/non-electrical features which should be precisely identified;^[13,15,16,28-30] the success of a NILM approach critically depends on the features identification. The electrical features are generally defined as a set of parameters which can be measured from aggregate load data.^[31] Real power^[17,32-35] reactive power,^[36-40] harmonic signals^[41,42] power factor,^[43] shape features of voltage-current trajectory,^[44,45] voltage noise,^[46,47] and transient power^[48-52] are the electrical features mainly utilized by conventional NILM approaches. Non-electrical features of appliances such as usage duration and time of the day also contributes to more accurate load disaggregation performance.^[53,54] For example, a printer in an office space is not used from 6:00PM to 7:00AM and this non-electrical feature could tell that any information derived by an NILM algorithm regarding printer usage during this time could be incorrect.

With the significance of features in mind and seeking to develop a NILM-based solution for monitoring occupant-specific energy consumption, identifying electrical/non-electrical features related to energy-consuming behaviors of occupants is necessary. Therefore, this paper identifies and examines occupancy-related energy-consuming features which could be utilized in developing NILM-based disaggregation approaches for estimating occupant-specific electrical energy consumption in office buildings, which is still an extremely challenging issue in

these buildings^[9]. The paper is structured as follows: Section 2 introduces the features. The research methodology, experiment and hypotheses are presented in Section 3. Section 4 provides the results and discussion. In section 5, the limitations of this study are presented. Finally, conclusions are provided in Section 6.

2. Occupancy-Related Energy-Use Features

In general, to understand energy-use behaviors of occupants, literature has typically studied their energy-use intensity, energy-use efficiency, and energy-use entropy patterns^[8,12,20,55]. In particular, the energy-use intensity patterns account for the amount of energy that occupants consume during working hours. Due to this fact that a NILM approach estimates how much energy is consumed by an appliance, the energy-use intensity patterns could be utilized as the occupancy-related energy-use features in developing a NILM-based approach for monitoring occupant energy consumption. To this end, finding such the patterns of individual occupants is favorable. In^[19,56], by collecting data through an ILM method, it was statistically confirmed that major energy-use actions (turn on/off appliances) of individual occupants are predominantly occurred right after entering to a building (entry event) and right before leaving a building (departure event). Therefore, it is of interest to extract energy-consuming information of individual occupants at these events. Through^[19,56], it was also revealed that each occupant has a recurring pattern for the power changes at the entry and departure events since she typically use a same set of personal appliances repeatedly across different days. With these findings in mind and seeking to find occupants' energy-consuming features, the recurring patterns of occupants' power changes (as an energy-use intensity patterns) at entry and departure events could be utilized as a feature in load disaggregation processes.

Additionally, it was also found^[19,56] that there is a delay interval between an occupants' entry/departure event to a building and the start/end of her energy-consuming behaviors (the creation of power changes at entry/departure events). Then, it was statistically proofed that each occupant has a recurring consistent pattern for the delay intervals at entry and departure events. This interval allows finding an occupant's time of starting/ending energy consuming behavior based on the time of her entry/departure event. Therefore, in a disaggregation procedure, the delay interval could act as a feature to detect the time when an occupant creates a power change at an event.

In summary, it can be concluded that there are two features related to occupant energy-consuming behavior at entry/departure events in office buildings: (1) delay

interval (ΔT), and (2) magnitude of power change (ΔP). The information of these features can be collected through existing sensing infrastructures (occupancy attendance systems and electricity meters) of office buildings. Figure 1 shows an example of these features for an entry event. Since each occupant has a recurring pattern for each of ΔT and ΔP ^[19,56], incorporating the information of these features might allow extracting the power changes caused by occupants at the occupancy events (i.e., entry/departure events).

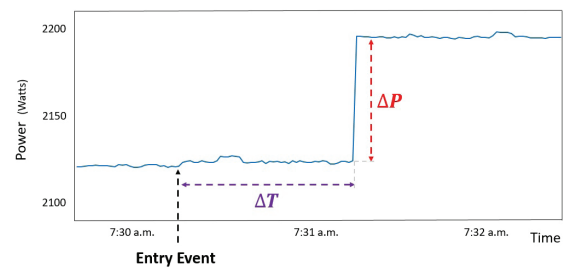


Figure 1. Occupancy-related energy-use features: delay interval (ΔT) and power change (ΔP)

In order to investigate this, an experiment was conducted to collect required data in office building and then to analyze the data through conventional supervised prediction methods used in NILM literature. In addition, hypotheses tests were also statistically checked the significant of features. The following sections provide the detailed description of the methodology and results.

3. Methodology

3.1 Experiment Design and Data Acquisition

An experiment was designed and conducted in an office building over two months. The entire building has 2200 square feet and it was fully occupied by eighteen staffs. Due to the different usage for each room of the building, various office building appliances such as personal computers, laptops, printers, scanners, video projectors, desk lamps, microwaves, refrigerators, and coffee makers, were used during the experiment. Five groups of staff were chosen as target occupants for this study.

In order to acquire the aggregate load data, a smart meter which collected data with 1-second interval resolution, was installed on a circuit which covered all outlets and end-users within the office space. Ground-truth load data with 1-second interval resolution was also collected through plug load meters installed at the occupants' workstations. To detect the entry and departure events, a Wi-Fi sniffer was installed at the building to passively track the transmitted Wi-Fi packets of the occupants' smartphones.

3.2 Method Selection

Aggregate energy-use data correlated with occupancy events during the experiment was identified and collected for each occupant. Figure 2 shows data points correlated with entry events (i.e., data points captured after the entry events) of one occupants in 20-min time-windows. Each data point is plotted by two features: ΔT measured in seconds, and ΔP measured in watts. The vertical axes in figure 2 were limited to the range of -200 to 200 watts for better visual demonstration of power changes caused by occupants. Positive ΔP at the entry events suggest the occupant increased their loads when entered.

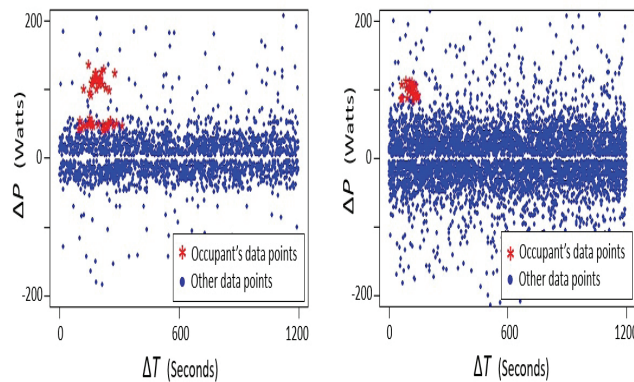


Figure 2. Power changes correlated with entry events of an occupant; other data points are the power changes are not caused by the occupant

Figure 2 particularly demonstrates that aggregate data points (i.e., power changes) correlated with an occupant's events could be divided into two groups: (1) power changes caused by the occupant (group 1), and (2) power changes not caused by the occupant (group 2). Figure 2 particularly shows that the data points caused by each occupant are within a specific range of ΔT and a few values of ΔP among aggregate data provided by meters. Therefore, the specific ranges/values might allow to utilize these features' information for extracting data points caused by occupants.

To check this, logistic regression model (logit model) was selected as a predictor to investigate the significance of ΔT and ΔP in predicting the correct group of the data points. Logit model is the most common and widely used statistical regression method utilized in the terms of prediction when there is a set of m independent predictor variables $X = \{X_1, X_2, \dots, X_m\}$, and one binary response variable, Y [57,58]. Y determines two groups into one of which, a data point can be assigned. In general, a logit model is expressed by:

$$\text{Logit}(\pi) = \beta_0 + \beta_1 X_1 + \beta_2 X_2 + \dots + \beta_m X_m \quad (1)$$

Where $\beta = \{\beta_0, \beta_1, \dots, \beta_m\}$ is a set of regression parameters, and π ($0 < \pi < 1$) is the estimated of Y and determines

the value of probability which is used to predict the group of a data point.

In addition, the logit model through estimated values for the set of regression parameters (β), particularly provides an opportunity to statistically test the importance of features (X) used in the prediction process. Therefore, in this research, the feasibility of ΔT and ΔP in the correct prediction of the groups of data points also tested through the following hypotheses:

- Hypothesis 1. Predicting the correct group of data points by using ΔT as a predictor is feasible.
- H0: ΔT is not statistically significant in the prediction process.
- HA: ΔT is statistically significant in the prediction process.
- Hypothesis 2. Predicting the correct group of data points by using ΔP as a predictor is feasible.
- H0: ΔP is not statistically significant in the prediction process.
- HA: ΔP is statistically significant in the prediction process.

3.3 Data Selection

Correct performance of the selected classifiers and predictor depends to the size of time windows which capture the data points correlated with occupancy events. The points within these time windows are the input data for the classifiers/predictor. Figure 2 as an example shows data points captured through a 20-min time window. Selecting a big size for time windows (e.g., 2-hour time windows) provides a lot of data points which are not caused by a specific occupant and could disturb the performance of a technique which derive the occupant's data points. On the other hand, small size time windows (e.g., 3-min time windows) could lead to losing some data points caused by occupants.

To address this issue, a size for time windows was selected in this study as follow. For entry events of an occupant, the maximum time of ΔT was estimated by the ground-truth data acquired for his/her entry events and considered as the size of the time window for his/her entry events. Then, this time window captured data points correlated with his/her entry events and put into a dataset which will be analyzed by the classifiers and predictor. Similarly, the size of time window for his/her departure events was also estimated and data points correlated with his/her departure events (data points caused before his/her departure events) were captured and put into another dataset. Figure 3 shows a time window which selected the data points for departure event of an occupant. The negative ΔP suggests that this occupant reduced energy load when left the building.

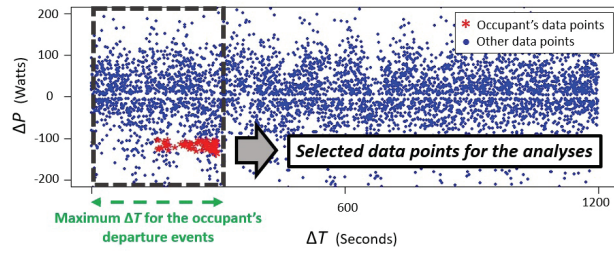


Figure 3. A time-window captures data points correlated with departure events of an occupant; other data points are not caused by the occupant

4. Results and Discussion

In order to run the predictor, and hypothesis testing on the datasets, R-programming, an open-source statistical language, was selected. The following results were achieved through the predictor implementations.

4.1 Predictor Performance

In this study, there were two possible groups for a data point: group 1 and group 2. ΔT and ΔP also act as independent predictors. Therefore, the logit model used in predicting the correct group of the data points was expressed by $\text{Logit}(\pi) = \beta_0 + \beta_1 \Delta T + \beta_2 \Delta P$.

The performance of a logit model in predicting processes significantly depends on the cutoff point which is a threshold defined for . In this study, for each occupant, all possible values of the cutoff point (all values between 0 and 1) were examined to understand how the logit regression model performs for different cutoff values. Accordingly, receiver operating characteristic (ROC) curves were

utilized to illustrate the performance of the logit model for all cut off values; a ROC curve visually demonstrates the performance of a binary classifier or predictor when the threshold is varied.^[59,60] For each value of the cutoff point, a confusion matrix returned number of true positives (TP), true negatives (TN), false positives (FP), and false negatives (FN). Then, the curve is allowed to show the tradeoff between true positive rates (TPR) against false positive rate (FPR) for all values of the point. TPR and FPR are defined as follows:

$$TPR = \frac{TP}{TP + FN} \quad (2)$$

$$FPR = \frac{FP}{FP + TN} \quad (3)$$

These metrics are ranged between 0 and 1. While the higher value of TPR indicates the more accuracy, the lower values of FPR indicate the better results. Figure 4 demonstrate the ROC curve generated for the occupants' events. TP, FP, TN, and FN contributed with the same weight to TPR and FPR and the equal error cost was considered during the process.

The ROC curves in figure 4 typically demonstrate the higher TPR compared to FPR for all occupancy events. In particular, the curves for few events (e.g., entry events of occupant 2) touched the 45-degree line in a few points which indicates some values of cutoff points for these events led to worthless predictions (FPR is equal to TPR). The stochastic nature of ΔT and the possibility of coincidence in ΔP with similar magnitude could be the main source of errors in the prediction procedure. Fur-

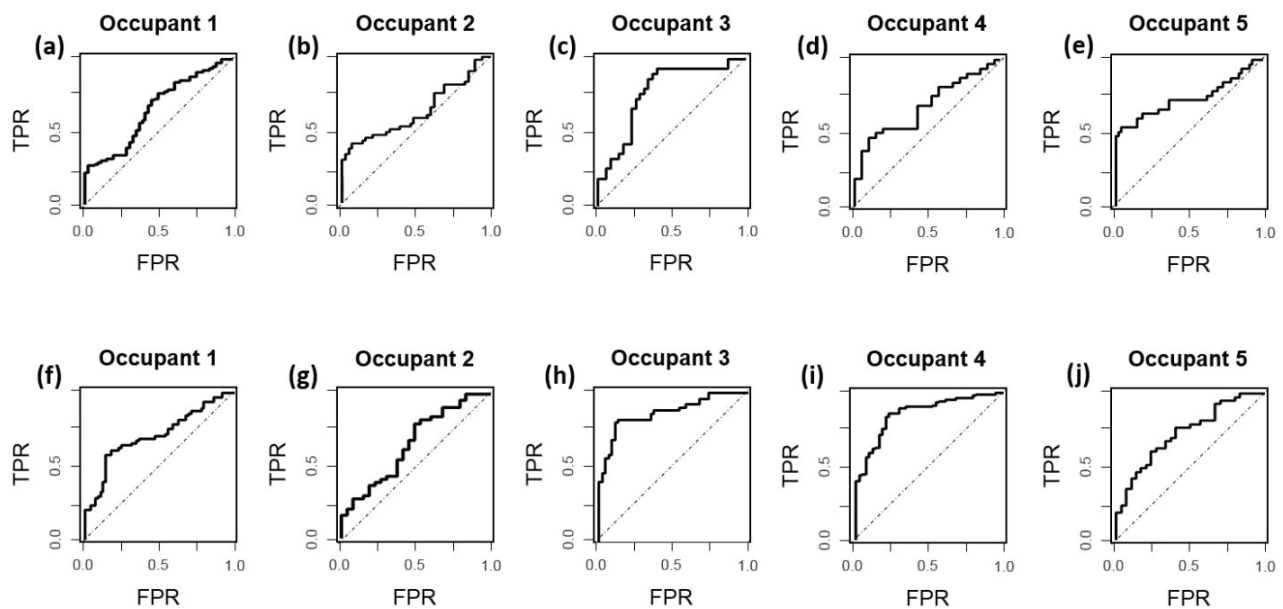


Figure 4. Roc curves: (a, b, c, d, e) entry events, (f, g, h, i, j) departure events

thermore, more the area under curve (AUC) for departure events of occupant 3 compared to the events of all occupants, indicating more accurate prediction for data points of this occupant at departure events. Overall, the ROC curves in figure 4 demonstrated that using ΔT and ΔP for appropriately predicting power changes caused by occupants with higher TPR to FPR rates is feasible.

4.2 Hypotheses Test Results

For entry and departure events of each occupant, the maximum likelihood estimation was used to estimate the set of parameters for . Then, the estimated values were tested through Wald and Likelihood-Ratio (LR) tests for the constructed hypotheses; Wald and LR tests are the tests mainly utilized to statistically investigate the importance of parameters in a regression analysis ^[61]. Table 1 lists the results of the tests.

The results of LR and Wald test draw a same conclusion for events of individual occupants. The statistically significant p-values give evidences for rejecting null hypotheses for all events and indicate that ΔT and ΔP are statistically significant to derive power changes caused by occupants among aggregate data points.

4.3 Further Discussion on the Results

The ROC curves achieved through the logit model, and the statistically significant p-values obtained for the hypothesis tests revealed that using ΔT and ΔP for extracting power changes caused by occupants from data provided in building operations is feasible. The information of ΔT and ΔP is collected from existing occupancy and energy sensing infrastructures in office buildings, without installing new hardware. As discussed, the possibility of coincidence in data points with similar ΔT and ΔP could

be interpreted as the main source of error which did not allowed the classifiers and predictor to achieve the maximum performance (highest accuracies).

Furthermore, Figure 2 and 3 demonstrate data points caused by occupants are limited to the few value of ΔP which means these data points caused by personal appliances typically used during the experiment. Through the help of the acquired ground truth data, it was finally found that these data points were caused by the personal computers used at the workstations. In fact, since the personal computers were typically used every day during the experiment, their caused data points (power changes) had most frequently in datasets which allowed making dense clusters; such clusters were utilized by classifiers/predictor.

Currently, NILM techniques typically provide the energy-use information of the major appliances (use the most energy) in a building ^[13,15,16], this information is valuable in enhancing overall energy efficiency in built environments. Similarly, ΔT and ΔP helped extracting energy-use information of the personal computers which were the major appliances with maximum frequency of usage at the occupants' workstations during the experiment. Accordingly, the energy-use data of personal computers could provide valuable information for understanding occupants' energy-use behaviors.

5. Limitations

While current energy and occupancy sensing infrastructures in offices building have not been demonstrated to be suitable to provide real-time occupants' energy-use behavior information, the results of this study indicated that such infrastructures have capacity to provide occupant-specific energy-use information at entry and depar-

Table 1. Wald and LR tests results

Occupant	Hypothesis	Entry Events				Departure Events			
		Wald Test		LR test		Wald Test		LR test	
		Z-value	P-Value	-2log(Λ)	P-Value	Z-value	P-Value	-2log(Λ)	P-Value
1	1	2.637	0.00837	7.531	0.00606	2.722	0.00648	7.648	0.00568
	2	2.028	0.04258	9.527	0.00202	-3.419	0.00062	11.504	0.00069
2	1	2.504	0.01229	11.350	0.00075	-2.279	0.02266	12.151	0.00049
	2	-3.867	0.00011	16.942	3.85e-05	4.724	2.31e-06	24.688	6.74e-07
3	1	2.391	0.01679	14.831	0.00011	-3.416	0.00063	12.213	0.00047
	2	-5.029	4.94e-07	37.395	9.64e-10	4.753	2.01e-06	36.208	1.77e-09
4	1	1.960	0.04999	13.342	0.00025	-5.119	3.07e-07	37.654	8.447e-10
	2	4.707	2.51e-06	53.612	2.44e-13	6.279	3.40e-10	60.741	6.51e-15
5	1	2.471	0.01347	9.978	0.00158	2.911	0.00360	8.124	0.00436
	2	-3.750	0.00017	46.557	8.90e-12	3.559	0.00037	26.585	2.52e-07

ture events. The main objective of this paper was to assess whether the two proposed features are able to derive occupant-specific power changes based on the NILM concept. This objective was confirmed through the results from the logit model. However, this research is subject to some limitations.

As discussed, the results significantly depend on the size of time-windows which select data points. In this research, the size was selected based on the maximum ΔT in each dataset. In fact, due to the lack of enough data, no analysis such as a sensitivity analysis could result in strong conclusions. Accordingly, further research into different sizes of time windows through various datasets would be beneficial to recommend the optimal size for a time window which lead to higher accuracies.

Furthermore, in this study, all data points correlated with an occupancy event were studied together in a time window. However, considering one time-window for each day based on its ΔT and studying data points in individual daily time windows might suggest an optimal size for the time window. Such individual daily time windows might also help looking more in depth into occupants' energy-use information.

6. Conclusion

This research was the first step in developing a non-intrusive occupant load monitoring approach in office buildings. The results from implementing the predictor and hypothesis tests on aggregate load data from a building confirmed the feasibility of ΔT and ΔP in non-intrusively extracting power changes caused by occupants at entry/departure events. Compared to the previous research extended the NILM concept for occupancy sensing, this research extended this concept for monitoring occupant-specific energy consumption. Furthermore, within the office settings, building management systems have utilized increasingly extensive sensor networks, but these networks fail to leverage aggregate load data as a measurement of occupant-specific energy consumption. However, this study particularly shows that without installation any additional hardware in an office building, the information provided by current infrastructures (i.e., Wi-Fi networks and metering devices) could be utilized for monitoring individual occupants' energy-use information. Overall, this study presents promising options for future research into occupant energy sensing in office buildings at minimal costs.

Acknowledgement

The Authors would like to acknowledge Dr. Changbum Ahn, Professor at Texas A&M University, and Dr. Kent Eskridge, Professor at the University of Nebraska-Lincoln, for their valuable advice during the data collection/

analysis process.

References

- [1] Godfried Augenbroe, Daniel Castro, Karthik Ramkrishnan, Decision model for energy performance improvements in existing buildings, *J. Eng. Des. Technol.* 2009,7,21–36. doi:10.1108/17260530910947240.
- [2] J. Chen, C. Ahn, Assessing occupants' energy load variation through existing wireless network infrastructure in commercial and educational buildings, *Energy Build.* 2014,82,540–549. doi:10.1016/j.enbuild.2014.07.053.
- [3] A. Ghahramani, C. Tang, B. Becerik-Gerber, An online learning approach for quantifying personalized thermal comfort via adaptive stochastic modeling, *Build. Environ.* 2015,92,86–96. doi:10.1016/j.buildenv.2015.04.017.
- [4] H.N. Rafsanjani, Factors Influencing the Energy Consumption of Residential Buildings: A Review, in: *Constr. Res. Congr. 2016, American Society of Civil Engineers*, 2016, 1133–1142. <http://ascelibrary.org/doi/abs/10.1061/9780784479827.114> (accessed on May 25, 2016).
- [5] C. Clevenger, J. Haymaker, M. Jalili, Demonstrating the Impact of the Occupant on Building Performance, *J. Comput. Civ. Eng.* 2014,28,99–102. doi:10.1061/(ASCE)CP.1943-5487.0000323.
- [6] K. Anderson, S. Lee, C. Menassa, Impact of Social Network Type and Structure on Modeling Normative Energy Use Behavior Interventions, *J. Comput. Civ. Eng.* 2014,28, 30–39. doi:10.1061/(ASCE)CP.1943-5487.0000314.
- [7] A. Ghahramani, F. Jazizadeh, B. Becerik-Gerber, A knowledge based approach for selecting energy-aware and comfort-driven HVAC temperature set points, *Energy Build.* 2014,85, 536–548. doi:10.1016/j.enbuild.2014.09.055.
- [8] E. Azar, C. Menassa, Framework to Evaluate Energy-Saving Potential from Occupancy Interventions in Typical Commercial Buildings in the United States, *J. Comput. Civ. Eng.* 2014,28,63–78. doi:10.1061/(ASCE)CP.1943-5487.0000318.
- [9] H.N. Rafsanjani, C.R. Ahn, M. Alahmad, A Review of Approaches for Sensing, Understanding, and Improving Occupancy-Related Energy-Use Behaviors in Commercial Buildings, *Energies*. 2015,8,10996–11029. doi:10.3390/en81010996.
- [10] N. Murtagh, M. Nati, W.R. Headley, B. Gatersleben, A. Gluhak, M.A. Imran, D. Uzzell, Individual energy use and feedback in an office setting: A field trial, *Energy Policy*. 2013,62, 717–728. doi:10.1016/j.enpol.2013.07.090.
- [11] H. Staats, E. van Leeuwen, A. Wit, A longitudinal study of informational interventions to save energy in an office building., *J. Appl. Behav. Anal.* 2000,33,101–104. doi:10.1901/jaba.2000.33-101.
- [12] A. Khosrowpour, R. Gulbinas, J.E. Taylor, Occupant Workstation Level Energy-use Prediction in Commercial

- Buildings: Developing and Assessing a New Method to Enable Targeted Energy Efficiency Programs, *Energy Build.* (n.d.). doi:10.1016/j.enbuild.2016.05.071.
- [13] A. Zoha, A. Gluhak, M.A. Imran, S. Rajasegarar, Non-Intrusive Load Monitoring Approaches for Disaggregated Energy Sensing: A Survey, *Sensors*. doi:10.3390/s121216838.
- [14] R. Gulbinas, J.E. Taylor, Effects of real-time eco-feedback and organizational network dynamics on energy efficient behavior in commercial buildings, *Energy Build.* doi:10.1016/j.enbuild.2014.08.017.
- [15] M. Zeifman, K. Roth, Nonintrusive appliance load monitoring: Review and outlook, *IEEE Trans. Consum. Electron.* 57 (2011) 76–84. doi:10.1109/TCE.2011.5735484.
- [16] G.W. Hart, Nonintrusive appliance load monitoring, *Proc. IEEE*.1992, 80,1870–1891. doi:10.1109/5.192069.
- [17] L.K. Norford, S.B. Leeb, Non-intrusive electrical load monitoring in commercial buildings based on steady-state and transient load-detection algorithms, *Energy Build.* 1996,24, 51–64. doi:10.1016/0378-7788(95)00958-2.
- [18] N. Batra, O. Parson, M. Berges, A. Singh, A. Rogers, A comparison of non-intrusive load monitoring methods for commercial and residential buildings, in: 2014.
- [19] H.N. Rafsanjani, C. Ahn, M. Alahmad, Development of Non-Intrusive Occupant Load Monitoring (NIOLM) in Commercial Buildings: Assessing Occupants' Energy-Use Behavior at Entry and Departure Events, in: *First Int. Symp. Sustain. Hum.-Build. Ecosyst. ISSHBE*, American Society of Civil Engineers, Pittsburgh, PA, 2015,44-53.
- [20] R. Gulbinas, A. Khosrowpour, J. Taylor, Segmentation and Classification of Commercial Building Occupants by Energy-Use Efficiency and Predictability, *IEEE Trans. Smart Grid*. PP 2015, 1-1. doi:10.1109/TSG.2014.2384997.
- [21] H.N. Rafsanjani, C. Ahn, Linking Building Energy-Load Variations with Occupants' Energy-Use Behaviors in Commercial Buildings: Non-Intrusive Occupant Load Monitoring (NIOLM), *Procedia Eng.* 2016,45,532–539. doi:10.1016/j.proeng.2016.04.041.
- [22] Measurement science roadmap for net-zero energy buildings workshop summary report, 2010.
- [23] H.N. Rafsanjani, C.R. Ahn, J. Chen, Linking Building Energy Consumption with Occupants' Energy-Consuming Behaviors in Commercial Buildings: Non-Intrusive Occupant Load Monitoring (NIOLM), *Energy Build.* 2018,172,317–327. doi:10.1016/j.enbuild.2018.05.007.
- [24] D. Chen, S. Barker, A. Subbaswamy, D. Irwin, P. Shenoy, Non-Intrusive Occupancy Monitoring Using Smart Meters, in: *Proc. 5th ACM Workshop Embed. Syst. Energy-Effic. Build.*, ACM, New York, NY, USA, doi:10.1145/2528282.2528294.
- [25] W. Kleiminger, C. Beckel, T. Staake, S. Santini, Occupancy Detection from Electricity Consumption Data, in: *Proc. 5th ACM Workshop Embed. Syst. Energy-Effic. Build.*, ACM, New York, NY, USA, doi:10.1145/2528282.2528295.
- [26] W. Kleiminger, C. Beckel, S. Santini, Household Occupancy Monitoring Using Electricity Meters, in: *Proc. 2015 ACM Int. Jt. Conf. Pervasive Ubiquitous Comput.*, ACM, New York, NY, USA, 2015, 975–986. doi:10.1145/2750858.2807538.
- [27] O. Ardakanian, A. Bhattacharya, D. Culler, Non-Intrusive Techniques for Establishing Occupancy Related Energy Savings in Commercial Buildings, in: *Proc. 3rd ACM Int. Conf. Syst. Energy-Effic. Built Environ.*, ACM, New York, NY, USA, 2016, 21–30. doi:10.1145/2993422.2993574.
- [28] Y.F. Wong, Y.A. Şekercioğlu, T. Drummond, V.S. Wong, Recent approaches to non-intrusive load monitoring techniques in residential settings, in: *2013 IEEE Comput. Intell. Appl. Smart Grid CIASG*, 2013, 73–79. doi:10.1109/CIASG.2013.6611501.
- [29] Characteristics and Performance of Existing Load Disaggregation Technologies, United States. Dept. of Energy. , Washington, D.C., 2015.
- [30] R. Bonfigli, S. Squartini, M. Fagiani, F. Piazza, Unsuper-vised algorithms for non-intrusive load monitoring: An up-to-date overview, in: *2015 IEEE 15th Int. Conf. Environ. Electr. Eng. IEEEIC*, 2015, 1175–1180. doi:10.1109/IEEEIC.2015.7165334.
- [31] M.B. Figueiredo, A. de Almeida, B. Ribeiro, An Experimental Study on Electrical Signature Identification of Non-Intrusive Load Monitoring (NILM) Systems, in: *Adapt. Nat. Comput. Algorithms*, Springer, Berlin, Heidelberg, 2011, 31–40. doi:10.1007/978-3-642-20267-4_4.
- [32] H.-H. Chang, C.-L. Lin, H.-T. Yang, Load recognition for different loads with the same real power and reactive power in a non-intrusive load-monitoring system, in: *2008 12th Int. Conf. Comput. Support. Coop. Work Des.*, 2008,1122–1127. doi:10.1109/CSCWD.2008.4537137.
- [33] A. Shrestha, E.L. Foulks, R.W. Cox, Dynamic load shedding for shipboard power systems using the non-intrusive load monitor, in: *2009 IEEE Electr. Ship Technol. Symp.*, 2009, 412–419. doi:10.1109/ESTS.2009.4906545.
- [34] L. Farinaccio, R. Zmeureanu, Using a pattern recognition approach to disaggregate the total electricity consumption in a house into the major end-uses, *Energy Build.* 1999,30, 245–259. doi:10.1016/S0378-7788(99)00007-9.
- [35] M.L. Marceau, R. Zmeureanu, Nonintrusive load disaggregation computer program to estimate the energy consumption of major end uses in residential buildings, *Energy Convers. Manag.* 2000,41,1389–1403. doi:10.1016/S0196-8904(99)00173-9.
- [36] A.J. Bijker, X. Xia, J. Zhang, Active power residential non-intrusive appliance load monitoring system, in: *AFRICON 2009*, 2009, 1–6. doi:10.1109/AFR-

- CON.2009.5308244.
- [37] H.H. Chang, K.L. Chen, Y.P. Tsai, W.J. Lee, A New Measurement Method for Power Signatures of Nonintrusive Demand Monitoring and Load Identification, *IEEE Trans. Ind.* 2012,48, 764–771. doi:10.1109/TIA.2011.2180497.
- [38] H.H. Chang, C.L. Lin, J.K. Lee, Load identification in nonintrusive load monitoring using steady-state and turn-on transient energy algorithms, in: 2010 14th Int. Conf. Comput. Support. Coop. Work Des., 2010, 27–32. doi:10.1109/CSCWD.2010.5472008.
- [39] H.H. Chang, L.S. Lin, N. Chen, W.J. Lee, Particle Swarm Optimization based non-intrusive demand monitoring and load identification in smart meters, in: 2012 IEEE Ind. Appl. Soc. Annu. Meet., 2012,1–8. doi:10.1109/IAS.2012.6373990.
- [40] S. Drenker, A. Kader, Nonintrusive monitoring of electric loads, *IEEE Comput. Appl. Power.* 1999,12, 47–51. doi:10.1109/67.795138.
- [41] A. Cole, A. Albicki, Nonintrusive identification of electrical loads in a three-phase environment based on harmonic content, in: *IEEE*, 2000.
- [42] J. Liang, S.K.K. Ng, G. Kendall, J.W.M. Cheng, Load Signature Study #x2014;Part I: Basic Concept, Structure, and Methodology, *IEEE Trans. Power Deliv.* 2010,25,551–560. doi:10.1109/TPWRD.2009.2033799.
- [43] A.G. Ruzzelli, C. Nicolas, A. Schoofs, G.M.P. O'Hare, Real-Time Recognition and Profiling of Appliances through a Single Electricity Sensor, in: 2010 7th Annu. IEEE Commun. Soc. Conf. Sens. Mesh Ad Hoc Commun. Netw. SECON, 2010, 1–9. doi:10.1109/SECON.2010.5508244.
- [44] W.K. Lee, G.S.K. Fung, H.Y. Lam, F.H.Y. Chan, M. Lucente, Exploration on Load Signatures Abstract, (n.d.). <http://citeseerx.ist.psu.edu/viewdoc/citations;j-sessionid=93C520073BC7C992B8FF8B8A41880153?-doi=10.1.1.120.5328> (accessed February 20, 2017).
- [45] H.Y. Lam, G.S.K. Fung, W.K. Lee, A Novel Method to Construct Taxonomy Electrical Appliances Based on Load Signaturesof, *IEEE Trans. Consum. Electron.* 2007,53, 653–660. doi:10.1109/TCE.2007.381742.
- [46] S. Gupta, *ElectriSense: Single-Point Sensing Using EMI for Electrical Event Detection and Classification in the Home*, Thesis, 2015. <https://digital.lib.washington.edu/443/researchworks/handle/1773/26334> (accessed February 20, 2017).
- [47] S.N. Patel, T. Robertson, J.A. Kientz, M.S. Reynolds, G.D. Abowd, At the Flick of a Switch: Detecting and Classifying Unique Electrical Events on the Residential Power Line (Nominated for the Best Paper Award), in: *UbiComp 2007 Ubiquitous Comput.*, Springer, Berlin, Heidelberg, 2007, 271–288. doi:10.1007/978-3-540-74853-3_16.
- [48] Y.C. Su, K.L. Lian, H.H. Chang, Feature Selection of Non-intrusive Load Monitoring System Using STFT and Wavelet Transform, in: 2011 IEEE 8th Int. Conf. E-Bus. Eng., 2011, 293–298. doi:10.1109/ICEBE.2011.49.
- [49] H.-H. Chang, Non-Intrusive Demand Monitoring and Load Identification for Energy Management Systems Based on Transient Feature Analyses, *Energies.* 2012,5, 4569–4589. doi:10.3390/en5114569.
- [50] C. Laughman, K. Lee, R. Cox, S. Shaw, S. Leeb, L. Norford, P. Armstrong, Power signature analysis, *IEEE Power Energy Mag.* doi:10.1109/MPAE.2003.1192027.
- [51] H.-H. Chang, H.-T. Yang, C.-L. Lin, Load Identification in Neural Networks for a Non-intrusive Monitoring of Industrial Electrical Loads, in: *Comput. Support. Coop. Work Des. IV*, Springer, Berlin, Heidelberg, doi:10.1007/978-3-540-92719-8_60.
- [52] S.R. Shaw, S.B. Leeb, L.K. Norford, R.W. Cox, Non-intrusive Load Monitoring and Diagnostics in Power Systems, *IEEE Trans. Instrum. Meas.* doi:10.1109/TIM.2008.917179.
- [53] H. Kim, M. Marwah, M. Arlitt, G. Lyon, J. Han, Unsupervised Disaggregation of Low Frequency Power Measurements, in: *Proc. 2011 SIAM Int. Conf. Data Min.*, Society for Industrial and Applied Mathematics, doi:10.1137/1.9781611972818.64.
- [54] J.T. Powers, B. Margossian, B.A. Smith, Using a rule-based algorithm to disaggregate end-use load profiles from premise-level data, *IEEE Comput. Appl. Power.* doi:10.1109/67.75875.
- [55] A. Albert, R. Rajagopal, Smart Meter Driven Segmentation: What Your Consumption Says About You, *IEEE Trans. Power Syst.* doi:10.1109/TPWRS.2013.2266122.
- [56] H.N. Rafsanjani, C. Ahn, K. Eskridge, Understanding the Recurring Patterns of Occupants' Energy-Use Behaviors at Entry and Departure Events in Office Buildings, *Build. Environ.* 2018,136,77–87.
- [57] J.M. Hilbe, *Logistic Regression Models*, CRC Press, 2009.
- [58] J.M. Hilbe, *Practical Guide to Logistic Regression*, CRC Press, 2016.
- [59] D.M. Powers, Evaluation: from Precision, Recall and F-measure to ROC, Informedness, Markedness and Correlation, <http://dSPACE.flinders.edu.au/xmlui/handle/2328/27165> (accessed September 26, 2016).
- [60] *Signal Detection Theory and ROC Analysis in Psychology and Diagnostics: Collected Papers - 1996*, Page iii by John A. Swets. Online Research Library: Questia, (n.d.). <https://www.questia.com/read/91082370/signal-detection-theory-and-roc-analysis-in-psychology> (accessed September 26, 2016).
- [61] R.F. Engle, Wald, likelihood ratio, and Lagrange multiplier tests in econometrics, Elsevier, 1984. <https://ideas.repec.org/h/eee/ecochp/2-13.html> (accessed September 26, 2016).

REVIEW

Early Stage Design Workflow for High Energy Performance Multi-storey Residential Buildings

Caroline Hachem* Robert Beckett

Faculty of Environmental Design, University of Calgary, Calgary, T2N 1N4, Canada.

ARTICLE INFO

Article history:

Received: 29 October

Accepted: 16 November

Published: 30 November

Keywords:

Multi-storey buildings

Residential

Energy performance

Design performance models

Modelling analysis techniques

ABSTRACT

This paper presents a methodology to optimize building envelope energy performance for multi-storey residential buildings using a design performance model approach. Five analysis techniques, applied to a database of parametric simulation results, are proposed to derive information on various building performance features that can support early design decisions. Information may include optimal combination of design parameter values to achieve lowest energy consumption, or the relative impact of design parameters on a given design, such as a base case. A workflow template is established to provide support for the design process of energy efficient multi-storey residential buildings. This template can form a basis for the development of an interactive tool that integrates energy performance principles into early stage design decisions. The application of this methodology to a building in Vancouver (BC, Canada, 49°N) is presented as a case study. Results of this application demonstrates that adopting a specific combination of building envelope parameters, thermal load can be reduced by up to 85% as compared to a base case designed according to commonly built apartment buildings in the studied location.

1. Introduction

The achievement of a highly energy efficient buildings, which aim at minimizing negative environmental impact, requires implementing energy efficiency principles at early design stages, with particular attention to envelope design^[1,2]. Building envelope design plays a significant role in the energy performance of

multi-storey buildings, both residential and commercial. Increasing the efficiency of building envelope, coupled with improved climate control technologies, is considered as one of the main design strategies in achieving highly sustainable buildings^[3,4,5]. Moreover, the design of building envelope can be manipulated to increase the potential of buildings to generate renewable solar energy^[6,7].

**Corresponding Author:*

Caroline Hachem,

Faculty of Environmental Design,

University of Calgary, Calgary, T2N 1N4, Canada;

E-mail: caroline.hachem@ucalgary.ca.

Building simulation tools that allow flexibility in design, combined with feedback on energy performance, can be instrumental in exploring design solutions and their impact on building performance. Implementation of design performance models (DPM) is a convenient strategy for optimizing building envelope for energy performance at early design stages, allowing flexibility and ease of application in responding to design changes^[8]

Several researchers have attempted to develop tools to facilitate the design and energy performance analysis of buildings, both in new buildings and for retrofit purposes. Ochoa and Capeluto^[9] propose an interactive tool, based on the EnergyPlus simulation software, to provide alternative facade design configurations to support decision making during the early design stages of homes in hot climates. Alternative facade design scenarios are provided based on geographical location, building orientation, occupancy type, degree of automation, natural lighting, contextual setting, and building depth.

Attia et al.^[10] propose an interactive tool, ZEBO, which employs a DPM approach to provide support for early design decisions based on building envelope parameters including orientation, shape, window size/type, wall/roof insulation, and passive solar shading controls. Hemsath^[11] discusses the importance of using building performance simulations to inform decisions during the early stages of design for buildings. Conceptual design elements include building orientation, geometry/shape, envelope material/thermal resistance, window to wall ratio (WWR), shading, thermal mass, renewable energy, infiltration, and others. The parameters that need to be considered in modelling buildings' energy performance in a given geographic location vary according to, the type of building, the stage of design and its complexity and the objectives to be achieved. A large body of research discusses various parameters implemented in the simulation of energy performance, methods of modelling of buildings, and different methods of performance analysis. Yıldız, and Arsan^[12] employ sensitivity analysis to identify building parameters that influence thermal energy loads of apartment buildings in hot-humid climates, including design parameters such as window size, indoor space height, and features of materials. Samuelson et al.^[13] employ an exhaustive parametric method to calculate all possible combinations of a discrete set of building envelope parameters, including WWR, glass type, building orientation, building shape and wall insulation. Echenagucia et al^[14] employ genetic algorithm optimization to minimize the energy need of a 5-story office building for heating, cooling and lighting, by varying building envelope design parameters. These parameters include thickness of the masonry walls, number, position

and shape of the windows and the type of windows.

Statistical methods are employed to obtain information related to the impact of various design parameters on performance. Hygh et al.^[15] use a Monte Carlo algorithm and EnergyPlus simulations to develop a multivariate linear regression model based on a large number of design parameters for a rectangular office building. Standardized regression coefficients are calculated to show the relative impact of each of the input parameters on heating, cooling, and total energy loads. Tian^[16] discusses a variety of sensitivity analysis methods that are applicable to building energy analysis.

While a rich literature exists on optimizing energy performance of buildings of specific configurations and environments^[17,18], the objective of this paper is to present a generalized methodology to optimize building envelope energy performance of multi-storey buildings during the early design stage, while providing flexibility in setting design parameters. Despite the fact that the proposed methodology is developed with residential buildings in mind, it can be extended to include other types of buildings, including multifunctional.

The proposed methodology includes five modelling analysis techniques that can be employed to analyse the output of exhaustive parametric study of building envelope design parameters. A simplified flow-chart is provided to illustrate the main stages of this methodology and the potential of each of these techniques to provide specific information to support design decisions.

A case study of a residential building in Vancouver (BC, Canada, 49°N) serves to illustrate the application of the methodology in a specific design.

2. Methodology and Simulations

The methodology presented in this paper consists of the following stages. First, a base model is developed at the suite level to represent typical multi-storey residential buildings in the relevant location (Vancouver, Canada in the case study). Next, a parametric study is designed to investigate the effects of selected building envelope parameters on energy performance. Finally, the output of the parametric study is analysed using design performance modelling techniques.

2.1 Parametric Study

An extensive parametric study is developed to investigate parameters associated with the building envelope expected to influence energy performance. Each of the parameters is incremented at discrete input intervals over a range of values expected to be valid for the considered design and combinations of parameters are simulated to measure the predefined energy performance. Once every combination

of the parameter values has been evaluated, a database of response variables corresponding to all parameter combinations is created to serve as a base for further analysis. The simulations are performed separately for each residential unit of the base model, in order to account for differing climatic effects on energy performance of units of differing positions and orientations. The following sections summarize the simulation software utilized in this research, details of the parametric workflow, definitions of design parameters, and the response variables that are included in the analysis.

2.1.1 Simulations

EnergyPlus v8.5 is selected to conduct all building design simulations. These simulations aim at determining the annual thermal energy required for heating and cooling of the studied apartments, as well as the electric load for appliances and equipment, and the PV electricity generation potential. The weather file for the studied region (Vancouver, Canada in the case study – section 3, ^[19]) is employed in the simulations. The parametric study is conducted following the methodology of software package jePlus ^[20], where discrete values are assigned to variables defined in an EnergyPlus input data file. EnergyPlus simulations are performed for each combination of the input parameter values to build a database of annual energy performance associated with each of the residential suites.

This approach allows a full set of results to be computed without reference to order of precedence of parameters. There is, however, a practical limit to the number of simulations that can be included in the study, based on software and data processing resources. This limitation needs to be considered when selecting ranges and intervals of parameter values.

In the proposed modelling, residential suites are simulated individually, assuming that only the exterior wall interacts with the outside environment. All interior walls, floors, and ceilings are set to 'adiabatic', implying no heat transfer through these surfaces. This assumption reflects the scenario where the suite is mid-level in the building, and has neighbouring suites with similar temperature settings.

2.1.2 Input Parameters and Response Variables

Input parameters are selected, based on their anticipated influence on energy performance, as identified by large body of research ^[1,17,18,21]. The nature, and particularly values of parameters, depend on the climatic region considered. While the ten parameters considered in this investigation (see case study, section 3) are selected with northern climate in mind, primary parameters, such as wall insulation, thermal mass represented by a concrete

slab, glazing size and properties, are expected to feature in the majority of climatic conditions, albeit at varying ranges of viable values. The increment of values for each parameter is set to provide sufficient data to define a trend, while keeping the overall number of simulations to a manageable number (due to software limitations, as mentioned above).

Typical response variables employed to indicate the performance of various building envelope designs are heating and cooling loads, heating and cooling energy consumption, electrical loads (including lighting, domestic hot water, and appliances), and, optionally, photovoltaic electricity generation potential. Heating and cooling loads account for various heat transfer mechanisms through the building envelope, solar heat gain and various internal heat gain sources (e.g. people, lights and appliances). Heating and cooling energy is based on heating and cooling loads, but may be modified by climate control devices, such as a heat pump. PV potential represents the amount of energy generated by photovoltaic cells integrated into the opaque surfaces of exterior façade surfaces, as well as the upper surface of window overhangs (when available).

The results from each simulation have a unique pattern of heating and cooling loads (and PV potential), depending on the geometry and materials used in the design. It is important to keep in mind that heat gain or loss can be either beneficial or costly depending on the need for heating or cooling. For example, solar heat gain can be beneficial to supplement mechanical heating during the winter, but can contribute to overheating of the suite during the summer. Similarly, the heat gains from internal loads (occupants, lighting, and equipment) can be a benefit or a cost depending on the interior temperature balance.

2.2 Design Performance Modelling Analysis Techniques

The American Institute of Architects (AIA) distinguishes two concepts for evaluating energy related design: design performance modelling (DPM) and building energy modelling (BEM) ^[18]. Whereas a BEM is designed to reflect the detailed geometry and materials for a building to ensure compliance with energy codes and targets, DPM is a less complex and time-consuming procedure to evaluate energy use at the design stage before the building is finalized. The methodology employed in this study follows the concept of DPM by generalizing basic envelope parameters to allow designers to get rapid feedback on various configurations of envelope components without expending the effort to build a detailed energy model. EnergyPlus simulations are primarily based on forward modelling ^[22], and it supports both BEM and DPM approaches.

In this section, five data analysis techniques are pre-

sented to analyse data created by the parametric simulation. These methods include reduction, extreme scenarios, sensitivity analysis, trend analysis and optimization. Trend analysis was employed by RDH Building Engineering^[23] to optimize a base model for a typical multi-storey residential building in Vancouver. The sensitivity analysis technique is a statistical method applied by Hygh et al^[15] to prioritize the significance of input variables. Extreme scenarios were introduced for an exhaustive parametric study by Samuelson et al^[13]. The Reduction and optimization techniques are proposed in this research to explore the full population of simulation results created in the parametric study. Any combination of these analysis techniques can be employed in a given design based on design priorities.

2.2.1 Reduction

The reduction technique allows the user to set a performance threshold to remove design options that do not achieve the desired performance level. Some values of envelope parameters are complementary, while others are in conflict, resulting in poor energy performance. For example, designs that combine large windows, high solar heat gain coefficient (SHGC), and no solar shading controls are conducive to high cooling loads. On the other hand, designs that combine high infiltration rates, large windows, low U- values, and low wall insulation values have high heating loads. The worst performing designs combine parameters that result in high heating and cooling loads.

This analysis technique is proposed to allow users to filter out design options based on a threshold of energy performance. Using the results from all simulations in the parametric study, and a threshold setting for one or more response variables, a subset of the available design options is removed from consideration. In some instances, a design parameter will only be available when combined with certain elements. For example, if larger windows are desired, it may be necessary to include shading overhangs and low SHGC glazing in order to minimize cooling load requirements.

2.2.2 Extreme Scenarios

This technique, which is, in fact, a simplified optimization technique, queries the simulation database for extreme scenarios based on a selected metric. Examples of extreme scenarios include lowest net energy, lowest heating load, lowest combined heating and cooling load, and highest PV generation. Since the parametric study is conducted at the suite level, it is possible to query the database for scenarios where all suites have the same parameter values, as well as scenarios where heterogeneous designs among various suites are allowed. For example, the optimal win-

dows to minimize net energy for the suites on the south orientation may differ from the north-oriented suites.

This DPM technique is a quick method to identify combinations of envelope parameters which yield the best outcome for a specific metric. When combined with the optimization technique, discussed in section 2.2.5 below, the designer can for instance start with an extreme scenario and make incremental changes until an acceptable balance between energy performance and other design requirements is achieved.

2.2.3 Sensitivity Analysis

Sensitivity analysis allows to recognise the most significant parameters, which affect building performance and, thus to concentrate design and optimization of buildings on these parameters^[24]. Standardized regression coefficients (SRCs) are calculated to indicate the relative impact that input variables have on a selected output metric^[25]. Hygh et al.^[15] calculated SRCs to investigate the sensitivity of input variable changes on heating and cooling loads for a commercial office building. Calculating SRCs for a given scenario provides valuable context to prioritize design decisions based on maximizing impact. For example, if during the design process, limitations exist to select a number of design element of the building envelope to optimize energy performance while responding to budget constraints, this technique allows selection of the most impactful design parameters to adopt.

While sensitivity analysis is initially applied to the base case design, it can be re-calculated to analyse a subset of the data that remains after employing one of the other techniques listed in this section. For example, the designer may want to know which input variables will be most influential at reducing the heating load of a design with 80% WWR. The results of the analysis of this subset of data may vary significantly from the original scenario.

Once the most important variables are identified, the designer will need to know whether there are trade-offs or synergies associated with them. This analysis is discussed below.

2.2.4 Trend Analysis

A significant aspect of design performance modelling is to delineate the relationships between input and response variables for various design scenarios. Trends that are observed when altering the base model may not be consistent with trends that are observed for alternative starting points for the conceptual design. For example, if the design is constrained to have high WWR and low wall insulation, the relationships between the remaining input variables and results can vary significantly from the base model trends.

Using the full set of results from the parametric study, or a subset of results defined by one of the other analysis techniques, trends can be investigated between the input and output variables. Plotting multiple input variables against a response variable can identify trade-offs or synergies that exist. For example, WWR and overhangs both affect the thermal loads of a building. As WWR increases, so does the heating load due to the relatively higher conductive heat losses through the glazed area. Also, as WWR is increased, the opaque area available to integrate solar technologies (if this is part of the design considerations) is reduced, limiting the capacity for renewable energy generation. As window overhangs are increased in length, cooling loads are decreased due to the reduction of unwanted solar heat gains, and available opaque area for potential integration of photovoltaic cells is increased. By combining these two input parameters in a trend analysis, the overall effect of these parameters on net energy consumption can be evaluated for a given design scenario.

This DPM analysis technique can be focussed by filtering the population of simulations to explore incremental changes to a specific design, or can be broadened by averaging a range of parameter values. It can be employed to showcase the interdependent nature of various design options. For example, the effect of changes in WWR, regardless of the window type, can be investigated by averaging the range of results for all values of U-value and SHGC.

2.2.5 Optimization

Optimization is defined, in the general sense, as a procedure minimizing or maximising the value of a parameter, subject to prescribed constraints. In the present context the parameters being optimised are energy performance parameters, in terms of selected response variables. Since all combinations of the input parameters are simulated in the parametric analysis and values of the response variables are stored in the data base, any design scenario that combines parameter values under given constraints can be investigated. The simplified optimization technique referred to under Extreme Scenarios (section 2.2.2), consists of selecting design parameter combinations that optimize selected response variables, such as minimizing total energy consumption or net energy consumption. The extreme scenario technique, which considers all parameter combinations in the data base can be modified to account for specific constraints applied to selected design parameter values, such as requiring a fixed value or a limited range of values. For instance, a minimal WWR or daylighting values may be prescribed for aesthetic and comfort considerations. However, the constraints may be more complex than specifying values to certain parameters. For

instance, limiting costs involves a wide range of parameters and determining the values of the main parameters that govern cost is a more rigorous procedure than the extreme scenario. This procedure, that involves incremental changes to input parameters, is illustrated in the case study presented below.

2.3. Interactive Workflow template for Design Performance Modelling

Although design is an iterative process, energy performance characteristics of the building envelope are often determined during the conceptual design stages^[8]. Design performance models (DPM) offer a direct, flexible approach to evaluating the energy performance at early stage building designs. The five design performance modelling techniques discussed above can be integrated into an interactive template of modelling workflow, to provide support for the design of multi-storey residential buildings. Figure 1 is a representation of the workflow template proposed in this paper. This template has the potential of being developed into an interactive tool for early design stage of energy efficient buildings.

The workflow consists of two phases. Phase 1 includes the construction of the base model and parametric simulation of energy performance of each unit to generate a data base of energy performance. Phase 2 involves the five data analysis techniques discussed above.

Stage 1 starts with input of the "background information" including location of the building, followed by geometric data and then followed by the parametric energy performance simulations and compilation of the database of response variables of all envelope parameter combinations (on individual unit basis). Stage 2 starts with reduction and the other analysis techniques, which produce as output the parameter levels and response variable values of the resulting design. Reduction technique is used to exclude all results that do not meet minimum energy efficiency requirements. An examination of the lowest net energy extreme case is presented to provide context around the range of possible outcomes. A sensitivity analysis indicates the parameters manipulation of which has the biggest impact on outcomes. Trend analysis is presented to showcase the interdependent nature of some of the design options. Optimization technique enables obtaining optimal set of parameter values that maintain specific constraints, such as relating to non-technical aspects like aesthetics, comfort etc.

An illustration of the implementation of the workflow template for design performance modelling of a residential building in Vancouver, Canada is presented in section 3.3 below.

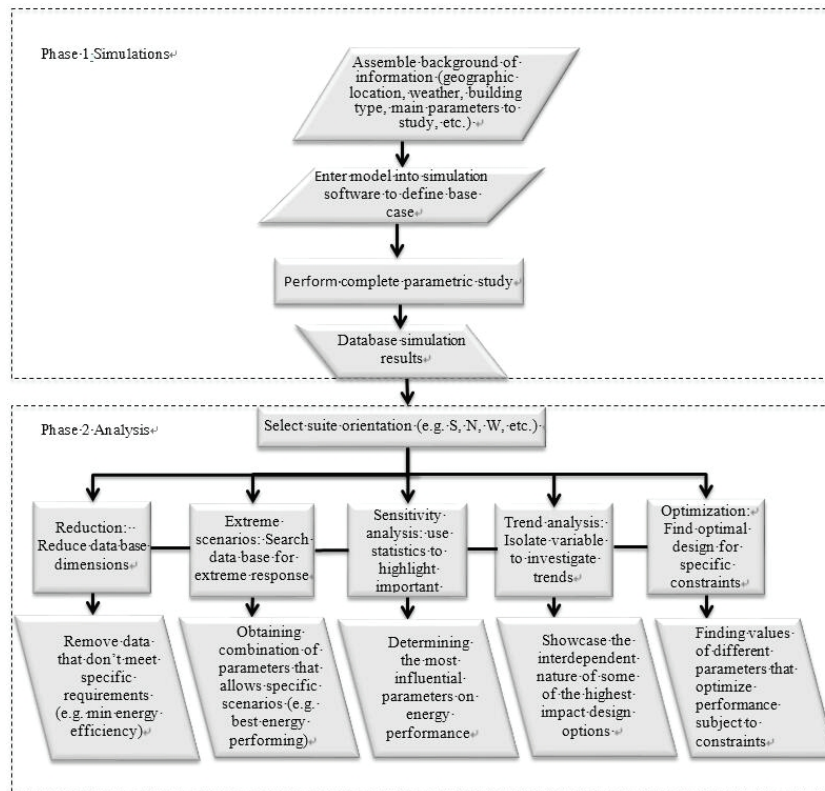


Figure 1. Design performance modelling workflow template

3. Case Study

In this section the methodology outlined in section 2 is applied to a residential building in Vancouver, Canada (49°N). The presentation of the analysis and design procedures follow the general layout of section 2.

3.1 Base Case

The geometry of the residential suites that make up a sample floor plan is shown in Figure 2. This floor is assumed to be located in the mid-section of a 12-story building. Each suite has the same floor area of 90m², with full width windows on each exposed façade. Consequently, the corner suites on the SW, SE, NW, and NE have double the glazed area as the single-façade suites on the S, E, W, and N sides of the building. The central area, labelled 'C', is

the common area that contains the corridors and service core of the building. This area is not included in the current study for the sake of simplicity.

The base case is designed to represent the existing multi-storey residential buildings in the Vancouver area built over the last 40 years, which is still representative of the majority of the existing building stocks. This base case is employed as a reference against which energy performance associated with building envelope improvements are measured. Table 1 shows the parameters adopted to represent the base case for the current study, together with the source for each parameter. Representative parameters for existing building stock are based on an analysis by RDH Building Engineering Ltd [23]. Data from Canadian Mortgage and Housing Corporation (CMHC) [26] is used

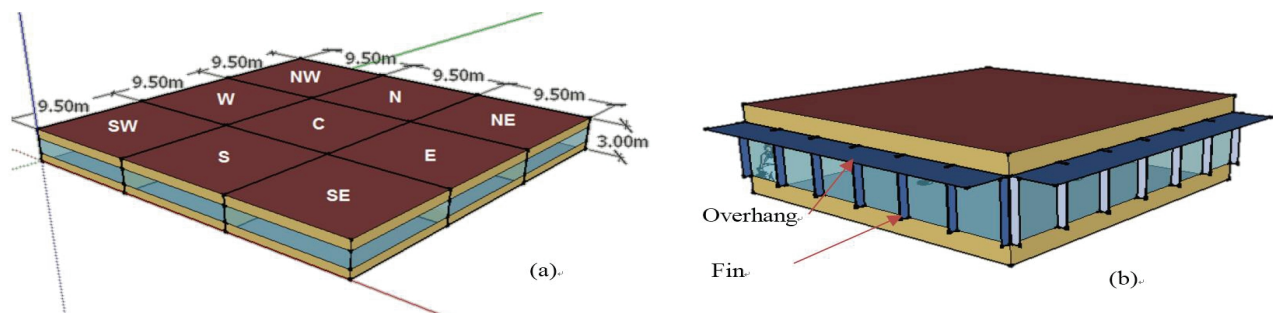


Figure 2. (a) Geometry of the eight unique suites of a story of the base case, and common area 'C'; (b) Illustration of the use of overhang and fins in the simulations.

Table 1. Base case parameter values

Parameter	Value	Units	Source
Plug Load	5.6	W/m ²	RDH, 2012
Suite Lighting Load	8.7	W/m ²	RDH, 2012
Infiltration Rate	0.572	ACH	RDH, 2012
Ventilation Rate	0.35	ACH	ASHRAE 62.1
Temperature Setpoint (day)	22	°C	RDH, 2012
Temperature Setback (night)	18	°C	RDH, 2012
People Load	1.9	Persons per suite	CMHC, 2013
Suite Area	90.67	m ²	RDH, 2012
Window to Wall Ratio	46	%	RDH, 2012
Overall Wall R-value	0.63	m ² K/W	RDH, 2012
Overall Window U-value	3.97	W/m ² K	RDH, 2012
Window SHGC	0.67	dimensionless	RDH, 2012
Storey Height	3	m	Modified from RDH, 2012
Occupancy Schedule		fractional	NRCAN, 2011
Suite Lighting Schedule		fractional	NRCAN, 2011
Plug Load Schedule		fractional	NRCAN, 2011
Weather Data	Vancouver	.epw file	U.S. Department of Energy, 2016
Photovoltaic Cell Efficiency	12	percent	Installed in all opaque areas

for occupancy levels, ASHRAE 62.1 is referenced for the ventilation rate, and the schedules from the National Energy Code (2011) for Buildings^[27] are used for all cases. PV panels are assumed to cover all opaque areas (excluding the north facades), including overhangs when applied. A 12% PV efficiency is assumed in the simulations (using EnergyPlus). The study assumes all-electric scenarios, to allow valid comparison of PV electricity generation potential of the residential units, to their total electricity consumption.

3.2 Parametric Study

3.2.1 Input parameters and Response Variables

Parameters identified, with the objective of optimizing the performance of the base case, are listed in Table 2, with the discrete values that are substituted in the simulations. Parameters include wall insulation, thermal mass, represented by a concrete slab, infiltration rates, shading overhangs (presented as the ratio of overhang width to the height of the window), window fins (measured as ratio of the fin width to the window width) (see Fig 2), internal blinds, window U-value and solar heat gain coefficient (SHGC), window to wall ratio (WWR), ventilation heat recovery, and façade orientation. Although concrete slab and ventilation heat recovery are not associated with the envelope design of the building, they constitute important

factors in designing energy efficiency, when considering passive solar gains capture and energy transfer mechanisms. The number of values for each parameter are set to provide sufficient data to define a trend, while keeping the overall number of simulations manageable.

The window U-value/SHGC values shown in Table 2 correspond to the window assemblies presented in Table 3. The base case window (see Table 1) is representative of the existing multi-story residential building stock in the Vancouver area^[23]. The NECB 2011 minimum window is the prescribed U-value under NECB 2011 8 with an assumed solar heat gain coefficient (SHGC) and visible transmittance (VT) based on the triple, low-e, high SHGC, argon filled window.

The main response variables employed to indicate the performance of various building envelope designs are heating and cooling loads, heating and cooling energy consumption, electrical loads, and potential photovoltaic electricity generation assuming BIPV installed on all opaque surfaces and overhangs of east, south and west facades. Net energy is calculated for each suite based on the heating energy, cooling energy, electrical loads, and PV potential using the following formula:

Net Energy=Heating+Cooling+Lighting+Equipment+Hot Water-PV

Heating and cooling energy is calculated assuming

Table 2. Envelope parameters and values considered in this research

Parameters	Units	Values							
Wall RSI	m ² K/W	1.76	3.6	6.2	8.8				
Thermal Mass		10cm slab with carpet	10cm slab	20cm slab					
Infiltration	ACH	0.03	0.09	0.27	0.57				
Overhang/Window Ratio	%	0	33	66	100				
Fin/Window Ratio	%	0	16	48	100				
Window U-value/SHGC	W/m ² K	0.77 / 0.41	1.08 / 0.18	1.14 / 0.41	2.2 / 0.41	3.57 / 0.26	3.63 / 0.38		
Window/Wall Ratio	%	20	40	60	80				
Internal Blinds		zone > cooling SetPoint	Always Off						
Heat Recovery	% Sensible	0	65	85					
Façade Orientation		SW	S	SE	W	E	NW	N	NE

Table 3. Window assemblies used for the base case and parametric study ^[28]

Assembly	Frame	U-Value	SHGC	VT
Base case window (RDH 2012)		3.97	0.67	0.7
Double, low-e, high SHGC, argon filled	Aluminium	3.63	0.38	0.61
Double, low-e, low-SHGC, argon filled	Aluminium	3.57	0.26	0.49
NECB 2011 minimum U-value window (NRCAN 2011)		2.2	0.41	0.50
Triple, low-e, high SHGC, argon filled	Improved non-metal	1.14	0.41	0.5
Triple, low-e, low SHGC, argon filled	Improved non-metal	1.08	0.18	0.37
Quadruple, low-e, high, SHGC, krypton filled	Improved Non-metal	0.77	0.41	0.36

that a heat pump with Coefficient of Performance (COP) of 4.0 is used to deliver heating and cooling to the suites. Electrical loads are associated with lighting and electrical equipment, excluding the heat pump. Energy requirements for lighting and equipment are based on NECB 2011^[27], and domestic hot water requirements are set to 2.62 KWh/occupant/day^[29]. Assuming an average occupancy of 1.9 people per suite^[26] the energy required for domestic hot water (DHW) is 1817 KWh/year/suite. The energy requirements for the common areas (i.e.: corridor heating and lighting) and centralized services (i.e.: elevators, lobby) and the solar energy generation from the roof of the building are not included in the calculation.

3.3 Design Performance Modelling

This section details the application of the workflow template for design performance modelling (DPM) as outlined in Figure 1. The analysis techniques employed in the performance modelling in this case study are carried out primarily through Excel spreadsheet processing of the database generated by EnergyPlus simulations.

3.3.1 Sample Case

The example presented below represents an updated scenario of the base case corresponding to NECB 2011 minimum

requirements (Tables 2, 3). A PV system, which is not included in the minimum requirements, is assumed. Figure 3 shows the total heating energy, cooling energy, PV potential, and electrical loads for this energy code scenario for the eight-suite floor plate. The Ratio of energy generation to total consumption for all eight suites reaches 26%.

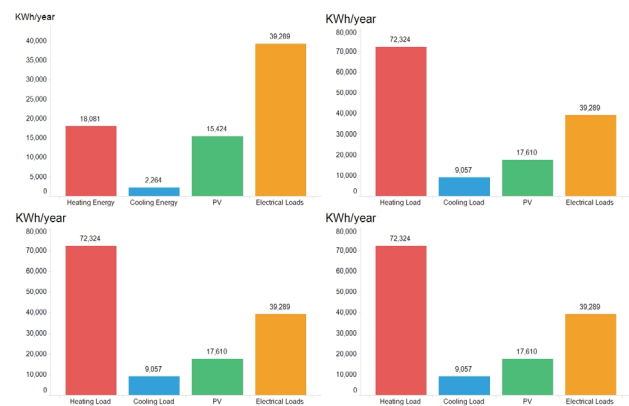


Figure 3. Sample case heating, cooling, PV, and electrical loads for the eight suite floor plate

At this point, the optimization technique (presented in detail below) can be used to explore the effects of modifying individual input parameters. However, for this case study, the reduction technique is used first to limit the field of

possibilities to exclude any options that do not meet the minimum energy performance required by the energy code.

3.3.2 Reduction

In this stage of the workflow, design options that do not achieve the minimum standard set out in NECB 2011 are removed from the analysis. Figure 4 shows the range of combined heating and cooling loads for each of the eight suite locations for varying levels of WWR. The dotted line shows the minimum standard associated with NECB 2011 for each suite. Any simulations that have combined heating and cooling loads above the line are excluded from further analysis steps. Although the minimum standard for NECB 2011 can be achieved with any WWR from 20% to 80%, there are many combinations of input parameters that do not make the cut. For example, designs that combine large windows, low U values, low wall RSI, high infiltration rates, and no solar shading controls fail to achieve the minimum energy efficiency levels dictated by NECB 2011.

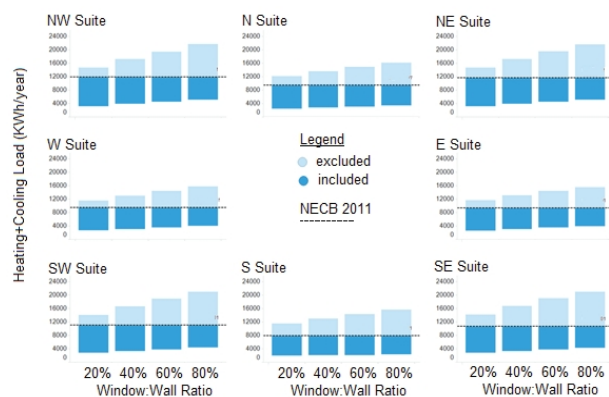


Figure 4. Range of combined heating and cooling loads for various windows to wall ratios by suite orientation

As performance requirement is set to stricter levels to achieve standards set by building certification programs, lower performing design parameters can be further eliminated from the list of acceptable combinations.

3.3.3 Extreme Scenarios

As mentioned in Section 2.2.2, this is a simplified optimi-

zation technique consisting of scanning the (reduced) data base for parameter combination that optimize a selected response variable, in the present example net energy consumption. Table 4 shows the parameters that combine to give the lowest net energy consumption for each of the eight suites.

The envelope parameter values for the eight suite types are uniform, except for the window type and shading control parameters. The N suite has a zero shading overhang and fin length with a relatively high SHGC window type (SHGC=0.41) and automated blinds. E and W suites have no shading fins, 100% window overhangs, U-value/SHGC of 1.08/0.18 and no shading blinds. The remaining suites (NW, NE, SW, SE, S) have no shading fins, 100% window overhangs, U-value/SHGC of 0.77/0.18, and automated blinds. These differences highlight the benefit of non-uniform designs that optimize each face separately.

Figure 5 shows the detailed response variables related to heat gain and heat loss for each of the eight suites for the lowest net energy scenario. Heat gains and losses translate into heating and cooling loads only when the suite temperature crosses either the heating or cooling set-point.

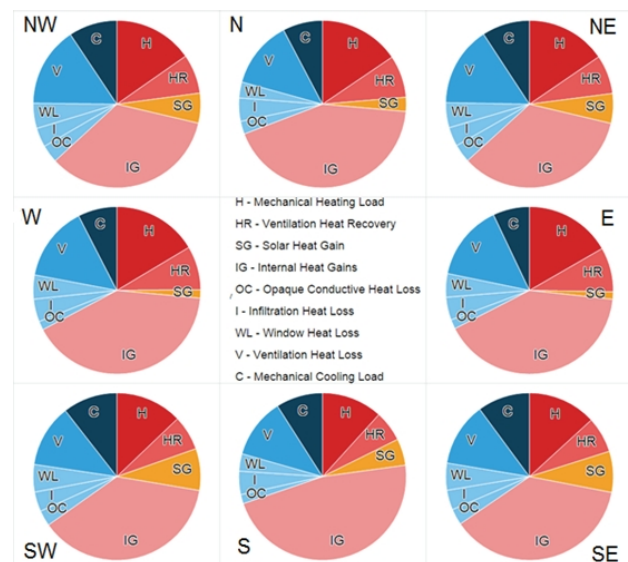


Figure 5. Response variables for lowest net energy scenario (heat losses in blues, heat gains in reds/orange)

Each of the heat loss categories (ventilation, window

Table 4. Parameters for lowest net energy scenario

Suite	Wall (RSI)	Thermal Mass	Infiltration (ACH)	Fin/Win-dow	Overhang/Window	Window U-value (W/m ² K)	Window SHGC	WWR	Heat Recovery	Blinds
N	8.8	20cm Slab	0.03	75%	0%	0.77	0.41	20%	85%	On When Zone \geq Cooling SP
E, W	8.8	20cm Slab	0.03	0%	100%	1.08	0.18	20%	85%	Always Off
NW, NE, SW, SE, S	8.8	20cm Slab	0.03	0%	100%	0.77	0.41	20%	85%	On When Zone \geq Cooling SP

losses, infiltration, and opaque conductive losses) have been minimized in this scenario due to the selection of small, high quality windows, a high level of airtightness, good wall insulation, and ventilation heat recovery. The amount of solar heat gain is optimized to offset heating loads in winter, while avoiding unwanted heat during summer. The corner suites have higher solar heat gains due to the double glazed area compared to the N, E, S, W suites. Internal heat gains (lighting, occupants, and equipment) are the same for all suites, representing the dominant heat source affecting the suites. These loads can be further reduced by careful selection of equipment. Moreover, passive cooling strategies, such as natural ventilation, have the potential of further reducing cooling loads.

3.3.4 Sensitivity Analysis

In the example presented in this paper, the range of performance results is trimmed through the minimum requirements of the energy code and extreme performance scenario. The next step in the workflow is to highlight which of the envelope parameters has the highest impact on improving outcomes.

At this stage, the population of data is analysed statistically to highlight the relative significance of input variables. For the following analysis, only simulations that produce net energy performance greater than the NECB 2011 case are included. Figure 6 shows the standardized regression coefficients (SRCs) for each of the input variables to show their relative impact on net energy performance. Variable importance, using SRCs is a measure of the standard deviation change in the output variable (response parameter) that corresponds to standard deviation changes of the input variables (design parameters). Standardized regression coefficients permit comparisons of predictor-response variable relationships across studies in which the variables are measured using different units of measure ^[30].

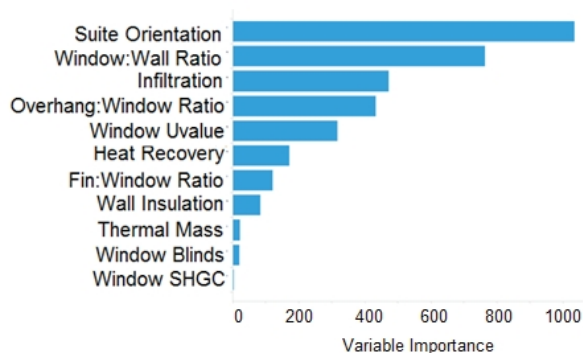


Figure 6. Relative impact of Input variable on net energy

Within the set of data and corresponding parameters values, the orientation of the suite has the highest influence on the net energy performance. The next highest impact parameter is the window to wall ratio (WWR). This

parameter affects the overall insulation value of window and opaque areas, the amount of area available for solar cells, and the window area available for passive solar heat gain.

Four out of the six highest priority envelope parameters are related to windows – window to wall ratio, overhang to window ratio, window U-value, and fin to window ratio. For the next step in the workflow, trends in the data are identified to better understand the effects that window parameters have on the suite performance.

3.3.5 Trend Analysis

Windows play an important role in the design of multi-storey residential buildings. As the sensitivity analysis section shows, decisions on the size and characteristics of glazed areas and passive solar controls play an important role in the energy performance of the finished building. This section shows two types of trend analysis that delineate the relationships between input parameters and energy performance results. In the first representation, the values of each individual input parameter is plotted against the major response variables – heating and cooling loads, and PV potential. The second representation provides information on the interaction between pairs of input parameters by plotting them against a single response variable, in this case, net energy.

Figure 7 shows the relationship between WWR and the major response variables; heating load, cooling load, and PV potential for the average simulation in the parametric study.

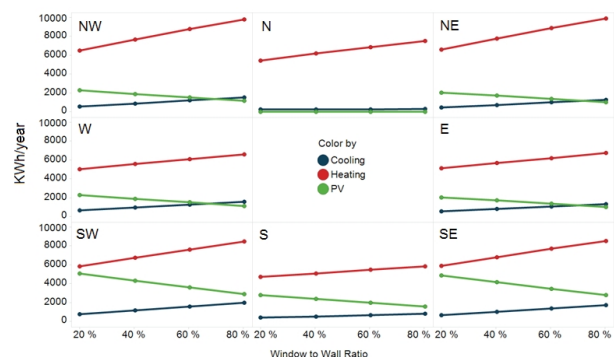


Figure 7. WWR vs heating and cooling loads and PV potential for eight suite types (all simulations)

PV potential is reduced with increasing WWR for each suite type due to the reduction in opaque area available for PV, except for the N suite, which has no photovoltaic cells. Cooling loads increase moderately for each of the eight suite types, except for the N suite, due to the increase in passive solar gains. Heating loads increase for each of the eight suites due to the relatively lower thermal resistance of glazing compared to opaque wall surfaces. These relationships represent a very broad view of the data, since they represent the average of all available

simulations, and are not necessarily representative of all design scenarios in the study.

Figure 8 shows the same set of relationships for the subset of simulations that include quadruple pane windows with high SHGC. (U-value 0.77, SHGC 0.41) The trends for PV potential are naturally not affected by window type, but heating and cooling load trends are significantly affected. The trends of increasing cooling load with increasing WWR are more pronounced, especially for the SW and SE suites that sustain increased solar exposure. Heating load trends, on the other hand, are flattened for all suites, showing a slight increase with WWR on the north side, and slight decrease on the south side. The additional solar energy captured by this subset of designs offset heat losses through the larger window surface area.

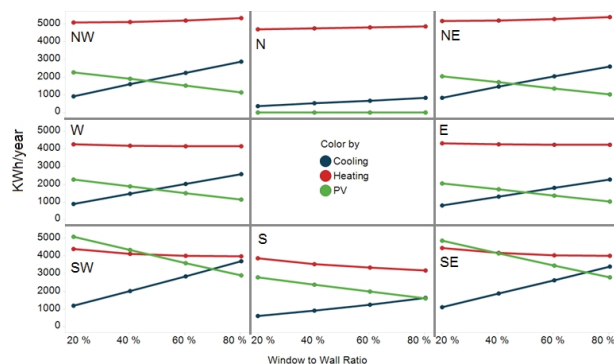


Figure 8. WWR vs heating and cooling load and PV potential for eight suite types with quadruple glazed, high SHGC windows

Figure 9 shows the interrelated nature of window size and shading devices. Darker colours on the map represent a relative improvement in energy performance, and the star marks the lowest net energy case. It is clear from the contrast between Figure 8 and Figure 9 that there is interaction between the input parameters that needs to be better

understood.

In general, the performance of the average suite improves as window size is reduced relative to opaque areas, and as the shading overhang length is increased relative to the window height. It is noted by the darkening colors of the cells in the chart that increasing overhang lengths are beneficial regardless of window size. Figure 9a shows that, for the average of the eight suites, the highest performing scenarios are related to a WWR=20%, while the lowest performance level is associated with WWR=80% and no shading overhangs, increasing the net energy consumption by 51% compared to the lowest net energy case. Figure 9b shows the relationship between window to wall ratio and fin to window ratio with respect to net energy. The effect of window size is dominant in this relationship, with a very moderate net energy performance trend towards shorter fins. Minimizing the width of fins is associated with a moderate improvement in performance, regardless of window size. Figure 9c shows the relationship between the length of fins and length of overhangs. The trend shows that higher net energy performance tends towards maximizing overhangs and minimizing fins.

3.3.6 Optimization

The Extreme Scenario example (section 3.3.3) demonstrates a simple optimization technique, consisting of scanning the data base for parameter combinations that optimize a selected response variable. It can be extended to allow for specific constraints on input parameters, such as prescribed values or range of values. The more rigorous procedure presented in this section can be applied to constraints that are not directly related to parameter values, such as material and construction costs and human comfort. The technique consists of determining incremental changes to the response variable being optimized (net energy in the present example) due to successive incremental changes to all parameter values, from a given set point. As the set point is moved in optimal trend, the interaction

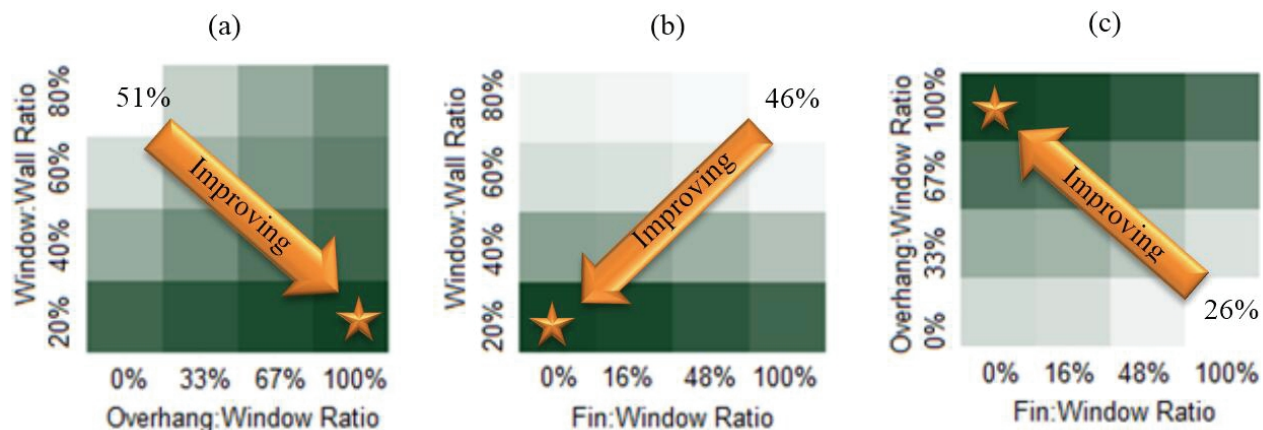


Figure 9. Qualitative trends in average net energy consumption for a) window to wall ratio vs. overhang to window ratio, b) fin to window ratio vs. overhang to window ratio, and c) overhang to window ratio vs. fin to overhang ratio

between parameters takes effect. It is, in a sense, a complex, sequential trend analysis.

Figure 11 shows the percentage difference dashboard for the average of all eight suites, evaluated against net energy consumption, with the objective of minimizing net energy. The 'Current Value' column shows the NECB 2011 minimum case, as discussed in section (3.3.1). Percentage differences in net energy consumption are shown in the '%diff' columns for incremental changes to each parameter (with + sign for increasing and – for decreasing increments), based on the discrete values defined in the parametric study (Table 2). Since the energy code case is the minimum (as set by the reduction technique in Section 3.3.2) there are only %diff+ viable options for improvement at this stage. Cells in the dashboard labelled 'min' and 'max' indicate that there are no further options of parameter values within the scope of the parametric study.

It can be observed for instance that the best incremental change is to improve the WWR by one step (i.e. from 40% to 20%), resulting in a 19% reduction in net energy consumption, while three increments (i.e. Increments by 3 consecutive values of the specific parameter- see values in Table 2) of infiltration have the highest potential for reducing net energy consumption, at 20% reduction. Since this is a live dashboard, each change to a parameter in the 'Current Model' will update all of the %diff values for each parameter. Using this technique, the user can 'wander' through the database to evaluate the energy performance of changing various design parameters.

The dashboard allows the user /designer to understand the impact of changing the value of individual parameters, and how this will affect the values of other parameters as well as the output in energy.

4. Discussion

This study presents a methodology to optimize the energy performance of building envelope of residential multi-storey buildings throughout the early design stage, using design performance modelling strategy. The methodology consists of applying a selection of analysis techniques to a

database obtained from the results of extensive parametric simulations performed on an assumed base case design. The parameters selected for the simulations are based on their expected impact on the energy performance of buildings^[18,1,21].

The objective of the five proposed analysis techniques is to explore impacts of various building envelope parameters on energy performance and to assist in selecting an optimal combination of parameter values. The analysis techniques include the following: Reduction – reducing the database to filter out all cases that fall below a certain threshold (for instance specific energy standards such as the NECB); Extreme Scenarios – searching the data base for parameter combinations that maximize or minimize selected performance criteria (e.g. total energy consumption, net energy consumption, etc.); Sensitivity Analysis– assessing the relative impact of design parameters on specific energy performance criteria; Trend Analysis – evaluation of the effect of varying a parameter value on a selected response; Optimization – evaluation of design parameter combinations that optimize a selected energy performance response, subject to constraints, through an incremental process of varying parameter values. The designer has the option of selecting the techniques that best fit the specific design under consideration.

Although a number of existing research focus on developing tools for early building design stages in specific applications, using, in some cases, some of the discussed techniques, the present methodology consists of a template that can be generally applicable to residential buildings. The originality of the proposed template resides in assembling a number of analysis techniques, which permit the user to extract useful information for specific design cases. In addition, the proposed method allows the user to visualize, and interactively appreciate, the impact of design decisions on the performance of the building and how this will affect the values of other parameters (as presented in Figure 10). Due to this, flexibility in the design can be attained, as wider understanding of the impact

Parameter	%diff--	%diff-	Current Value	%diff+	%diff++	%diff+++
Wall Insulation (m2K/W)	min	min	3.6	-1%	-2%	max
Thermal Mass	min	min	10cm slab, carpet	-1%	-2%	max
Infiltration (ACH)	min	min	0.572	-13%	-19%	-20%
Fin:Window	min	min	0%	max	max	max
Overhang:Window	min	min	0%	-7%	-12%	-15%
Window Uvalue (W/m2K)/SHGC	min	min	2.2/0.41	-6%	-6%	-8%
WWR	min	min	40%	-19%	max	max
Heat Recovery (% Sensible)	min	min	65	-2%	max	max
Blinds	min	min	Always Off	-1%	max	max

Figure 10. Optimization dashboard showing NECB 2011 parameter values and incremental %diff for net energy consumption

of design parameters is gained. While the current methodology was developed with residential buildings in mind, it can be readily applicable to a variety of building types.

A case study is employed to illustrate the application of this methodology to a residential multi-storey building in a cold climatic zone (Vancouver, BC, Canada, 49°N). The case study demonstrates that achieving high performance is significantly affected by the design of envelope parameters such as wall insulation, window type and size, air tightness, PV generation, and passive solar controls. For instance, combined heating and cooling load can be reduced by up to 85% as compared to the base case designed according to commonly built apartment buildings in the studied location (Vancouver, Canada). This performance is associated with a number of high-energy performance measures including the application of high insulation in opaque portions of the envelope, high performance windows (e.g. triple glazing, low-e coating, argon fill), relatively small window size constituting 20% of the façade area, and airtightness. Sensitivity analysis indicates that for the studied location and the range of parameters considered, apartment orientation, window-to-wall ratio (WWR) and airtightness have the highest impact on energy performance, respectively.

The case study presented in this paper relates to a simple rectangular geometry. Often in the design of buildings, variations of design are expected, including shape, height, and façade details. Some of these design aspects may affect the performance as for example a self-shading geometry (e.g. L shape, U shape,^[31]). Representing this variability in detailed building energy models requires significant effort, and therefore a barrier to improving energy performance, in the early design stage. The presented methodology can constitute a first stage in the design process, applied to demonstrate the impact of building envelope components, to achieve high-energy performance, generally applicable regardless of geometry variations. A second stage might consist of integrating shape and other geometrical aspects that can affect building loads, and often implying change in some design elements (e.g. location of windows, size and type of shading devices, etc.).

Decisions made during the early design stages set the foundation for the energy performance of the final building model. By focusing efforts on the most relevant interdependencies, trends, and sensitivities that influence energy performance, rather than on the construction of fully detailed building models, design professionals can build knowledge to improve the energy performance of buildings. The workflow provided in this study allows for a staged and customizable presentation of results depending on the nature of the inquiry and the level of knowledge of the user. As the questions into energy performance impacts become more sophisticated, the template provides options to explore varying frames of reference based on

the five data analysis techniques presented. The ability to drill down into individual response variables allows professionals with advanced levels of training to leverage the data to develop more advanced scenarios. For a more accurate assessment of full building energy performance, additional information about energy flows between adjacent suites and between floors, as well as energy requirements of common areas and mechanical systems, should be implemented in the energy models, in more advanced stages.

5. Concluding Remarks

This study provides a novel approach to influencing energy performance design decisions for multi-storey residential buildings during early design stages. The proposed approach allows the visualization of the impact of specific design decisions on the overall building performance as well as on other design parameters. This approach permits customizable presentation of results, depending on the nature of the inquiry and the level of knowledge of the user. The methods of interpretation of energy performance results, proposed in the template, allow the user to extract information that can be tailored to specific design cases. The methodology provides basic knowledge of the influence and interrelation between different components of building envelope, that can be applied to high-energy performance building regardless of other design elements (such as shape).

By understanding envelope energy performance of a residential multi-storey building at the suite level, and standardizing parameters based on an analysis of local building stocks, the task of optimizing the entire building is greatly reduced. This methodology can be further developed into an interactive tool that can support professionals in building design, with possibility of extending the type and range of parameters.

The methodology presented can be applied to other types of buildings such as office or institutional building, with some modification to the type of parameters and their range, taking into account the internal thermal building loads that may affect this selection.

Acknowledgements

The authors gratefully acknowledge the financial support of BC Housing as part of the Building Excellence Research & Education Grants Program.

References

- [1] Hachem, Caroline, Andreas Athienitis, and Paul Fazio. 2014. "Energy Performance Enhancement in Multistorey Residential Buildings." *Applied Energy*, 2014, 116, 9–19. doi:10.1016/j.apenergy.2013.11.018.
- [2] Sozer, H., 2010. Improving energy efficiency through the design of the building envelope. *Building and environment*, 2010, 45(12), 2581-2593.

- [3] Li, D.H., Yang, L. and Lam, J.C., 2013. Zero energy buildings and sustainable development implications—A review. *Energy*, 2013, 54, 1-10.
- [4] West, S., 2001. Improving the sustainable development of building stock by the implementation of energy efficient, climate control technologies. *Building and Environment*, 2001, 36(3), 281-289.
- [5] Khan, M.A., Mishra, S. & Haque, A. A Present and Future State of Art Development for Energy Efficient Buildings using PV Systems. *Intelligent Building International* (Taylor and Francis), 2018.
- [6] Hachem, Caroline, and Mohammed Elsayed. "Patterns of Facade System Design for Enhanced Energy Performance of Multistory Buildings." *Energy and Buildings*, Elsevier B.V. 2016, : 366–77. doi:10.1016/j.enbuild.2016.08.051.
- [7] Khan, M.A., Mishra, S. & Harish, V.S.K.V. Grid Connected Energy Efficient Building with Roof Top SPV. *IEEE second International Conference on Recent Developments in Control, Automation and Power Engineering (RD-CAPE)*, Amity University, Noida, <https://ieeexplore.ieee.org/document/8358252/>.
- [8] (AIA) The American Institute of Architects. 2012. "An Architect's Guide to Integrating Energy Modelling in the Design Process."
- [9] Ochoa, Carlos Ernesto, and Isaac Guedi Capeluto. 2009. "Advice Tool for Early Design Stages of Intelligent Facades Based on Energy and Visual Comfort Approach." *Energy and Buildings*, 2009, 41 (5), 480–88. doi:10.1016/j.enbuild.2008.11.015.
- [10] Attia, Shady, Elisabeth Gratia, André De Herde, and Jan L.M. Hensen. 2012. "Simulation-Based Decision Support Tool for Early Stages of Zero-Energy Building Design." *Energy and Buildings*, 2012, 49, 2–15. doi:10.1016/j.enbuild.2012.01.028.
- [11] Hemsath, Timothy L. "Conceptual Energy Modelling for Architecture, Planning and Design: Impact of Using Building Performance Simulation in Early Design Stages." *Proceedings of BS 2013: 13th Conference of the International Building Performance Simulation Association*, 2013, 376–84. <http://www.scopus.com/inward/record.url?eid=2-s2.0-84886645991&partnerID=tZOTx3y1>.
- [12] Yıldız, Y. and Arsan, Z.D.. Identification of the building parameters that influence heating and cooling energy loads for apartment buildings in hot-humid climates. *Energy*, 2011, 36(7), 4287-4296.
- [13] Samuelson, Holly, Sebastian Claussnitzer, Apoorv Goyal, Yujiao Chen, and Alejandra Romo-Castillo. "Parametric Energy Simulation in Early Design: High-Rise Residential Buildings in Urban Contexts." *Building and Environment*, doi:10.1016/j.buildenv.2016.02.018.
- [15] Hygh, Janelle S., Joseph F. DeCarolus, David B. Hill, and S. Ranji Ranjithan. "Multivariate Regression as an Energy Assessment Tool in Early Building Design." *Building and Environment*. doi:10.1016/j.buildenv.2012.04.021.
- [16] Tian, Wei. "A Review of Sensitivity Analysis Methods in Building Energy Analysis." *Renewable and Sustainable Energy Reviews*. doi:10.1016/j.rser.2012.12.014.
- [17] Harish, V. S. K. V., and Arun Kumar. "Reduced Order Modeling and Parameter Identification of a Building Energy System Model Through an Optimization Routine." *Applied Energy*, 2016a, 162: 1010–1023.
- [18] Harish, V. S. K. V., and Arun Kumar. "A Review on Modeling and Simulation of Building Energy Systems." *Renewable and Sustainable Energy Reviews*, 2016b, 56, 1272–1292. doi:10.1016/j.rser.2015.12.040.
- [19] U.S. Department of Energy. 2016. "EnergyPlus." <https://energyplus.net/downloads>.
- [20] Zhang, Yi. 2012. "Use jEPlus as an Efficient Building Design Optimisation Tool." *CIBSE ASHRAE Technical Symposium*.
- [21] Hachem C., A. Athienitis, Effect of Residential Building Design on Energy Performance, *ASHRAE journal*, 2013, 55(1), 72-74.
- [22] Crawley, Drury B., Linda K. Lawrie, Frederick C. Winkelmann, W. F. Buhl, Y. Joe Huang, Curtis O. Pedersen, Richard K. Strand, et al. 2001. "EnergyPlus: Creating a New-Generation Building Energy Simulation Program." *Energy and Buildings*, 2001, 33 (4), 319–31. doi:10.1016/S0378-7788(00)00114-6.
- [23] (RDH) RDH Building Engineering Ltd. "Energy Consumption and Conservation in Mid- and High-Rise Residential Buildings in British Columbia." doi:10.1017/CBO9781107415324.004.
- [24] Heiselberg, P., Brohus, H., Hesselholt, A., Rasmussen, H., Seinre, E. and Thomas, S., Application of sensitivity analysis in design of sustainable buildings. *Renewable Energy*, 2009, 34(9), 2030-2036.
- [25] Schroeder, Larry D. 1986. *Understanding Regression Analysis An Introductory Guide*. Beverly Hills: Sage Publications.
- [26] (CMHC) Canada Mortgage and Housing Corporation. 2013. "CANADIAN HOUSING OBSERVER." <http://www.cmhc-schl.gc.ca/odpub/pdf/67989.pdf>.
- [27] (NRCAN) National Research Council Canada. *National Energy Code of Canada for Buildings*. 2011.
- [28] Carmody, John, and Kerry Haglund. "Measure Guideline : Energy-Efficient Window Performance and Selection," 2012.
- [29] Sartori, Igor, Sonja Geier, Roberto Lollini, Andreas Athienitis, and Lorenzo Pagliano. "Comfort and Energy Efficiency Recommendations for Net Zero Energy Buildings." *Energy*, doi:10.1111/j.1945-1474.2011.00166.x.
- [30] Landis, R.S., *Standardized regression coefficients*. Wiley StatsRef: Statistics Reference Online. 2005.
- [31] Hachem C., A. Athienitis, P. Fazio, Parametric investigation of geometric form effects on solar potential of housing units, *Journal of Solar Energy*, 2011, 85(9), 1864-1877.

REVIEW

Anthropic Principle Algorithm: A New Heuristic Optimization Method

Elder Oroski^{1*} Beatriz S. Pês² Rafael H. Lopez³ Adolfo Bauchspiess⁴

1. Universidade Tecnológica Federal do Paraná (UTFPR), Curitiba, Brazil

2. Instituto Federal do Paraná (IFPR), Campo Largo, Brazil

3. Universidade Federal de Santa Catarina (UFSC), Florianópolis, Brazil

4. Universidade de Brasília (UnB), Brasília, Brazil

ARTICLE INFO

Article history:

Received: 26 November 2018

Accepted: 12 December 2018

Published: 31 December 2018

Keywords:

Heuristic optimization

Anthropic principle

System identification

ABSTRACT

Heuristic optimization is an appealing method for solving some engineering problems, in which gradient information may not be available, or yet, when the problem presents many minima points. Thus, the goal of this paper is to present a new heuristic algorithm based on the Anthropic Principle, the Anthropic Principle Algorithm (APA). This algorithm is based on the following idea: the universe developed itself in the exact way to allow the existence of all current things, including life. This idea is very similar to the convergence in an optimization process. Arguing about the merit of the Anthropic Principle is not among the goals of this paper. This principle is treated only as an inspiration for heuristic optimization algorithms. In the end of the paper, some applications of the APA are presented. Classical problems such as Rosenbrock function minimization, system identification examples and minimization of some benchmark functions are also presented. In order to validate the APA's functionality, a comparison between the APA and the classic heuristic algorithms, Genetic Algorithm (GA) and Particle Swarm Optimization (PSO) is made. In this comparison, the APA presented better results in the majority of tested cases, proving that it has a great potential for application in optimization problems..

1. Introduction

In the last decades, optimization problems have motivated great improvements in mathematics and engineering. Methods like Newton, steepest descent and Levenberg-Marquardt have made possible the solution of a series of design optimization problems^[1]. How-

ever, these methods require strong conditions to have their convergence proved, such as availability of gradients, convexity, and so on^[2,3]. It is important to point out that in several industrial applications the designer has to deal with some peculiarities such as non-linearity, non-convexity, existence of several local minima, presence of discrete

*Corresponding Author:

Elder Oroski

Universidade Tecnológica Federal do Paraná (UTFPR), Curitiba, Brazil

Email: oroski@utfpr.edu.br

and continuous design variables, among others^[4].

One class of optimization methods, which are potentially able to handle these characteristics, are the metaheuristic algorithms. Known advantages of these algorithms include the following: (i) they do not require gradient information and can be applied to problems in which the gradient is difficult to obtain or simply is not defined; (ii) they do not become stuck in local minima if correctly tuned; (iii) they can be applied to non-smooth or discontinuous functions; (iv) they furnish a set of sub-optimal solutions instead of a single solution, giving the designer a set of options from which to choose; and (v) they can be easily employed to solve mixed variable (discrete and continuous) optimization problems^[5]. Among the most popular metaheuristic algorithms are the Genetic Algorithm (GA)^[5], the Ant Colony Optimization (ACO)^[6], and the Particle Swarm Optimization (PSO)^[7], all of them inspired by biological principles.

Other principles have been employed for the development of metaheuristic optimization algorithms, such as the Imperialist Competitive Algorithm^[8], based on the imperialist policy of extending the power and rule of a government beyond its own boundaries, Group Search Optimizer inspired by animal searching behavior^[9], and the Biogeography-Based Optimization, that uses the geographical distribution of biological organisms as inspiration for algorithms in the optimization area^[10].

Following the line of nature inspired algorithms, this paper proposes a new metaheuristic optimization algorithm based on the Anthropic Principle, originated in Physics. According to the Anthropic Principle, uncountable factors had to converge, in the history of the universe, to make the human existence possible^[11]. Thus, the universe evolution can be seen as an optimization process whose objective function aims to minimize the effects that go against the human existence.

Details as the low eccentricity of the Earth's orbit, the relationship between the Sun's mass and distance from the Earth to the sun are examples in the set of suitable conditions for human existence^[11]. If just one element in this set were different, life as it is known could probably not be developed. In other words, the constants of the universe seem to be evolved in such a manner to assume ideal values to make life possible^[11]. This concept is very similar to "fine-tune" performed in a metaheuristic optimization algorithm.

This paper is organized as follows: in section 2, the Anthropic Principle is conceptually detailed. In section 3, the necessary concepts to the Anthropic Principle Algorithm (APA) are exposed and its operators are described. In section 4, the pseudo-code related to the proposed al-

gorithm is presented. Section 5 presents some examples of applications of the proposed algorithm, and finally, the concluding remarks are in section 6.

2. Anthropic Principle

The anthropic principle was formally defined by astrophysicist Brandon Carter in 1974^[12]. Following, John D. Barrow and Frank J. Tipler improved the ideas of this principle and compiled their formulations in the book, *Cosmological Principle*^[13].

In order to achieve suitable conditions for human existence, there is a series of necessary factors. Details such as a different ratio between the electron and proton masses could derail the existence of more complex structures of matter^[11]. If the electromagnetic force were changed for a small quantity, the organic molecules could not be able to group themselves^[11]. If, for example, the distance between sun and earth had been changed, mankind would not have developed. If the gravitational force were minimally changed, planets orbits would not be formed, and consequently, there would be no life^[14].

In fact, the reasoning of the anthropic principle starts with the premise that given the existence of mankind, only the universe stories compatible with that fact can be considered as physical models of this universe. This principle is known as the Weak Anthropic Principle (WAP). By this idea, it is understood that the characteristics of our universe and its physical laws allowed the existence of mankind. Due to the great number of coincidences necessary to create life in a universe, some physicists developed a theory in which the universe developed itself with the objective of allowing the existence of life. This concept is known as Strong Anthropic Principle (SAP) and it is very controversial in Physics^[15]. According to the SAP, the universe evolved in such a way as to make possible the existence of mankind^[11]. In other words, the physical and cosmological quantities evolved to promote the creation of life.

The anthropic principle in its strong version is rather controversial. There are many arguments contrary to it, as the fact that values of the fundamental constants incompatible with the development of intelligent life will never be observed^[16]. In this paper, the Anthropic Principle is only considered as an inspiration for the development of a new metaheuristic optimization algorithm. The idea behind the anthropic principle seems to be promising for a meta-heuristic algorithm. In this context, we propose the Anthropic Principle Algorithm (APA), which makes use of the ideas presented above and apply them in an optimization framework. In the next section, the concepts required for this new algorithm are presented.

3. Anthropropic Principle Algorithm: APA

The APA has an universe U as its basic element. Its structure can be defined as:

$$U = \{C, L\}, \quad (1)$$

in which C represents the characteristics and L the physical laws of that universe U .

These concepts can be better defined in the following form:

(i) Characteristics: set of attributes that characterize a universe, for example, some of the characteristics which were cited in the previous section such as distance between the Earth and the Sun, ratio between the electron and proton masses, and so on. In an optimization algorithm scheme, the characteristics of the universe represent the n design variables of the optimization problem. These characteristics are grouped into the vector C :

$$C = \{c_1, c_2, \dots, c_n\}. \quad (2)$$

(ii) Physical laws: set L of equations that update the characteristics of a universe:

$$L = \{l_1, l_2, \dots, l_n\}. \quad (3)$$

The relation between C and L can be expressed in many forms, among them, there is:

$$c_i^{(k+1)} = l_i \{c_i^{(k)}\}, \quad (4)$$

in which k stands for the k^{th} iteration of the algorithm. Equation (4) proposes that the i^{th} characteristic of the universe be updated by the i^{th} physical law, using only the current characteristic value.

The "manner" in which the characteristics of a universe U are updated is called the History of U .

The History of an universe is represented by H and it expresses the evolution of this universe between its initial state $U^{(0)}$ and its current state $U^{(k)}$:

$$H : U^{(0)} \rightarrow U^{(k)}, \quad (5)$$

in other words, the History "tells" the story of the characteristics of the best universe, through its laws and operators:

$$\{C^{(0)}, L\} \rightarrow \{C^{(k)}, L\}.$$

An individual I can be generated in a universe, U , if the characteristics of this universe are favorable for the creation of this specific kind of life. The notation used for representing the generation of an individual in a universe is:

$$U \Rightarrow I.$$

An individual generated by a universe U is called product individual: $U \Rightarrow I_p$. Here, we introduce the concept of the reference individual I_R . That is, an idealized individual generated by an ideal universe U_R , whose characteristics C_R are the most favorable for some specific kind of life, thus, $U_R \Rightarrow I_R$. Therefore, we may consider that there exists a specific kind of life in the universe U , if its product individual I_p is similar to the reference individual I_R . We propose to measure this similarity with the aid of the function $F(\cdot)$. That is, the universe U generates this specific kind of life if its image in the function $F(I_R, I_p)$ breaks up a threshold α_v . In other words, if $F(I_R, I_p) < \alpha_v$, there is this specific kind of life in the universe U and, consequently, the universe can be now designated as an "alive universe", which is called U'' .

In the APA, the reference individual, I_R is represented by the set of requisites expected to be reached by the problem's optimal solution. For instance, if the optimization problem is the minimization of the function, $f(x_1, x_2, \dots, x_n)$, in which $f: \mathbb{R}^n \rightarrow \mathbb{R}$, the I_R is represented by the minimum image of the $f(x_1, x_2, \dots, x_n)$. If the problem is the minimization of a multi-objective function, the set of desired values for the variables, involved in the optimization process, represents the restrictions that characterize the reference individual. In a system identification problem, each pair of samples (input and output signals) is considered as a restriction for the existence of the life, and the set of these restrictions represents the reference individual.

Now, the development above can be associated to the optimization algorithm presented in this paper. In the APA, the design variables are represented by the characteristics of a universe, e.g. the values of the global solution of the optimization problem are the characteristics C_R of the reference Universe U_R . The function $f(\cdot)$ may be set as the difference between the objective function of a given product individual and:

- 1) the global solution provided by I_R in the case of a target optimization problem, or,
- 2) the best solution found up to the current iteration of the algorithm in the minimization of a given function.

The APA was developed as a multi-agent optimization algorithm, consequently, there is a set of candidate universes for life creation. In this context, the set M of universes $\{U_1, U_2, \dots, U_m\}$ is called Multiverse and it can be expressed as:

$$M = \{U_1, U_2, \dots, U_m\} \quad (6)$$

In the initialization of the algorithm, the characteristics $C = \{c_1, c_2, \dots, c_n\}$ of each universe are randomly generated, and the physical laws of each universe are randomly generated, and physical laws of each universe can have

different kind of rules of update. For example, consider as possible laws the difference equations in the form:

$$l_i: c_i^{(k+1)} = a_1 c_i^{(k)} + a_2 c_i^{(k-1)} + \dots + a_n c_i^{(k-n-1)}, \quad (7)$$

in which the coefficients a_1, a_2, a_n , are randomly initialized. The initial conditions for equation (7) can be computed with the previous values of the characteristic, c_i . If these variables are unavailable, their values are assumed to be zeros.

Another example of a possible kind of physical law is presented in equation (8),

$$l_i: \begin{cases} \Delta c_i^{(k+1)} = a_1 c_i^{(k)} \Delta c_i^{(k)} + a_2 \Delta F^{(k)}(.) \\ c_i^{(k+1)} = c_i^{(k)} + \Delta c_i^{(k+1)} \end{cases} \quad (8)$$

in which the coefficients $a_1, a_2 \in \mathbb{R}^{+}$ are also randomly initialized and $\Delta F^{(k)} = F^{(k)} - F^{(k-1)}$. In this kind of laws, the update of the characteristics is indirect, using steps Δc_i , and there is a feedback, implemented by the last image of evaluation function, $F(.)$, aiming at choosing adequately the size of the step.

The coefficients a_1 and a_2 are initially all positives, but its signals are changed, as it is shown in table 1, at each iteration. This is valid if the characteristic, c_i , is positive. Otherwise the signals of a_1 and a_2 , presented in this table, are inverted.

Table 1. Signals of the coefficients a_1 and a_2 related to the physical law (8)

$\Delta c^{(k)}$	$\Delta F^{(k)}$	a_1	a_2	$\Delta c^{(k+1)}$
-	-	-	-	-
-	+	-	+	+
+	-	+	-	+
+	+	-	-	+

The objective of this permutation of signals is to keep $\Delta F^{(k)}$ negative. The signals of the coefficients a_1 and a_2 are chosen depending on the signals of the two first columns of table 1, aiming to obtain the correct signal for $\Delta c^{(k+1)}$, shown in the third column of the same table.

It is important to mention that only two kinds of physical laws were presented here, but many others are possible.

In order to continue the presentation of the proposed algorithm, we define in the sequel three different classes of universes. The universe U_i of M which presents the best characteristics C , e.g. the lowest objective function value, is denoted as propagating universe U^* . It receives this name because it propagates its characteristics to some least developed universes, as it will be shown in section 3.2.

Two other classes of universes can also be defined: the

promising U° and the stagnated U^\dagger universes. The former are the ones which have favorable physical laws for the universe evolution. In other words, universes with physical laws that improve, in one iteration, the image of the evaluation function, $F^{(k+1)}(.) < F^{(k)}(.)$, in a minimization problem. In the opposite way, the universes with physical laws that go against the universe evolution in p iterations, i.e., $F^{(k+p)}(.) > F^{(k)}(.)$, are called stagnated U^\dagger universes.

It is important to mention that, in APA, the reference IR , is fixed and the environment, U , is "adapted" to him, while in classic Genetic Algorithm (GA) the environment is fixed and the individuals are evolved.

In order to construct the APA, the main operators proposed for this algorithm are presented next.

3.1 Characteristic's Update

The characteristic update operator has the objective of systematically change the characteristics C of a universe U , through its physical laws L . It is done, in such a manner, that each characteristic, c_i , is updated by its corresponding physical law, l_i , as it is illustrated in figure 1.

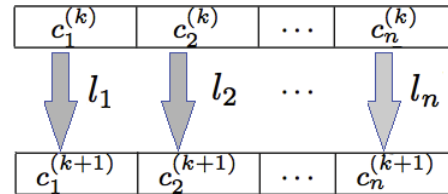


Figure 1. Update of the Universe's characteristics, $C = c_1, c_1, \dots, c_n$, through the physical laws, $L = l_1, l_2, \dots, l_n$

The update operator can be implemented in different ways, depending on how the structure of the laws is used. In order to exemplify this, two kinds of update are presented here:

- 1) The direct update: in which the law, l_i , acts directly over the characteristic, c_i , as it is shown in equation (7). In this kind of physical law, each characteristic has its own dynamic, and the algorithm have to select the laws that has the tendency to lead the evaluation function to a lower value;
- 2) The update by Δc : in which the law, l_i , creates some quantity Δc_i , which is summed to the characteristic c_i , as it is shown in equation (8). In this kind of physical law, the step $\Delta c^{(k+1)}$ is calculated taking into account its last value $\Delta c^{(k)}$ and the last value of the evaluation function $F(.)$. Thus, the law creates a control mechanism, a feedback, aiming to avoid or at least decrease the fast divergence of a given universe from the solution.

It should be pointed out that since the physical laws of each universe are not the same, the characteristics will be updated in different manners, sweeping the searching

space in different ways.

It is worth mentioning that APA has no fixed kind of physical laws. Differently of Ant Colony Optimization^[6] and Particle Swarm Optimization^[7], and many others heuristic algorithms, in APA the kind of actualization rule of the parameters can be chosen by the user, or by the algorithm itself, depending on the kind of problem being treated.

3.2 Characteristic's Propagation Operator

The propagating universe may transfer its characteristics integrally to less suitable universes. The characteristic propagation operator is represented by the symbol and express the propagation of all characteristics, $C = [c_1, c_2, \dots, c_n]$, from the propagating universe, U^\square , to the universe U :

$$\{C^*, L^*\} \gg \{C, L\},$$

or simply:

$$U^* \gg U.$$

The action of this operator can be seen in the figure 2.

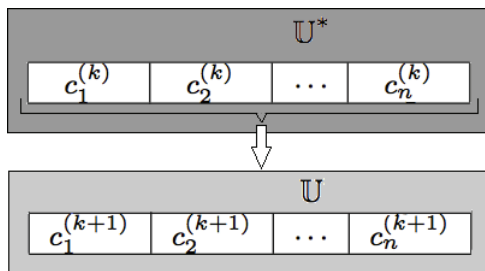


Figure 2. Characteristic Propagation Operator from propagating universe, U^* , to the universe U

It is worth to mention that this operator only acts on universe characteristics, C , not changing the physical laws, L , of any universe. In this context, this operator can also be applied from an alive universe U^\vee to a promising universe U^\diamond :

$$U^\vee \gg U^\diamond.$$

This procedure aims to spread all the best characteristics, C^\vee of the alive universes, U^\vee , to the promising universes, U^\diamond , that have favorable physical laws, L^\diamond . Thus, potential characteristics are lead to potential laws and its values can be evolved.

3.3 Big Bang Operator

From Physics, one may understand that our universe was generated by a "Big Bang"^[11]. In the proposed algorithm, this idea can be useful. In the APA, the physical laws can be difference equations, system of equations, among others. As the initialization of these equations is a random process, then some physical laws, l_i , could lead the characteristics, c_i , of the universe U to instability. In this scenario, the Big Bang Operator, $B(\cdot)$ can discard these universes and create new ones, and the process go on.

Another possible application of the "Big Bang" Operator is randomly generating new universes and replaces the stagnated ones. In other words, the operator discards non-promising regions of the design domain and restarts the search randomly in a new location of the searching space.

In order to avoid the random search caused by the "Big Bang Operator", the occurrence rate of this operator should be inferior to 15% of the universes in the multi-universe, at each iteration.

3.4 Armageddon Operator

Similarly to a natural catastrophe, the Armageddon operator, $A(\cdot)$, disturbs some characteristics of a universe. The Armageddon operator perturbs the characteristics of a universe by having small constants, Δc , added to their current values, as can be seen in figure 3.

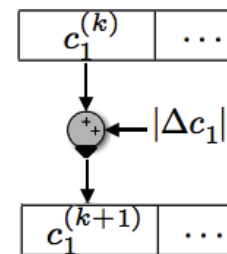


Figure 3. Armageddon Operator, $A(\cdot)$, acting over characteristic c_1

The effect of this operator can be tuned by the Armageddon operator rate, allowing the algorithm to perform local searches around the current characteristics of the universes.

4. Application Example

In this section, some examples of the use of APA for optimization problems will be presented. The experiments were carried out on a Macbook with 2.2 GHz Intel Processor and 4.0 GB RAM. All the codes were written and executed in Matlab R2013. The operating system was Mac OS Lion.

4.1 Rosenbrock Function Example

In order to exemplify the solution of an optimization problem using the APA, consider the Rosenbrock function:

$$f(x) = (a - x_1)^2 + b(x_2 - x_1^2)^2, \quad (9)$$

in which $f: \mathbb{R}^2 \rightarrow \mathbb{R}$ is a non-convex function, with $a = 1$ and $b = 100$, used in tests for global optimization. The objective of the optimization is to find the vector $x^* = [x_1, x_2]$ that minimizes $f(x)$:

$$x^* = \operatorname{argmin} \{f(x)\} \quad (10)$$

the global optimum of this function is located at $x^\square = [1, 1]$, the objective function is $f^\square = 0$.

In this example, each universe has 2 characteristics, $[c_1,$

c_2], which represent the values $[x_1, x_2]$ of the Rosenbrock function, and two laws, $[l_1, l_2]$ responsible for updating these characteristics. It is worth to mention that the physical laws, L , used in this example, were a class of equations with the structure presented in (8). In addition, the APA evaluation function is $f(x)$.

In order to illustrate the progress of the algorithm, the Rosenbrock function was minimized using the APA. In all runs of this section, the APA uses 200 universes, characteristics propagation rate starting with 50% and ending with 30%, the Big-Bang rate starting with 5% and ending with 10% and the Armageddon rate starting with 5% and ending with 15%, varying linearly.

For illustration purposes, the algorithm was run only for 10 iterations. The best solution found for each iteration is plotted in figure 4 and detailed in table 2.

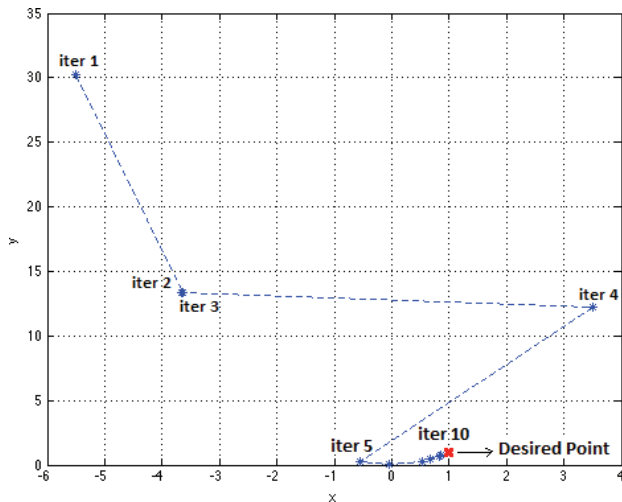


Figure 4. History of a Multiverse. The evolution of the characteristics of an universe during the APA's convergence

Table 2. Characteristics for the best Universe in each iteration

Iter.	c_1	c_2	Δc_1	Δc_2	ΔF
1	-5.5024	30.2659	NA	NA	NA
2	-3.6278	13.3869	-39.2095	-7.2623	-1.5511×10^8
3	-3.6582	13.3894	0.0305	0.0025	-72.4581
4	3.4940	12.2212	-7.1522	-1.1682	-8.0588×10^7
5	-0.5403	0.2111	-0.4129	-2.9837	-523.4355
6	-0.0485	0.0877	-0.9072	-2.3368	-230.3496
7	0.5232	0.2301	-0.6340	-0.3256	-1.9760
8	0.6736	0.4385	0.0023	0.2083	-1.9823×10^4
9	0.8378	0.7159	0.1642	0.1693	-1.3187×10^4
10	0.8448	0.7276	0.0070	0.0117	-1.2819×10^5

From table 2, one may see that the APA did not reach the optimal point $[1, 1]$ in only 10 iterations, however the convergence process of the proposed algorithm can be clearly observed. In order to further investigate this process, we present the laws (represented by the coefficients a_1 and a_2) of the best universe at each iteration in table 3.

Table 3. The laws for the best Universe in each iteration

Iter.	l_1		l_2	
	a_1	a_2	a_1	a_2
1	0.0556	2.0082×10^{-8}	0.6309	6.5930×10^{-8}
2	0.3287	9.9367×10^{-8}	0.1148	2.3732×10^{-8}
3	0.7401	1.6827×10^{-8}	0.3792	2.0312×10^{-8}
4	0.3889	9.225×10^{-8}	0.4464	1.5073×10^{-8}
5	0.2505	5.4600×10^{-8}	0.6141	2.7179×10^{-8}
6	0.4815	1.5400×10^{-8}	0.2903	7.9859×10^{-8}
7	0.5318	5.4355×10^{-8}	4.1028	7.9859×10^{-8}
8	0.1386	7.8980×10^{-8}	0.4280	7.8184×10^{-8}
9	0.4242	3.9651×10^{-8}	0.2491	5.8548×10^{-8}
10	0.4428	7.6638×10^{-8}	0.4401	7.2683×10^{-8}

Most of the universes presented in table 2 are not totally connected in an evolutionary way. In other words, they evolved from other universes, in the multiverse, which were not the best in the previous iteration of the algorithm.

In table 2, in 4 iterations the best universe evolved from itself: iterations 2 to 3, 3 to 4, 8 to 9 and 9 to 10. In these cases, it is possible to calculate manually the evolution of these universes using the values presented in tables 2 and 3, since the physical laws were responsible for the characteristics update that resulted in the decrease of the objective function. In the other iterations, the best universe was reached by the action of the APA operators. In the transition from iteration 4 to 5, 6 to 7 and 7 to 8 the best universe was reached by propagation of the best characteristics to universes with physical laws that allowed decreasing the evaluation function. In the transition from iteration 1 to iteration 2, the best universe was reached by the Armageddon Operator. In this example, the Big Bang operator did not generate best universes.

Now, we run the APA for 50 iterations, and then compare its results to two well-known metaheuristic algorithms: GA and PSO. In this situation, the proposed algorithm reached as best solution $x^* = [1.0001, 1.0002]$. As it is known that the optimum of the Rosenbrock function is $[1, 1]$ [17], one can consider that it is a close result, reaching an evaluation function equal to 1.1125×10^{-8} . The APA's convergence curve for this run is illustrated in figure 5.

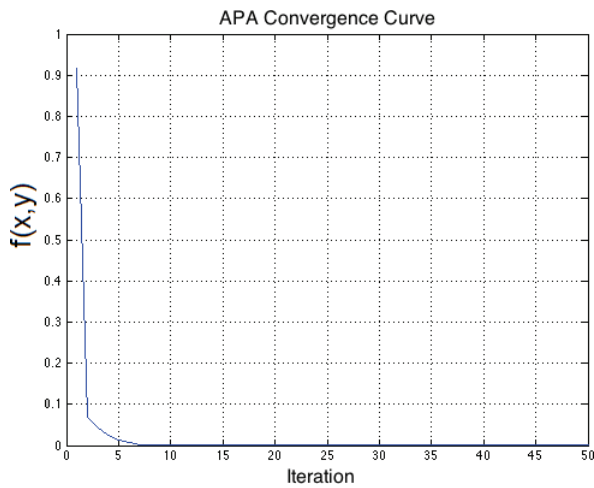


Figure 5. Convergence curve of the Anthropic Principle Algorithm

In order to compare the APA to a GA and a PSO, table 4 shows the objective function reached by these algorithms in a single optimization run. The stopping criterion for all the algorithms was 50 iterations. The APA and GA results were generated by the authors and the PSO result was taken from the literature^[18].

Table 4. Minimization of the Rosenbrock Function Results

Method.	APA	GA	PSO
Function value	1.1125×10^{-8}	0.0018	0.001341

In the GA, 200 chromosomes were used, with cross-over rate starting in 80% and ending with 60%. The mutation rate starting in 5% and ending in 10%, varying linearly. For the PSO, were used 200 particles with social adjustment equal to the self adjustment (1.49).

One can see in table 4 that the lowest value of the Rosenbrock function was obtained with the APA, outperforming in this case, the other metaheuristic algorithms.

4.2 System Identification Example

System Identification deals with the problem of building approximated mathematical models of dynamic systems based on observed (experimental) data^[19]. In this section, we briefly present the problem to be solved, thus the interest reader is referred to^[20] and^[21] for further details. In this section, the APA is applied to a system identification problem. In this context, consider the following stable, linear and time invariant system, with input $u(k)$ and output $y(k)$:

$$H(z) = Z \left\{ \frac{y(k)}{u(k)} \right\} = \frac{Y(z)}{X(z)} = \frac{2z - 1}{z^2 - 0.2z + 0.26} \quad (11)$$

in which Z represents the Z transform and z is the complex variable associated to this transform. Consider also that one can seek an approximated model for such a sys-

tem using linear combinations of Laguerre functions, as expressed in (12):

$$M(z) = d_1 L_1(z) + d_2 L_2(z) + \dots + d_r L_r(z) = \sum_{i=1}^r d_i L_i(z), \quad (12)$$

in which $M(z)$ is the approximated model of the system $H(z)$ based on Laguerre functions, given by:

$$L_i(z) = \frac{\sqrt{1-p^2}}{z-p} \left(\frac{1-pz}{z-p} \right)^{i-1}, \quad (13)$$

in which $p \in R$ is the pole of the Laguerre functions.

Thus, in order to identify the system $H(z)$, expressed in (11), it is necessary to find the pole, p and the coefficients d_i that minimize $F(\cdot)$, as expressed in equation (14),

$$x^* = \operatorname{argmin} \{ F(I_R, I_p(x)) \} \quad (14)$$

in which $x = [d_1, \dots, d_r, p]$ is the design vector comprised by the r coefficients d_i and the pole p ; $F(I_R, I_p)$ is the evaluation function of the algorithm, expressed by the mean square error (MSE), of the approximated model output with respect to the observed (measured) system output. It is important to mention here that, in the identification problem, the image I_R of the reference universe U_R is known from experimental data. Hence, the evaluation function can be constructed as detailed above.

In order to identify the system $H(z)$, one can resort to an input $u(k)$, PRBS type, Pseudo Random Binary Signal. For the identification step, it was used 128 input/output system samples. Another 128 samples were reserved for the validation step. In this example, we constructed the approximated model using three Laguerre functions, i.e., $r=3$ in (12). Thus, the resulting optimization problem has 4 design variables: 3 coefficients d_i and the pole p .

In order to solve such a problem a multiverse with 200 universes was employed for 50 iterations. The algorithm ran with characteristic propagation rate starting with 50% and ending with 30%, the Big-Bang rate starting with 5% and ending with 10% and the Armageddon rate starting with 5% and ending with 10%, varying linearly. In addition, it is worth to mention that the physical laws, L , used in this example, were a class of difference equations of first order, in which a_1 and $a_2 \in R$ are generated by random values in each law of each universe.

The general structure of these laws is:

$$l_i: c_i^{(k+1)} = a_1 c_i^{(k)} + a_2 \quad (15)$$

in which $c_i^{(k+1)}$ is the i -th characteristic of a universe, updated by equation (15), in the iteration $(k+1)$ of the algorithm.

The best characteristics obtained by the APA are given in (16), which resulted in a $MSE = 6.011 \times 10^{-4}$.

$$\begin{aligned} d &= [1.4350 \ 2.1601 \ -0.1512], \\ p &= 0.1868. \end{aligned} \quad (16)$$

Now, using the information provided by APA, through the pole p , one can generate the Laguerre function basis, $[L_1(z), L_2(z), L_3(z)]$, used in the model (12):

$$L_1(z) = \frac{0.982}{z-0.187}, \quad (17)$$

$$L_2(z) = \frac{-0.184z + 0.982}{z^2 - 0.374z + 0.035} \quad (18)$$

$$L_3(z) = \frac{0.034z^2 - 0.367z + 0.982}{z^3 - 0.560z^2 + 0.105z - 0.0065} \quad (19)$$

and finally construct the approximation model $M(z) \approx \frac{Y(z)}{X(z)}$ as shown in (20).

$$M(z) = 1.4350L_1(z) + 2.1601L_2(z) - 0.1512L_3(z) \quad (20)$$

the pole, p , that has parameterized $L_1(z)$, $L_2(z)$ and $L_3(z)$ was 0.1868, as can be seen in (16).

The measured output of the system and the output obtained by the approximated model $M(z)$ are illustrated in figure 6. From this figure, we may see that the approximation model represents well the experimental data, thus successfully solving the identification problem.

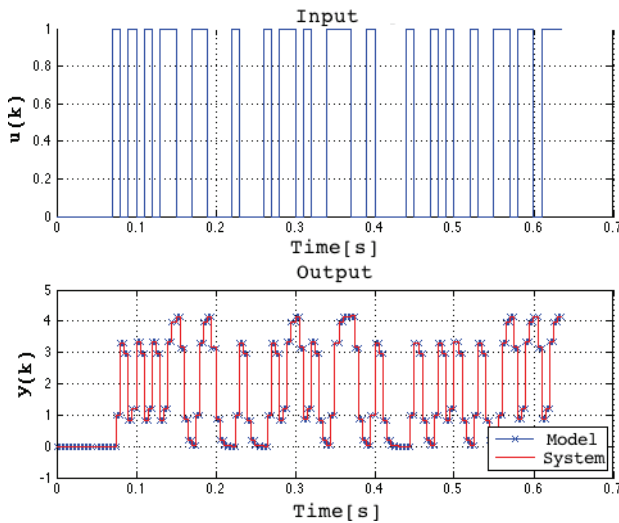


Figure 6. Input signal $u(k)$ applied to the system $H(z)$ and its output $y(k)$

The convergence curve of APA for this problem is shown in figure 7.

In figure 7, one can see that the APA convergence process is more intense in the first iterations and, then, evolves slowly to the end value.

In order to make a comparison between the performance of the APA and a classic GA, this identification problem was solved by both algorithms using the same

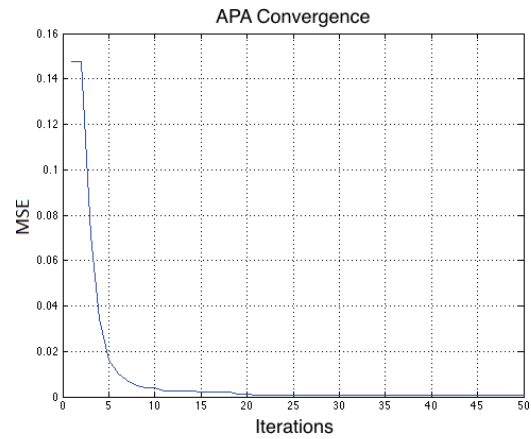


Figure 7. Anthropic Principle Algorithm Convergence stopping criterion: 100 iterations. In the GA, the crossover rate starting in 80% and ending with 60%, the mutation rate starting in 5% and ending in 10%. The resulting MSE of the approximated model provided by the APA and GA are given in table 5.

Table 5. Results of the minimization of MSE in the identification system problem with Laguerre functions

Method.	APA	GA
MSE	6.011×10^{-4}	7.110×10^{-4}

As it can be seen in table 5, the APA also provided a slightly better solution than the GA for this example.

It is import to mention that the APA was developed focusing in system identification problems, because the restrictions that characterize the IR are achieved directly from the sampled input/output data. However, is possible to infer that the APA algorithm can be applied for general optimization problems as can be seen in the next sections.

5. Statistical Analysis

In order to pursue a fair comparison among the APA and other metaheuristic algorithms, not only the best design found using each method should be compared, but also the statistics of each algorithm due to their stochastic nature. Thus, here, each optimization problem is run independently several times and the statistics of these runs are computed, such as the optimum mean value and coefficient of variation (C.O.V.) of the optimum objective function. The number of independent runs (NIR) for all the problems is taken as 50. Also, the stopping criterion used in all the problems is the number of iterations, which is set to 100.

The seven classical test functions shown in table 6 are analyzed. Functions f_1 , f_2 and f_3 are unimodal functions, with dimension equal to 30; f_3 is a random function; functions f_4 , f_5 and f_7 are multimodal, with 30 dimensions and

many local minima, while function f_6 is a polynomial type with 2 dimensions^[9].

The results of the comparison between the APA and the others algorithms is presented in table 7. The GA and PSO results were taken from the literature, in He et. al., (2009)^[9].

Table 6. Seven Benchmark functions, in which n is the dimension of the function, S represents the function domain and f_{min} is the global minimum value of the function

Test function	n	S	f_{min}
$f_1(x) = \sum_{i=1}^n x_i^2$	30	$[-100, 100]^n$	0
$f_2(x) = \sum_{i=1}^n (\sum_{j=1}^n x_j)^2$	30	$[-100, 100]^n$	0
$f_3(x) = \sum_{i=1}^n ix_i^2 + \text{rand}[0, 1]$	30	$[-1.28, 1.28]^n$	0
$f_4(x) = \sum_{i=1}^n (x_i^2 - 10 \cos(2\pi x_i) + 10)^2$	30	$[-5.12, 5.12]^n$	0
$f_5(x) = \frac{1}{4000} \sum_{i=1}^{30} (x_i - 100)^2 - \prod_{i=1}^n \cos(\frac{x_i - 100}{\sqrt{i}}) + 1$	30	$[-600, 600]^n$	0
$f_6(x) = 4x_1^4 - 2.1x_1^2 + \frac{1}{5}x_1^6 + x_1x_2 - 4x_2^2 + 4x_2^3$	2	$[-5, 5]^n$	-1.0316
$f_7(x) = 20 \exp(0.2 \sqrt{\frac{1}{n} \sum_{i=1}^n x_i^2}) - \exp(\frac{1}{n} \sum_{i=1}^n \cos(2\pi x_i)) + 20 + e$	30	$[-32, 32]^n$	0

It is worth to mention that the domain and correct minima of the functions are shown in table 6 on the third and fourth column. In the APA, the initialization of Universe's characteristics has followed the range expressed in these domains. From table 7, one can see that the APA reached better values than GA on functions f_1, f_2, f_5, f_6 and f_7 . In comparison with the PSO, the APA results were better on functions f_2, f_5, f_6 and f_7 . GA and PSO algorithms presented better results for the cases expressed by the functions f_3 and f_4 . The stochastic nature of the function f_3 can explain why the APA did not return the best result for this case. Concerning function f_4 , since it is a multimodal function, the conclusion is that APA got stuck in a local minimum, even though its result is a value near to the one presented by the PSO.

Table 7. Results for the seven-benchmark functions expressed in table 6

Func.	Algorit.	Mean	Std.	C.O.V.
f_1	GA	3.1711	1.6621	0.5241
	PSO APA	3.6927×10^{-37} 1.5859×10^{-10}	2.4598×10^{-36} 1.6380×10^{-10}	6.6612 1.0329
f_2	GA	9749.9145	2594.9593	0.2661
	PSO APA	1.1979×10^{-3} 7.4209×10^{-6}	2.1109×10^{-3} 1.3054×10^{-5}	1.7622 1.7591
f_3	GA	0.1045	3.6217×10^{-2}	0.3466
	PSO APA	9.9024×10^{-3} 8.9354	3.5380×10^{-2} 0.5094	3.5729 5.7009×10^{-2}
f_4	GA	0.6509	0.3594	0.5521
	PSO APA	20.7863 34.6328	5.9400 36.8309	0.2858 1.0635
f_5	GA	1.0038	6.7545×10^{-2}	6.7289×10^{-2}
	PSO APA	0.2323 2.1888×10^{-4}	0.4434 2.4709×10^{-4}	1.9087 1.5857
f_6	GA	-1.0298	3.1314×10^{-3}	NA
	PSO APA	-1.0160 -1.0316	1.2786×10^{-2} 3.8328×10^{-16}	NA NA
f_7	GA	12.9804	0.5979	0.0461
	PSO APA	2.2500 0.0219	4.5895 0.1256	2.0398 5.7322

In summary, the APA reached reasonable results for the majority of tested cases, overcoming the others meta-

heuristic algorithms in many cases.

6. Conclusion

In this paper, the concepts related to the Anthropic Principle were presented, as well as a new metaheuristic algorithm based on it. This algorithm is conceptually simple and easy to implement. Regarding the study of the effect of the control parameters, the authors found that the APA is not so sensitive to most of parameters with the exception of the coefficients of the physical laws. With respect to the applicability of the algorithm, one can see that it is appealing for solving real world problems, since it is applicable to a variety of optimization problems.

In order to test APA capability to find the minimum of a non-convex function, the Rosenbrock function was analyzed and compared, in a single run, with GA and PSO. From this comparison, one can conclude that the APA reached a value close to the known minimum, with better results than GA and PSO.

In order to test the algorithm in a practical engineering application, the APA was applied to a system identification problem. In other words, the APA was used to find the parameters in a Laguerre model for a dynamic system. In the comparison between the algorithms, the APA outperformed the GA. By the lower MSE reached and from figure 6, one can see that the approximated model is very close to the experimental data. Therefore, one can conclude that the approximated model provided by the APA is representative.

In figures 5 and 7, one can see that, typically, the APA convergence process is more intense in the firsts iterations and then, evolves slowly, but almost continuously, as seen in these figures.

In order to compare the statistics of the APA, GA and PSO, a set of seven benchmark functions were employed. 50 runs of each algorithm were pursued for each function. From table 7, one can see that the APA reached better values than GA on functions f_1, f_2, f_5 and f_6 . In comparison with the PSO, the APA results were better on functions f_2, f_5 and f_6 .

Considering that the APA is in its initial development, it is reasonable to assume that many improvements are still possible in the algorithm. In future work, it is possible to use the gradient-based methods as physical laws for the APA, mixing the deterministic and metaheuristic optimization.

Is important to mention that, in APA, the reference individual, IR, is fixed and the environment, U, is "adapted" to him, while in GA, the environment is fixed and the individuals are evolved. It also is noteworthy that the APA differs from the GA in the issue of defining its search di-

rections. The spread of the characteristics of propagating universe to other universes generates a range of "direction searches". As the physical laws are random, it is likely that different universes have different physical laws, and the search space is swept in different manners.

In the comparison between the results obtained with application of Anthropic Principle Algorithm and other heuristic algorithms, one can conclude that the APA presented reasonable results in all studied cases, and reached the best values and statistics in the majority of the tested cases. Moreover, it is expected that APA can be used for general heuristic optimization problems.

References

- [1] Nocedal, Jorge and Stephen, Wright. Numerical Optimization. Springer Publisher, 1st edition, 1999.
- [2] Boyd, Stephen Vandenberghe L. Convex Optimization. Cambridge University Press, 4th edition, UK, 2004.
- [3] Rao, S. S. Engineering Optimization: Theory and Practice. Wiley Press: New York, NY, 1996.
- [4] Mockus, Jonas; Eddy, William and Reklaitis, Gintaras. Bayesian Heuristic Approach to Discrete and Global Optimization: Algorithms, Visualization, Software and Applications. Kluwer Academic Publishers, 1st edition, 1997.
- [5] Koza, John. Genetic Programming: On the Programming of Computers by Means of Natural Selection. MIT Press, 6th edition, 1998.
- [6] Solnon, Christine. Ant Colony Optimization and Constraint Programming. Wiley Press, 1st edition, 2010.
- [7] Olsson, Andrea E. Particle Swarm: Theory, Techniques and Applications. Nova Science Publishers, 1st edition, 2011.
- [8] Atashpaz, Esmail and Lucas, Caro. Imperialist Competitive Algorithm: An Algorithm for Optimization Inspired by Imperialistic Competition. IEEE Congress on Evolutionary Computation, IEEE, 2007, 4661-4667.
- [9] He, S. and Wu, K. H. and Saunders, J. R. Group Search Optimizer: An optimization Algorithm inspired by animal Searching Behavior. IEEE Transactions on Evolutionary Computation, 2009.
- [10] Simon, Dan. Biogeography-Based Optimization. IEEE Transactions on Evolutionary Computation, 2008.
- [11] Hawking, Stephen and Mlodinow, Leonard, The Great Project, Nova Fronteira Print, 1st edition, 2012.
- [12] Carter, B. Confrontation of Cosmological Theories with Observational Data. IAU Symposium, Krakow, 1973.
- [13] Barrow, J. D. and Tipler, F. J. The Anthropic Cosmological Principle. Oxford Univ. Press. Oxford. 1986.
- [14] Comitti, V. S., Princípio Antrópico Cosmológico, Revista Brasileira de Ensino da Física, 2011.
- [15] Kallosh, Renata and Linde, Andrei. M theory, Cosmological Constant and Anthropic Principle. Physical Review D 67, 023510, 2003
- [16] Starkman, Glenn D. and Trotta, Roberto. Why Anthropic Principle Cannot Predict α . Physical Review Letters, 2006.
- [17] Rosenbrock, H. H. An automatic method for finding the greatest or least value of a function. The Computer Journal 3, 1960.
- [18] Raval, Falguni and Makwana, Jagruti. Optimization of Resonance Frequency of Circular Patch Antenna at 5GHz Using Particle Swarm Optimization. International Journal of Advances in Engineering and Technology, 2011.
- [19] Ljung, Lennart. System Identification, Theory for the User. 2nd edition. Prentice Hall. 1999.
- [20] Oroski, E. and Holdorf R. and Bauchspiess, A. Nonlinear Buck Circuit Identification Using Orthonormal Functions with Heuristic Optimization. XX Congresso Brasileiro de Automática, 2014.
- [21] Rosa, Alex and Campello, Ricardo and Amaral, Wagner. Exact Search Directions for Optimizations of Linear and Nonlinear Models Based on Generalized Orthonormal Functions. IEEE Transactions on Automatic Control, 2009.

About the Publisher

Bilingual Publishing Co(BPC) is an international publisher of online, open access and scholarly peer-reviewed journals covering a wide range of academic disciplines including science, technology, medicine, engineering, education and social science. Reflecting the latest research from a broad sweep of subjects, our content is accessible worldwide – both in print and online.

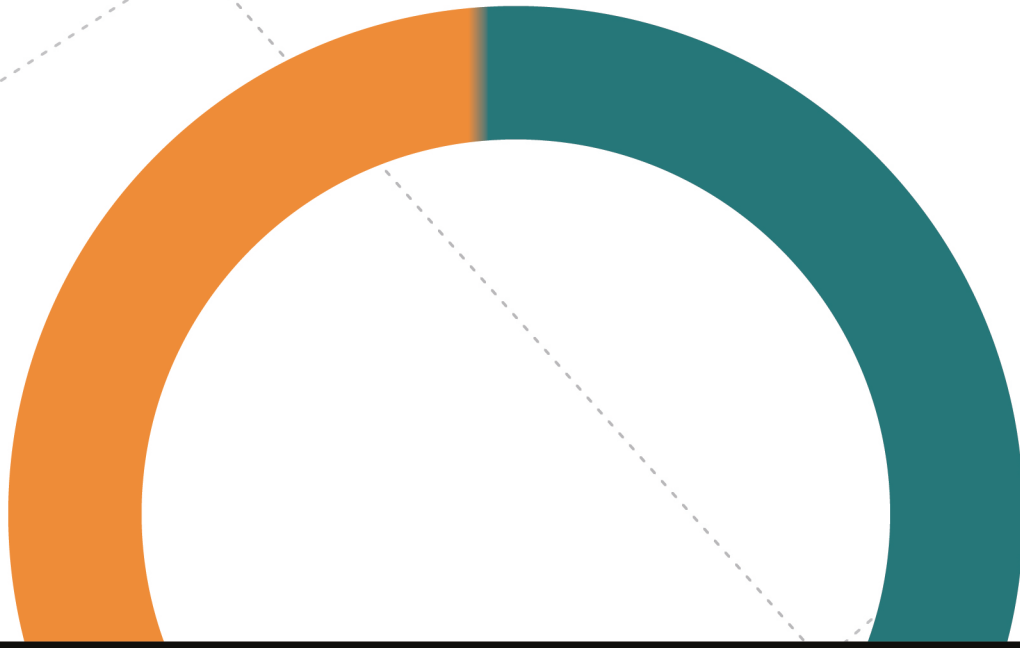
BPC aims to provide an academic platform for academic exchange and cultural communication that help organizations and professionals in advancing society for the betterment of mankind. BPC hopes to be indexed by well-known databases in order to expand its scope to the science community, and eventually grow to be a reputable publisher recognized by scholars and researchers around the world.

BPC adopts the Open Journal Systems, see on ojs.bilpublishing.com

About the Open Journal Systems

Open Journal Systems (OJS) is sponsored by the Public Knowledge Project Organization from Columbia University in Canada, jointly developed by PKP, the Canadian Academic Publishing Center and Canada Simon Fraser University Library. OJS can realize the office automation of periodical editing process, station build and full-text journals by network publishing. The system design is in line with international standards, and supports peer review. It is very helpful to improve the citation rate, academic level and publication quality of periodicals.





Bilingual Publishing Co. is a company registered in Singapore in 1984, whose office is at 12 Eu Tong Sen Street, #08-169, Singapore 059819, enjoying a high reputation in Southeast Asian countries, even around the world.



**BILINGUAL
PUBLISHING CO.**
Pioneer of Global Academics Since 1984

Tel: +65 65881289

E-mail: contact@blipublishing.com

Website: www.Blipublishing.com

